Dissertation der Graduate School of Systemic Neurosciences
der Ludwig-Maximilians-Universität München

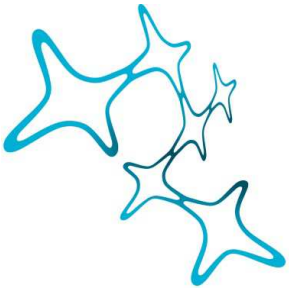

Graduate School of
Systemic Neurosciences
LMU Munich

Simultaneous Pupillometry and Functional Magnetic Resonance Imaging (fMRI) for the Detection of Stress-Related Endophenotypes

Submitted by
Maximilian Schneider
26th of July 2018

Date of Submission:	26th of July 2018
Date of Oral Defense:	15th of November 2018
First Supervisor/Reviewer:	Dr. Victor Spoormaker
Second Supervisor/Reviewer:	PD Dr. Mathias Schmidt

„Das schönste Glück des denkenden Menschen ist,

das Erforschliche erforscht zu haben

und das Unerforschliche zu verehren.“

– Johann Wolfgang von Goethe

Abstract

Mental diseases constitute a core health challenge of the 21st century. To date, diagnostics in psychiatry have been primarily based on subjective self-reports, largely bypassing the biological underpinnings and phenotypic heterogeneity of psychiatric disorders. As an effort to implement a more biologically valid classification of mental disorders, recent initiatives like the Research Domain Criteria (RDoC) project aim to identify endophenotypes that reflect transdiagnostic core mechanisms of psychiatric disorders. Stress is known to play a fundamental role in the development of mood and anxiety disorders. One key system involved in the physiological response to stress is the brainstem's noradrenergic (NA) arousal center located in the locus coeruleus (LC), and previous studies indicate that pupil size provides an indirect index for activity of the LC-NA system.

In order to investigate the relationship between spontaneous drifts in autonomic arousal and global brain activity in healthy human subjects, we first determined the fMRI correlates of spontaneous pupil fluctuations during the resting state. We found that pupil dilations are strongly coupled to activation of the dorsal anterior cingulate cortex (dACC) and bilateral insula (salience network [SN]). To assess whether this link between the pupil and the SN would also extend to emotional arousal, we next investigated the neural correlates of reward anticipation-induced pupil dilations in healthy subjects. Here, we could show that a cue signaling the possibility to receive a monetary reward evoked strong pupil dilations, the magnitude of which predicted response time to a target cue. Again, pupil dilations were strongly linked to SN activation. Furthermore, our results suggest that pupillometry is helpful to dissect different phases of reward anticipation and associated brain activity, disentangling reward prediction, arousal modulation and attention-related processes.

These observations led us to the conclusion that the SN modulates arousal levels to optimize task performance, that is, to counteract drowsiness/ transitions to sleep during the resting state and to facilitate reward-directed behaviors in the reward anticipation task. Taken together, pupillometry appears to provide a reliable index for activity of the SN, a core network related to

psychiatric disorders, making it a promising tool for the detection of stress-related endophenotypes.

Contents

List of Abbreviations

ACC	Anterior cingulate cortex
ACh	Acetylcholine
ACTH	Adrenocorticotropic hormone
BOLD	Blood oxygen level dependent
CRH	Corticotropin-releasing hormone
dACC	Dorsal anterior cingulate cortex
DMN	Default mode network
EU	European Union
EW	Edinger-Westphal nucleus
fMRI	Functional magnetic resonance imaging
GC	Ganglion ciliare
GLM	General linear model
HPA	Hypothalamic-pituitary-adrenal
HRF	Hemodynamic response function
IML	Intermediolateral cell column of the spinal cord
LC	Locus coeruleus
MDD	Major depressive disorder
mPFC	Medial prefrontal cortex
MRI	Magnetic resonance imaging
NA	Noradrenaline/noradrenergic
OFC	Orbitofrontal cortex
PFC	Prefrontal cortex
PLR	Pupillary light reflex
PTSD	Posttraumatic stress disorder
PVN	Paraventricular nucleus of the hypothalamus
RDoC	Research domain criteria
rs-fMRI	Resting state fMRI
SC	Superior colliculus
SCG	Superior cervical ganglion
SN	Salience network
SNS	Sympathetic nervous system
SSNRI	Selective serotonin and noradrenaline reuptake inhibitors
VS	Ventral striatum

1 Introduction

1.1 The need for individualized therapy in psychiatry

1.1.1 Mental disorders: the core health challenge of the 21st century

Recent reviews and meta-analyses indicate that around 50% of the general population in middle- and high income countries will develop at least one psychiatric condition at some point in their lives (Trautmann et al. 2016; Wittchen and Jacobi 2005; Wittchen et al. 2005). In the European Union (EU), mental disorders affect about 165 million people each year (Trautmann et al. 2016; Wittchen et al. 2011). Anxiety and mood disorders rank among the most frequent diseases, with 12-month prevalence rates of approximately 14% and 7% respectively, often starting in childhood or adolescence (Wittchen et al. 2011). Mental disorders typically have adverse effects on school achievement and professional career as well as somatic health throughout life. Also, they are linked to premature mortality due to suicide or as a consequence of associated risk factors and chronic diseases (Colton and Manderscheid 2006; McCarrick et al. 1986; Walker et al. 2015; Wittchen et al. 2011; Wittchen et al. 2005). According to the World Health Organization, at least 25% of all "Disability Adjusted Life Years" (a metric that captures the number of years lost due to any ill-health, disability, or early death) can be traced back to mental disorders (Wittchen et al. 2005). Psychiatric diseases not only involve severe distress for the affected individuals, but also impair their social- and work-related environments. Due to their high prevalence, early onset, and frequent long-term course, the economic burden associated with mental disorders is vast. In 2010, the economic costs of mental disorders were estimated at 2.5 trillion US dollars around the globe and at 798 billion euros for the EU. These costs are expected to double by 2030 (Gustavsson et al. 2011; Trautmann et al. 2016). The majority of the economic burden is not related to direct costs within the healthcare system (e.g. diagnosis and treatment), but rather to indirect costs such as income and production losses due to disability, early retirement and mortality (Gustavsson et al. 2011; Trautmann et al. 2016). As a consequence, mental disorders are among the most costly

medical conditions (Roehrig 2016; Soni 2009) and are thus considered a core health challenge of the 21st century.

1.1.2 Personalized medicine in psychiatry

Despite intense research efforts over the last decades, the exact pathogenesis of most mental disorders is still not fully understood. The discovery of pharmacological treatments against depression in the 1950s gave rise to theories that, for the first time, considered a physical basis for psychiatric diseases, suggesting imbalances in monoamine and (neuro-)hormonal systems (Bowrey et al. 2017; Nemeroff 1988; Prange 1964; Schildkraut 1965), among others. In line with this, different psychiatric disorders frequently involve similar symptoms, pointing towards overlapping biological underpinnings. Although these theories have greatly contributed to a better understanding of mental disorders as well as to the development of new medications, various issues remain unsolved.

Many psychiatric disorders show a high phenotypic heterogeneity. To fulfill the current diagnostic criteria for major depression, a patient has to suffer from any five out of nine symptoms, several of which have opposite polarity. This implies that a patient who, for example, shows psychomotor retardation, hypersomnia and an increase in body weight obtains the same depression score as another patient who is agitated and experienced poor sleep and weight loss (Goldberg 2011). It is long known that certain psychiatric diseases involve distinct subtypes (such as the psychomotor retarded and agitated subtype of depression) that need to be differentiated from each other when selecting the most suitable treatment.

Moreover, there are significant inter-individual differences in disease vulnerability, the time needed for a drug to elicit a therapeutic response, the size of the dose needed to produce an effect, the occurrence of adverse side effects, and even in the responsiveness to specific psychotherapeutic interventions (Costa e Silva 2013; Sambataro et al. 2018). Such inter-individual differences presumably arise from individually unique physiological characteristics, such as genetic alterations, epigenetic modifications or brain network connectivity (Costa e Silva 2013; Ozomaro et al. 2013). For instance, it has recently been shown that the volume of a specific

brain region, the anterior cingulate cortex (ACC), predicts response to cognitive behavioral psychotherapy (Sambataro et al. 2018). Taken together, recent findings increasingly challenge our understanding of mental disorders as homogeneous categorical entities (Goldberg 2011).

Receiving a therapy that is not tailored for the individual patient is likely to involve prolonged suffering as well as a greater risk for morbidity and mortality. To deal more effectively with phenotypic heterogeneity of mental disorders, increasing efforts were made in the past years to implement a personalized medicine approach in psychiatry. However, comparably little progress has been made in translating neurobiological research findings into clinical practice. This might, to some extent, be due to our current classification systems of mental disorders, which are based on a verbal categorization of reported symptoms instead of empirical data from genetics, neurobiology and behavioral science. Although these diagnostic criteria have provided clinicians with a common language and encouraged biological research, they are increasingly questioned due to their lack of biological validity. Nusslock and Alloy (2017) summarized this issue as follows: “diagnostic categories based on clinical consensus and self-reported symptoms (a) may fail to align with current findings from psychological science, neuroscience, and genetics, (b) are not predictive of treatment response, and (c) do not appear to capture the fundamental underlying mechanisms of dysfunction” (p. 3).

1.2 The search for biomarkers in stress-related disorders

1.2.1 RDoC, endophenotypes & biomarkers

As an effort to promote precision medicine in psychiatry, the National Institute of Mental Health proposed a new approach to classify mental disorders in 2012, focusing on observable behavior and neurobiological measures. The overarching goal of the so-called RDoC project is to establish a research framework based on core features that occur across traditional diagnostic boundaries (Cuthbert and Insel 2013; Kozak and Cuthbert 2016; Woody and Gibb 2015). More precisely, the initiative aims to identify mechanisms that are common to multiple psychiatric disorders, as well as mechanisms that are unique to specific psychiatric symptoms and reflect markers of differential

risk for these symptoms (Nusslock and Alloy 2017). For this purpose, dimensional psychological constructs are defined (e.g. “reward learning”), which, in turn, are grouped into higher-level domains relevant to human behavior and mental disorders (e.g. “positive valence systems”). The current RDoC matrix comprises five domains: 1) negative valence, 2) positive valence, 3) cognitive systems, 4) social processes and 5) arousal/regulatory systems. Methods used to investigate these domains/constructs range from molecular and genetic to neurocircuit and behavioral assessments (referred to as “units of analysis”).

Within RDoC, mental disorders are assumed to reflect disruptions in specific brain circuits that are linked to anomalies across multiple units of analysis (Cuthbert and Insel 2013; Woody and Gibb 2015). The RDoC research framework has been shown useful for identifying clusters of individuals based on genomics, physiological traits, or imaging findings, yielding specific biomarkers and endophenotypes (e.g. Clementz et al. 2016). The term endophenotype refers to “markers of an illness regardless of the phenotypic presence or absence of the illness” (Ozomaro et al. 2013, p. 9). Based on work by Gottesman and Gould (2003), Ozomaro et al. (2013) summarized the criteria for endophenotypes in psychiatry as follows: “The endophenotype should segregate with the illness in the population, and co-segregate with the illness within families; it should be heritable and more prevalent in affected than in unaffected families; it should not depend on whether the illness is currently clinically manifested, and finally, it should be specific to the illness and capable of being reliably measured” (p. 9). Furthermore, Ozomaro et al. (2013) outlined biomarkers as “measureable characteristics that reflect biologic function or dysfunction, response to a therapeutic measure, or indication of the natural progression of disease” (p. 9). While endophenotypes constitute trait markers, biomarkers can be state or trait markers (Beauchaine 2009; Ozomaro et al. 2013). Endophenotypes are expected to offer greater biological validity and better clinical predictability than current diagnostic categories, yielding better guidance to treatment and eventually better outcomes.

1.2.2 (Neuro)biology of stress

Stress is known to play a major role in the development of mental disorders. For instance, depressive episodes frequently follow exposure to stressful events such as divorce or death of a spouse, family member, or significant other (Juruena 2014). Acute stress evokes a physiological alarm response that is mediated by the sympathetic nervous system (SNS) and neuroendocrine systems, including the brain's NA system (Bremner et al. 1996; Morilak et al. 2005) and the so-called hypothalamic pituitary adrenal (HPA) axis (Herman et al. 2016; Pacak and Palkovits 2001). The NA center is located in the LC (see Figure 1), a small nucleus in the brainstem that is highly responsive to alerting stimuli and strongly involved in the regulation of autonomic arousal (Aston-Jones and Bloom 1981; Aston-Jones et al. 1994; Szabadi 2013). The LC responds to stress within a few seconds via the release of NA, followed by increased secretion of NA and adrenaline from the adrenal medulla after 20 to 30 s (Allen 1983; Krugers et al. 2012). The effects of NA and adrenaline are frequently referred to as the "fight-or-flight" response, involving increases in heart rate, blood pressure, muscle tension and pupil size, as well as an overall increase in metabolic rate (Cannon 1929; Szabadi 2013; Tank and Lee Wong 2015).

The fast stress response mediated by the SNS is complemented by a slower, prolonged response of the HPA axis, typically occurring after several minutes and lasting up to several hours (de Kloet et al. 2008; Herman et al. 2016; Krugers et al. 2012; Ulrich-Lai and Herman 2009). The HPA axis consists of the hypothalamus, the pituitary gland and the adrenal glands. It plays a central role in regulating physiological homeostasis (including metabolic, cardiovascular, immunological and reproductive processes) and mediates the endocrine component of the stress response (Habib et al. 2001; Smith and Vale 2006). Here, stress is known to trigger the secretion of two peptides − vasopressin and corticotropin-releasing hormone (CRH) − from the paraventricular nucleus (PVN) of the hypothalamus, which in turn stimulate the secretion of adrenocorticotropic hormone (ACTH) from the anterior lobe of the pituitary gland (Herman et al. 2016; Linton et al. 1985; Smith and Vale 2006; Whitnall et al. 1987). ACTH elicits the release of glucocorticoid hormones from the adrenal cortex, including cortisol, a major stress hormone in humans. Glucocorticoids mobilize energy by increasing blood glucose, potentiate

sympathetically-mediated effects (by promoting the effects of NA and stimulating the synthesis of adrenaline), and influence the expression of various genes via binding to mineralocorticoid and glucocorticoid receptors in the brain (De Kloet et al. 1998; McKay and Cidlowski 2003; Smith and Vale 2006; Ulrich-Lai and Herman 2009). Finally, they act back on the hypothalamus and pituitary in a negative feedback loop to limit prolonged exposure to glucocorticoids. Negative feedback is mediated mainly through corticoid receptors in the hippocampus, and prolonged glucocorticoid exposure has been linked to hippocampal degeneration and depressive symptoms (Frodl and O'Keane 2013; Juruena 2014; Sterner and Kalynchuk 2010).

Activity of the HPA axis has been shown to be modulated by the LC via excitatory NA projections to the PVN (Cunningham and Sawchenko 1988; Saphier 1993). Also, CRH has an excitatory influence on the LC (McCall et al. 2015; Page and Abercrombie 1999), indicating a reciprocal excitatory loop between the two structures (Dunn et al. 2004; Perez et al. 2006). Both systems are tightly linked to various brain regions involved in emotion and cognition (e.g. amygdala, prefrontal cortex and hippocampus), and chronic abnormal activity of either system has been associated with psychiatric conditions such as depression and anxiety (Faravelli et al. 2012; Sterner and Kalynchuk 2010; Stetler and Miller 2011).

Previous research on stress and its relationship to mental disorders has extensively focused on the HPA axis, using salivary or blood samples to measure cortisol levels and thereby investigate HPA axis activity in humans. Naturally, the LC-NA system too has received ample attention, but recent findings suggest a more complex pattern of LC function, going beyond its basic role in arousal regulation and pointing towards a strong implication in cognitive and affective processing. As a consequence, the LC-NA system has become a promising object of investigation in neuroscientific and psychiatric research.

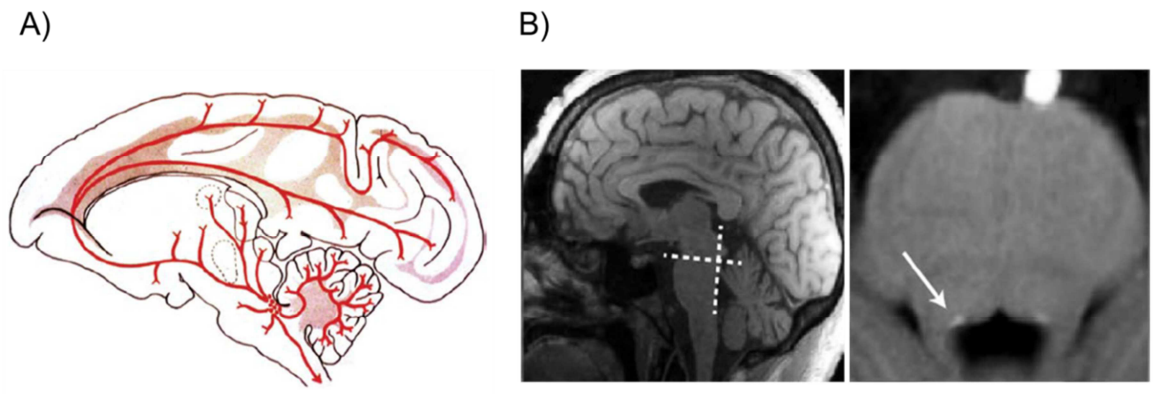

Figure 1. Locus coeruleus (LC). A) Illustration of the LC's efferent projections in the macaque monkey (sagittal view of the brain). The LC is a small nucleus in the dorsorostral pons of the brainstem that is strongly involved in the regulation of arousal. Moreover, the LC constitutes the brain's major noradrenaline source, sending widely distributed projections throughout the central nervous system. Figure reprinted with permission from Aston-Jones and Cohen (2005b). B) MRI-based visualization of LC in the human brain, seen in sagittal (left) and axial (right) planes. Figure adapted and reprinted with permission from Liu et al. (2017).

1.3 Locus coeruleus (LC): the brain's noradrenergic (NA) arousal center

1.3.1 Historical perspective: LC & arousal/vigilance

Traditional views of the LC-NA system emphasized its role in bottom-up processes such as general arousal, vigilance and environmental responsiveness. This understanding was based on early studies showing that LC neurons exhibit high tonic firing rates during wakefulness and low tonic firing rates during drowsiness and slow wave sleep, while being completely silent during rapid eye movement sleep (Aston-Jones and Cohen 2005b; Hobson et al. 1975; Rajkowski et al. 1998; Rasmussen et al. 1986). As a consequence, low tonic LC activity was associated with sleep and disengagement from the environment. An important role for environmental responsiveness was further supported by a number of studies reporting phasic bursts of LC activity following salient and arousing stimuli (Aston-Jones and Bloom 1981; Grant et al. 1988; Herve-Minvielle and Sara 1995). In addition, NA was found to enhance signal transmission through sensory networks (Devilbiss and Waterhouse 2000; 2004; Hurley et al. 2004; Waterhouse et al. 1998),

contributing to the idea that the LC-NA system may regulate arousal by modulating sensory processing, for instance by augmenting the processing of motivationally relevant stimuli (Aston-Jones and Cohen 2005b). Also, based on its widespread projections throughout the brain (see Figure 1A), LC activity historically was assumed to have a rather broad, nonspecific effect on cortical information processing (Aston-Jones and Cohen 2005b).

1.3.2 Updated view: LC & performance optimization

Recent research on LC functions points towards a more complex pattern, suggesting close interactions with top-down influences from cortical systems and an important role in optimizing behavior. Studies investigating the neural mechanisms involved in simple decision making provided evidence that phasic LC activity modulates specific behaviors rather than sensory processing (Aston-Jones and Cohen 2005b; Gold and Shadlen 2000; Hanes and Schall 1996; Schall and Thompson 1999). This conclusion was largely based on the results of numerous experiments in rats and monkeys: for instance, phasic LC activity was found to be more tightly time-locked to the subsequent motor response than to the preceding presentation of a task cue (Aston-Jones and Cohen 2005b; Clayton et al. 2004). Also, LC responses could not be linked to specific sensory attributes of task cues; faster reaction times were associated with shorter latency of LC firing, and no LC responses were observed during trials in which the animal made no response despite viewing the cue (Aston-Jones and Cohen 2005a).

Various studies investigating the relationship between LC activity and task performance concluded that LC neurons seem to exhibit two modes of activity during wakefulness: a phasic mode, during which "bursts of LC activity are observed in association with the outcome of task-related decision processes and are closely coupled with behavioral responses", as well as a tonic mode, in which "LC baseline activity is elevated but phasic bursts of activity are absent, and behavior is more distractible" (Aston-Jones and Cohen 2005b, p. 407). The phasic mode has been suggested to optimize performance during tasks that require selective attention by filtering responses to task-irrelevant and facilitating responses to task-relevant cues. In contrast, the tonic

mode has been proposed to serve flexible changes in behavior and adaptive disengagement from the current task to explore more beneficial alternatives.

According to Aston-Jones and Cohen (2005b), the dynamic adjustment of LC activity mode is essential for maximizing utility: the phasic LC mode promotes "optimization of current task performance as long as task-related utility remains sufficiently high" (p. 423), or more generally, exploitation of reward opportunities. The tonic mode supports "exploration when current task-related utility falls below an acceptable value" (Aston-Jones and Cohen 2005b, p. 423). The transition between the two LC modes has been suggested to be regulated by two frontal cortex structures which send direct projections to the LC: the ACC and orbitofrontal cortex (OFC). Both regions are known to receive inputs from various sensorimotor areas, as well as limbic structures such as the insular cortex, ventral striatum (VS), and amygdala (Carmichael and Price 1995a; 1995b; Devinsky et al. 1995; Ongur and Price 2000). The OFC and ACC have been shown to be involved in evaluating rewards and costs, respectively, and task-related responses in both regions are closely related to the motivational significance of the eliciting event (Aston-Jones and Cohen 2005b). Furthermore, numerous studies have linked ACC activity to performance monitoring and error detection (e.g. Botvinick et al. 2004; Carter et al. 1998; Ito et al. 2003; Miltner et al. 1997). According to Aston-Jones and Cohen (2005b), the dACC might play an important role for counteracting transient lapses in task performance by upregulating the phasic LC mode, restoring selective attention.

1.4 Pupillometry: an objective index for arousal

1.4.1 Pupillometry as an efficient alternative to LC fMRI

The human LC is located in the dorsorostral pons of the brainstem and consists of no more than approximately 16,000 neurons per hemisphere, spanning an average length of 14.5 mm with a thickness of 2.5 mm (Fernandes et al. 2012; Liu et al. 2017). A typical voxel size used in human neuroimaging studies is $3 \times 3 \times 3$ mm^3, implying that in these studies, LC neurons cover less than one voxel in the axial plane (see Figure 1B). In addition, the standard fMRI data preprocessing

procedure involves spatial smoothing of the data (using kernel sizes between 2 mm and 8 mm), which is typically applied to increase the signal-to-noise ratio. However, since smoothing allows neighboring voxels to contribute to the estimated signal, it simultaneously increases the likelihood that activity in a certain region is contaminated by signals from surrounding structures (Liu et al. 2017). This issue becomes particularly problematic when measuring the activity of tiny brain nuclei like the LC. However, if smoothing is not applied, outliers may strongly affect any further analyses. Finally, the brainstem is closely located to major arteries and pulsatile cerebrospinal fluid filled spaces, yielding a high proportion of physiological noise (i.e. cardiac and respiratory signals) in brainstem blood oxygen level dependent (BOLD) signals (Liu et al. 2017).

All of these factors make it difficult to reliably capture LC activity using standard neuroimaging techniques. Although special methods have been recently proposed to optimize brainstem fMRI and recover LC signaling (Beissner 2015; Liu et al. 2017), LC activity can instead also be indirectly measured via an organ that frequently has been described as the "window to the soul" by various cultures: our eyes, or in this case, the pupil. As already described earlier in the context of the NA stress response, increased activity of the LC (i.e. sympathetic activity) involves a dilation of the pupil. Modern eye tracking cameras allow for a precise recording of the pupil size (including eye gaze direction) at high sampling frequencies of up to 1000 Hz, providing a comparably inexpensive and easy-to-handle technique to investigate LC functions.

1.4.2 LC activity and pupil size

A direct link between LC activity and pupil size was first reported by Rajkowski et al. (1993), who recorded the firing rate of single LC neurons while simultaneously tracking pupil size in macaque monkeys. Rajkowski et al found that the time course of the pupil size was almost identical to the time course of LC neuron firing rate (Figure 2A), such that pupil size and LC activity were sometimes used interchangeably from then on. Using special techniques such as neuromelanin-optimized imaging (neuromelanin is a dark polymer pigment accumulating inside

LC neurons), this relationship has recently also been replicated to a given extent in humans (Alnaes et al. 2014; Murphy et al. 2014).

The size of the pupil is regulated by the dilator and constrictor muscle of the iris (Figure 2B). The dilator muscle is activated via NA by peripheral neurons located in the superior cervical ganglion, which in turn receive (acetylcholinergic) input from neurons in the intermediolateral cell column (IML) of the spinal cord (sympathetic pathway). The constrictor muscle is activated via acetylcholine (ACh) by peripheral neurons in the ganglion ciliare, which in turn are innervated by neurons of the Edinger-Westphal nucleus (EW) in the brainstem (parasympathetic pathway). The LC is known to have both an excitatory influence on the IML as well as an inhibitory influence on the EW (Samuels and Szabadi 2008), which explains why increased firing of LC neurons causes a dilation of the pupils.

1.4.3 Pupillometric readouts

As described earlier, LC activity can be subdivided into tonic and phasic activity, for which distinct pupil readouts exist. Baseline pupil size provides information about tonic LC activity and therefore has been linked to general arousal and environmental responsiveness: alertness (i.e. high tonic LC activity) typically involves a large (and stable) pupil size, whereas drowsiness (low tonic LC activity) has been linked to increasing fluctuations in pupil size (Figure 2C). These so-called "pupillary fatigue waves" have been claimed to arise from an increasing imbalance between the sympathetic and parasympathetic innervation (Loewenfeld 1993; Warga et al. 2009; Wilhelm et al. 2001) and can be quantified by the "pupillary unrest index" (PUI; Ludtke et al. 1998; Wilhelm et al. 1998). Pupillary fatigue waves are typically measured in complete darkness to avoid the simultaneous occurrence of similar-appearing, light-induced pupil oscillations, which have been associated with feedback mechanisms of the pupillary light reflex pathway (Longtin and Milton 1989; Longtin et al. 1990; Warga et al. 2009) and do not relate to vigilance level (Loewenfeld 1993; Warga et al. 2009).

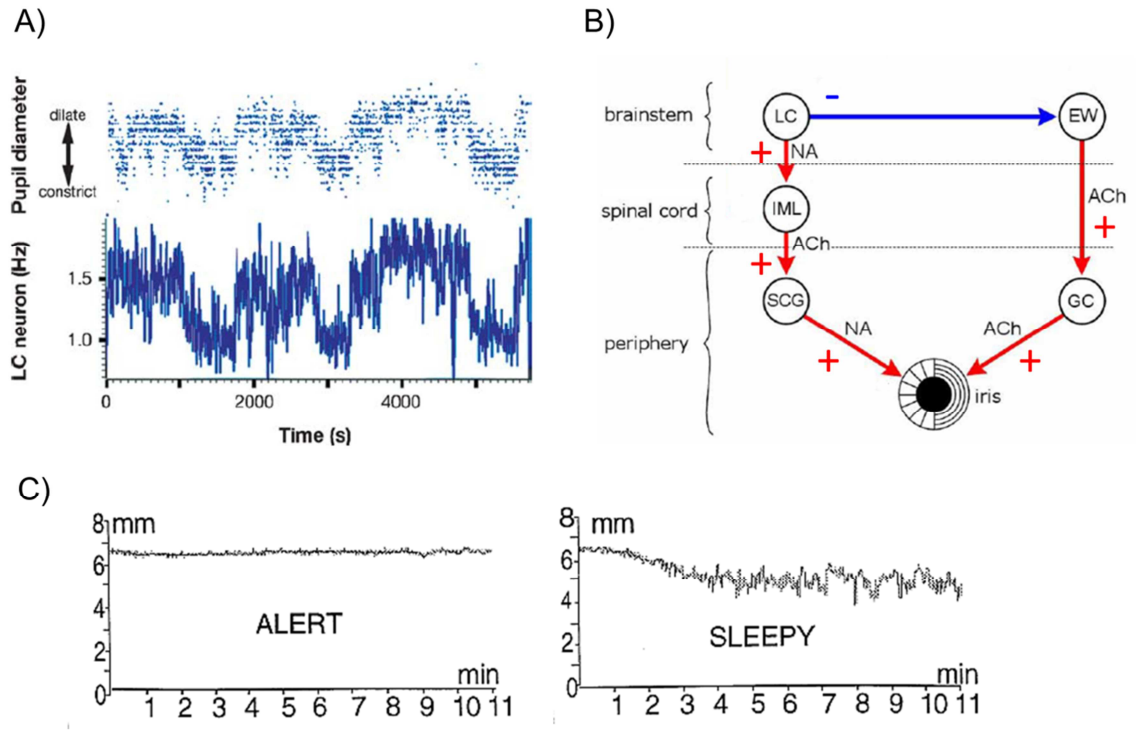

Figure 2. Locus coeruleus (LC) and pupil size. A) Relationship between tonic pupil diameter and baseline firing rate of an LC neuron in the macaque monkey. Pupil size was measured via a remote eye-tracking camera during fixation times of a visual spot within a signal-detection task. Figure reprinted with permission from Aston-Jones and Cohen (2005b). B) Innervation of the pupil dilator (radial; left half of iris) and constrictor muscles (circular; right half of iris). Red: excitatory connections, blue: inhibitory connections. LC: locus coeruleus; EW: Edinger Westphal nucleus; GC: ganglion ciliare; IML: intermediolateral column of spinal cord; SCG: superior cervical ganglion. ACh: acetylcholine; NA: noradrenaline. Figure adapted and reprinted with permission from Szabadi (2012). C) Infrared video-based recordings of pupil size in an alert (left) and sleepy (right) subject, who were instructed to maintain fixation on a group of infrared light-emitting diodes over a period of 11 min. Figure adapted and reprinted with permission from Wilhelm et al. (2001).

Transient pupil dilations in response to specific cues are assumed to reflect phasic LC activation associated with cognitive processes. Such task-related pupil responses typically occur with a delay of up to one second (Wierda et al. 2012) and can be quantified by computing the difference between the (average) pupil size value within a time window of interest and a pre-stimulus

baseline value (Reinhard and Lachnit 2002; Reinhard et al. 2006; Visser et al. 2015; Visser et al. 2013). While luminance-related dilations of the pupil are generally between 2–4 mm, pupil dilations associated with cognitive processes usually do not exceed .5 mm (Beatty and Lucero-Wagoner 2000; Heller et al. 1990; Kang et al. 2014). As described earlier, the LC is known to receive strong afferent projections from the OFC and ACC, which are strongly involved in a variety of cognitive and affective processes. Accordingly, pupil response magnitude has been shown to correlate with numerous concepts associated with OFC and ACC function, such as novelty, uncertainty, prediction error, surprise, attentional orienting, learning, and memory (e.g. Eldar et al. 2013; Koenig et al. 2018; Naber et al. 2013; Nassar et al. 2012; Preuschoff et al. 2011).

1.5 Aims of this thesis

1.5.1 Cortical and subcortical correlates of pupil size

As described in section 1.3, the LC sends widespread projections throughout the brain, and receives input from two cortical regions strongly implicated in various cognitive and affective processes (ACC and OFC). There is increasing evidence that the LC-NA system has a strong influence on cortical processing via the neuromodulatory effects of NA, involving adjustments in neural "gain" in cortical circuits (for review see Aston-Jones and Cohen 2005b). Neural gain has been described as an amplifier of neural communication, making highly active neurons become even more excited while further suppressing less-active neurons, and has been suggested to be upregulated via NA release (Eldar et al. 2013; Mather et al. 2016; Servan-Schreiber et al. 1990). In line with this, LC-mediated arousal has for instance been shown to increase processing of salient stimuli and to decrease processing of non-salient stimuli (Lee et al. 2018; Mather et al. 2016). Taken together, previous findings suggest that LC activity (i.e. arousal) is likely to have a strong impact on global brain activity and connectivity.

Up to now, little is known about which cortical and subcortical brain regions in humans show a strong link to the LC-NA system and arousal. However, MR-compatible eye trackers now allow simultaneous pupil size recordings during fMRI measurements, enabling the identification of BOLD correlates of pupil size fluctuations (as an index of LC activity/arousal). At the start of this thesis, only two research groups had addressed this issue by using such an approach, yielding mixed results: Murphy et al. (2014) found activity in the ACC, right insular cortex, visual cortex and medulla to correlate with pupil size during the resting state (here, subjects simply rest inside the scanner without performing any task) and during performance of an attention task. It is important to note that Murphy et al. additionally included the hemodynamic response function (HRF) derivatives in their analysis, which are typically used to capture neural correlates despite unknown variations in timing and duration of the HRF. Also, they only reported F-contrasts without further specifying the individual correlations (e.g. with respect to directionality). By contrast, Yellin et al. (2015) similarly investigated the BOLD correlates of pupil size during the

resting state and found positively correlated activity in regions of the default mode network (DMN), as well as negatively correlated activity in visual and sensorimotor areas. They suggested that the pupil dilation-related DMN activation and deactivation of visual areas might be related to visual imagery (which some authors have claimed to be typical for the resting state).

1.5.2 Neural correlates of arousal fluctuations during the resting state

To investigate which brain regions are particularly influenced in their activity and connectivity by spontaneous changes in arousal/vigilance during the resting state, the first goal of this thesis was to determine the BOLD correlates of spontaneous pupil fluctuations (beyond LC). The LC is innervated by the dACC, which is strongly involved in performance monitoring and has been suggested to modulate autonomic arousal according to situational requirements (Critchley 2005). In resting state studies, subjects are commonly instructed to keep their eyes open and fixate on a fixation cross. Remarkably, Tagliazucchi and Laufs (2014) revealed that a large portion of subjects tends to fall asleep during resting state. Therefore, the dACC might play an important role in modulating LC activity to maintain task performance (i.e. fixation) and inhibit a transition to sleep (Schneider & Spoormaker, personal communication). This hypothesis would be in line with the first fMRI/pupillometry study by Murphy et al. (2014) which revealed a link between ACC activity and pupil size during the resting state.

Apart from that, it would also be conceivable to find correlated activity in the DMN, as reported by Yellin et al. (2015). However, to us, it seems somewhat counterintuitive that increased DMN activity, which has been linked to daydreaming and mind-wandering (typically occurring in a state of mental relaxation), would actually involve a *dilation* of the pupil (indicating increased arousal). Therefore, we primarily expected to find positively correlated activity in the dACC. Together with bilateral anterior insula, the dACC is part of a classical resting-state network called the “salience network” (SN). Finding a link between pupil size and SN activity would strongly support the use of simultaneous pupillometry to control for arousal-related changes in brain activity/connectivity during the resting state.

1.5.3 Neural correlates of reward anticipation-related arousal

The second goal of this thesis was to examine whether the neural correlates of pupil size fluctuations during the resting state (as an index of spontaneous fluctuations in general arousal) would also extend to task-evoked (positive) emotional arousal. As described earlier, LC neurons exhibit two modes of activity, which are assumed to either facilitate an exploitation of a certain reward opportunity when utility is high (phasic mode), or a search for alternative reward opportunities when utility is low (tonic mode). Moreover, the LC receives cortical input from the OFC and ACC, which have been linked to reward and cost processing, pointing towards an important role of the LC-NA system in reward processing.

Reward processing has been proposed to involve two distinct temporal components, reward anticipation and reward consummation. Discrepancies in the reward anticipation phase have been associated with anhedonia (i.e. diminished interest or pleasure in activities), a key symptom of depression. Reward anticipation is characterized by an increase in autonomic arousal, which can be quantified via pupil size measurements. Rudebeck et al. (2014), for instance, used pupillometry to investigate reward anticipation-related arousal in macaque monkeys. They found that lesioning a specific brain region, the subgenual ACC, strongly reduced reward anticipation-related pupil dilations, concluding that this region appears to be crucial for sustaining elevated arousal in anticipation of rewards (see Figure 3). Interestingly, the authors remarked that the lesions might have involved damage to more dorsal parts of the ACC, and abnormal dACC activity has been linked to deficient reward anticipation in humans (Gorka et al. 2014; Knutson et al. 2008).

Pupillometry might provide an efficient method to objectively assess reward-related arousal in humans. Given previous findings, we expected to observe an (arousal-related) increase in pupil size during reward anticipation. To our knowledge, the neural correlates of pupil dilations during a reward task have not previously been addressed. Based on the recent observations in macaque monkeys by Rudebeck et al. (2014), we hypothesized that reward anticipation would induce pupil dilations in association with increased activity of the dACC.

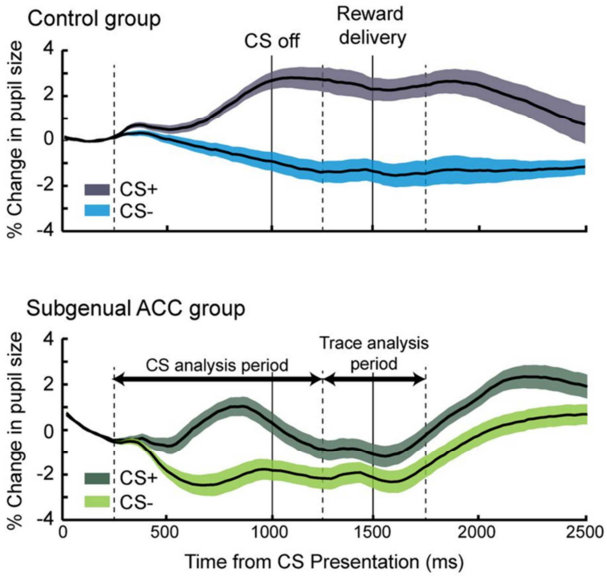

Figure 3. Effect of a (subgenual) ACC lesion on reward anticipation-related arousal, demonstrated by Rudebeck et al. (2014). Pupil responses to a reward predicting stimulus (CS+) and to a control stimulus (CS-) in a control group of macaque monkeys (top) and a group of monkeys with subgenual ACC lesion (bottom). Monkeys with lesions of the subgenual ACC showed initial, cue-evoked pupil dilations, but failed to maintain a large pupil size (i.e. high level of arousal) until the anticipated reward was delivered. Figure reprinted with permission from Rudebeck et al. (2014).

The measurements described in the following were part of a large scale study conducted at the Max Planck Institute of Psychiatry: Biological Classification of Mental Disorders ("BeCOME").

2 Spontaneous pupil dilations during the resting state are associated with activation of the salience network

2.1 Summary

In the first study, we investigated the BOLD correlates of spontaneous pupil size fluctuations in 32 healthy human subjects during the resting state. In order to increase variation in drowsiness and the extent of pupillary fatigue waves, subjects underwent a partial sleep deprivation procedure the night before testing. Furthermore, to assess a potential influence of light-induced pupil oscillations on sleepiness-related pupil fluctuations, two resting state scans of 12 min each were conducted, one with the lights in the scanner room switched on and the other in darkness. Pupil size was recorded with a MR-compatible eye tracker placed at the end of the scanner bore, capturing the subject's left eye via the head coil mirror.

Analysis of the neural correlates of pupil size primarily yielded negatively correlated activity in visual and sensorimotor areas, but no widespread positive correlations. Spontaneous dilations of the pupil were linked to increased activity of the SN, thalamus and frontoparietal regions. Spontaneous pupil constrictions involved increased activity in visual and sensorimotor regions. The pupil-BOLD correlations were very similar across lighting conditions and could be largely replicated in an additional sample of 36 healthy subjects who did not undergo any sleep restriction.

The results of the first study support our hypothesis that the dACC might play an important role in modulating LC activity to maintain task performance (i.e. fixation) and inhibit a transition to sleep. Taken together, simultaneous pupillometry appears an effective way to examine and control for arousal-related changes in brain activity during resting state fMRI.

2.2 Reference

This work was carried out under the supervision of Victor Spoormaker; M.S. and V.S. designed research and wrote the manuscript; M.S., P.H. and V.S. analyzed the data; M.S. and P.H. collected the data; L.L., P.S. and M.C. critically revised the manuscript.

The paper was published in *Neuroimage* under the following reference:

Schneider M, Hathway P, Leuchs L, Samann PG, Czisch M, Spoormaker VI. 2016. Spontaneous pupil dilations during the resting state are associated with activation of the salience network. *Neuroimage*. 139:189-201. DOI: 10.1016/j.neuroimage.2016.06.011

NeuroImage 139 (2016) 189–201

Contents lists available at ScienceDirect

NeuroImage

journal homepage: www.elsevier.com/locate/ynimg

Spontaneous pupil dilations during the resting state are associated with activation of the salience network

Max Schneider, Pamela Hathway, Laura Leuchs, Philipp G. Sämann, Michael Czisch, Victor I. Spoormaker *

Max Planck Institute of Psychiatry, 80804 Munich, Germany

ARTICLE INFO

Article history:
Received 23 December 2015
Revised 19 May 2016
Accepted 8 June 2016
Available online 9 June 2016

Keywords:
Arousal
Eye tracking
Pupillometry
Resting state fMRI
Vigilance

ABSTRACT

Resting state functional magnetic resonance imaging (rs-fMRI) is increasingly applied for the development of functional biomarkers in brain disorders. Recent studies have revealed spontaneous vigilance drifts during the resting state, involving changes in brain activity and connectivity that challenge the validity of uncontrolled rs-fMRI findings. In a combined rs-fMRI/eye tracking study, the pupil size of 32 healthy subjects after 2 h of sleep restriction was recorded as an indirect index for activity of the locus coeruleus, the brainstem's noradrenergic arousal center. The spontaneous occurrence of pupil dilations, but not pupil size per se, was associated with increased activity of the salience network, thalamus and frontoparietal regions. In turn, spontaneous constrictions of the pupil were associated with increased activity in visual and sensorimotor regions. These results were largely replicated in a sample of 36 healthy subjects who did not undergo sleep restriction, although in this sample the correlation between thalamus and pupil dilation fell below whole-brain significance. Our data show that spontaneous pupil fluctuations during rest are indeed associated with brain circuitry involved in tonic alertness and vigilance. Pupillometry is an effective method to control for changes in tonic alertness during rs-fMRI.

Introduction

Over the last decades, resting state functional magnetic resonance imaging (rs-fMRI) has been increasingly applied to identify functional biomarkers for mental disorders and brain pathology. During rs-fMRI, subjects are typically instructed to rest inside the scanner for 5 to 10 min and to think of nothing in particular. Despite promising new insights yielded by this method, experimental control over the subject's actual behavior during the resting state is low. For instance, it is unclear how well subjects manage to keep their eyes open and, if a fixation cross is used, how stable their gaze remains over time. It has been shown that the blood oxygen level dependent (BOLD) signal in occipital regions differs systematically between an eyes-closed and fixation rs-fMRI condition (Bianciardi et al., 2009; Marx et al., 2004). Furthermore, a recent study about rs-fMRI connectivity patterns by Tagliazucchi and Laufs (2014) indicated that a considerable portion of (healthy) subjects falls asleep during typical resting state experiments, involving changes in cortical and subcortical connectivity (Sämann et al., 2010; Spoormaker et al., 2010). Such vigilance-dependent changes may become particularly problematic when comparing rs-fMRI findings between healthy subjects and (psychiatric) patients with hypo- or hyper-arousal symptomatology.

Simultaneous eye gaze tracking and pupillometry allows for better experimental control of such confounds. Previous studies have shown that the fluctuations in the size of the pupil reflect activity of the locus coeruleus (Alnaes et al., 2014; Aston-Jones and Cohen, 2005; Murphy et al., 2014; Rajkowski et al., 1993), a cluster of brainstem nuclei involved in the regulation of vigilance through noradrenergic modulation (Aston-Jones et al., 1991; Berridge and Waterhouse, 2003). The locus coeruleus (LC) is located in the dorsolateral pons and, being part of the ascending reticular activating system (ARAS), has extensive wakefulness-promoting projections throughout the brain (Aston-Jones and Cohen, 2005). It is reciprocally innervated by the orbitofrontal cortex (OFC) and anterior cingulate cortex (ACC), which modulate LC function based on factors like goal-relevance (Aston-Jones and Cohen, 2005), motivational relevance (Mohanty et al., 2008) and conflict between competing responses (Sheth et al., 2012). The LC features both an excitatory connection to the sympathetic innervation pathway of the pupil (originating in the intermediolateral cell column of the spinal cord) and an inhibitory connection to the parasympathetic pathway (originating in the midbrain Edinger-Westphal nucleus; Szabadi, 2013). Consequently, increased LC activity involves increased sympathetic and decreased parasympathetic pupil innervation, causing a relative size increase (referred to as *dilation*) of the pupil (Szabadi, 2012). During low vigilance levels, the mean pupil diameter is reduced (Henson and Emuh, 2010; Ranzijn and Lack, 1997), reflecting low tonic firing rates of LC neurons and a dominant parasympathetic innervation of the pupil. Furthermore, during the transition from

* Corresponding author at: Max Planck Institute of Psychiatry, Department of Translational Research in Psychiatry, Kraepelinstr. 2-10, 80804 Munich, Germany.
E-mail address: spoormaker@psych.mpg.de (V.I. Spoormaker).

http://dx.doi.org/10.1016/j.neuroimage.2016.06.011
1053-8119/

wakefulness to drowsiness, spontaneous fluctuations in pupil size have been reported to increase (Lowenstein et al., 1963; Wilhelm et al., 1998). This behavior of the pupil has been referred to as "pupillary unrest" or "pupillary fatigue waves" and attributed to an imbalance between the sympathetic and parasympathetic innervation (Loewenfeld, 1993; Warga et al., 2009; Wilhelm et al., 2001). The extent of these sleepiness-related pupil fluctuations is quantified by the "pupillary unrest index" (PUI), which has been proposed to indicate the subject's level of vigilance (Ludtke et al., 1998; Wilhelm et al., 1998).

To our knowledge, only two studies have addressed the link between pupil size and the blood oxygen level dependent (BOLD) signal during rs-fMRI: Murphy et al. (2014) included a regressor for pupil size together with the hemodynamic response function (HRF) derivatives in their analysis and reported activity in the ACC, right insular cortex, visual cortex and medulla. These HRF derivatives are typically included to capture the BOLD response despite unknown variations in its timing and duration (Wall et al., 2009). Yellin et al. (2015) found positively correlated activity in regions of the default mode network (DMN), as well as negatively correlated activity in visual and sensorimotor areas. In clinical, non-fMRI studies employing pupillometry, the dynamic increase and decrease in pupil size is frequently analyzed in addition to pupil size alone. For instance, a recent study by Muppidi et al. (2013) provided evidence that several indices from the constriction and dilation phases of the pupillary light reflex can be used to disentangle parasympathetic and sympathetic pupil function, enabling a distinction between patients with autonomic dysfunction and healthy controls.

The aim of this study was therefore to investigate the neural correlates of pupil size and of *changes* in pupil size observed during spontaneous pupil fluctuations in resting healthy subjects. Simultaneous electroencephalography (EEG)/fMRI studies focusing on vigilance fluctuations have observed activity decreases in thalamus with increasing drowsiness (Olbrich et al., 2009; Sadaghiani and D'Esposito, 2015; Sadaghiani et al., 2010), short duration sleep periods referred to as micro-sleeps (Poudel et al., 2014), and light sleep stage 1 (Kaufmann et al., 2006). Moreover, neural correlates of EEG-defined tonic alertness extend to dorsal ACC (dACC) and anterior insula (Sadaghiani and D'Esposito, 2015; Sadaghiani et al., 2010). Activity increase associated with increasing drowsiness is typically reported for visual and sensorimotor areas (Olbrich et al., 2009; Sadaghiani et al., 2010), regions that also have a negative correlation with eye closure (Marx et al., 2003; Ong et al., 2015; Poudel et al., 2010) and pupil size (Yellin et al., 2015). We therefore hypothesized that activity in thalamus, dACC and anterior insula (salience network) is positively associated with pupil size and/or change (spontaneous dilations), whereas activity in visual and sensorimotor regions will be negatively correlated to pupil size and/or change (spontaneous constrictions). Finding such tonic alertness correlates would support the notion that pupillometry is an alertness/arousal marker with a less complicated setup (and data post-processing) than simultaneous EEG/fMRI, a higher sensitivity than manual scoring of eye closures, and an established link to a well-defined neurobiological system (Aston-Jones and Cohen, 2005).

Additionally, given the evidence for vigilance-dependent changes in DMN connectivity (Ong et al., 2015; Sämann et al., 2010) and the proposed link between pupil size and DMN activity (Yellin et al., 2015), we further expected pupil size to have an influence on functional connectivity within the DMN. Furthermore, previous studies have shown that thalamo-cortical connectivity undergoes widespread decreases during the transition from wakefulness to light sleep (Spoormaker et al., 2010; Tagliazucchi et al., 2013). Hence, we aimed to examine whether such changes in functional connectivity can already be observed when subjects become drowsy, as indicated by a reduction in mean pupil size and the occurrence of sleepiness-related fluctuations. To increase variation in drowsiness and fluctuations in pupil size, a mild sleep restriction procedure was employed. Finally, we applied the same pupil/fMRI analyses to a replication sample of 36 healthy subjects (who did not undergo sleep restriction).

Materials and methods

Subjects

The study protocol was in line with the Declaration of Helsinki and was approved by a local ethical review committee. Subjects provided their written informed consent after the study protocol had been fully explained, and were reimbursed for their participation. Thirty-two non-smoking, right-handed participants (mean age: 25.9 ± 4.1 years, range: 18–35 years, 17 female) underwent a general medical interview and clinical MRI to exclude present and past neurological, psychiatric, and sleep disorders. Additional exclusion criteria were regular intake of medication (except contraceptives), a change of time zone or night shift work in the last four weeks, current pregnancy, and generally acknowledged contraindications to MRI. During the MR sessions, short-sighted subjects with less than −3.0 diopters wore contact lenses to ensure normal vision.

Subjects were asked to refrain from caffeine consumption on the day of the experiment and to get up 2 h earlier than they would on a regular weekday. The aim of this mild sleep restriction procedure was to increase the variance of drowsiness levels among subjects. To assure an intact circadian rhythm, participants filled out a sleep diary for at least four nights before the MR session. The sleep diary assessed, among others, bed time, time of falling asleep, wake-up time and total sleep time. For each subject, sleep diary parameters (bed time, time of falling asleep and sleep duration) were averaged across the nights preceding the sleep restriction night and compared to the corresponding parameters for the sleep restriction night using paired *t*-tests.

Procedure

All subjects completed two resting state scans of 12 min each during which they were instructed to think of nothing in particular, to maintain their gaze on a red fixation dot presented on a black background, and to not fall asleep. If subjects had their eyes continuously closed over a period of more than 1 min without reacting to verbal instructions ("Please keep your eyes open"), the session was aborted. Sessions which required such verbal interventions were later excluded from analysis.

Pupil fluctuations as a marker of vigilance level are usually measured in total darkness in order to avoid the simultaneous occurrence of similar-appearing, so-called *light-induced* pupil oscillations (Loewenfeld, 1993; Warga et al., 2009) which do not relate to vigilance level. This type of pupil fluctuation can be observed at constant light intensities and has been associated with feedback mechanisms of the pupillary light reflex pathway (Longtin and Milton, 1989; Longtin et al., 1990; Warga et al., 2009). Since recordings in total darkness might not always be feasible in the MRI environment, we used two rs-fMRI sessions that differed only in their illumination settings to assess the potential influence of light-induced fluctuations on sleepiness-related ones: one run was conducted in darkness with lights in the scanner room and inside the scanner switched off ("dark condition"), while the other was conducted in an illuminated scanner environment, that is, lights in the scanner room and inside the scanner were switched on ("light condition"). The order of illumination condition was counterbalanced across subjects and established at least three to 4 min before the start of each run to ensure accommodation of the pupil. The fixation dot was presented with Presentation Software (version 16.3, Build 12.20.12, Neurobehavioral Systems Inc., Berkeley, California, USA) using a projector outside the MRI scanning room that displayed the stimuli onto a translucent screen located at the end of the scanner bore. Participants viewed the fixation dot through a first-surface reflecting mirror attached to the head coil. The color and luminance of the fixation dot were chosen in a way that subjects were able to see it clearly in both lighting conditions.

MR sessions were conducted during the afternoon. Participants were asked to rate their sleepiness level on the Karolinska Sleepiness Scale

(KSS; Akerstedt and Gillberg, 1990) before the start of the first run, between runs and after the second run. The KSS is sensitive to variation in drowsiness (Barbato et al., 2007; Curcio et al., 2001) and correlates with EEG and behavioral sleepiness parameters (Shahid et al., 2010). It consists of nine items describing various levels of wakefulness/sleepiness of which the participant chooses the one closest to their momentary condition. In order to assess whether subjects felt more or less drowsy after the rs-fMRI runs, the difference score (KSS after run minus KSS before run) was computed for each subject (with positive values reflecting an increase in subjective drowsiness) and averaged across subjects for the two lighting conditions. In addition, we computed a paired *t*-test in subjects who met analysis criteria for both conditions to assess whether the KSS difference score differed between the two lighting conditions.

Eye tracking

For pupil size recordings, an MR-compatible eye tracker (EyeLink 1000 Plus; SR Research, Osgoode, ON, Canada) was placed at the end of the scanner bore and below the presentation screen, such that the subject's left eye could be tracked via the head coil mirror. Pupil diameter was recorded in arbitrary units (as measured by the eye tracker) at a sampling rate of 250 Hz. Eye blinks are automatically detected by the EyeLink software, and blink-induced artifacts were corrected by interpolating values for the period from 100 ms before blink onset to 400 ms after blink offset (due to a tendency for light reflex-related artifacts within this range). Blinks that occurred shortly after each other (<100 ms) were combined and treated as one single blink. After this automated correction procedure, the data were visually inspected to make sure that all major artifacts had been successfully removed. No further manual corrections had to be applied.

Four runs had to be excluded due to technical problems (i.e. instable corneal reflection signal) and two because runs were aborted after subjects fell asleep. In addition, the following exclusion criteria were applied for further analyses: i) >15% blink/eye closure-related missing pupil data per run, ii) more than one eye closure longer than 5 s, and/or iii) eye closure(s) longer than 10 s per run. Compared to typical eye tracking studies, the rather high threshold of 15% was chosen to account for the low arousal levels of our participants caused by sleep restriction, which increases blink rate (Barbato et al., 2007) and thereby increases the amount of missing data (Regen et al., 2013). In total, this lead to the exclusion of 8 runs in the dark condition and 11 runs in the light condition, leaving 24 runs in the dark condition and 21 runs in the light condition for further analyses (see Supplementary Tables S1 and S2 for an overview of prolonged eye closures and proportion of blink/eye closure-related missing pupil data in individual subjects). To ensure that we did not miss effects of interest due to this exclusion, we re-ran the main analyses with all subjects included.

In order to account for the slow response time of the pupil to both luminance change and attentional events (Wierda et al., 2012; Yellin et al., 2015), the pupil time course was shifted forward 1 s (250 data points) before using it as regressor in the fMRI analyses. Since the power spectra of pupil and BOLD signal fluctuations, as well as their cross-spectrum, are dominated by frequencies between 0.01 and 0.1 Hz (Yellin et al., 2015), a Butterworth band-pass filter (0.01–0.1 Hz) was applied to correct for very slow drifts and high-frequency oscillations. We also performed a spectral analysis of the unfiltered, blink-interpolated pupil size data for both conditions (and the replication sample). Here, the entire run of 12 min was divided into eight segments of 90 s in line with previous work (Wilhelm et al., 1998). Next, a Fast Fourier Transform was applied to each time segment, and the mean power spectral density was computed across subjects for each condition. The spectral analysis (as well as the preprocessing of the pupil size data) was implemented in Matlab (version 2015a, MathWorks, Natick, USA).

After band-pass filtering of the pupil data, we computed the first order derivative of the pupil size vector ("pupil change"), which describes the slope of changes in pupil size, with positive values reflecting phases of pupil dilation and negative values reflecting phases of pupil constriction. To adjust the pupil time courses to the repetition time (TR; here: 2.56 s) of the fMRI, the pupil size and pupil change vectors were down-sampled by calculating the mean of each 640 consecutive data points (2.56 s), resulting in pupil time courses with 286 elements (corresponding to 12 min), equal to the number of volumes used for fMRI data analysis. These were later convolved with the canonical HRF (as well as the temporal and dispersion derivative functions of the informed basis set provided by SPM8, see section fMRI) and entered into a general linear model (GLM).

Additional physiological parameters were determined for each subject: i) the average pupil diameter per run, ii) the proportion of blink/eye closure-related missing pupil data per volume and per run, iii) average blink duration per run, iv) number of eye closures longer than 1 s, as well as v) the so-called pupillary unrest index (PUI). The proportion of blink/eye closure-related missing data over the whole run was determined by summing the data points during which pupil size equalled zero (detected blink), divided by the total number of data points per run. The proportion of missing data per *volume* was determined in an analogous manner for time windows of 2.56 s and, after convolution with the canonical HRF, used as a regressor in a GLM.

The PUI is defined as "cumulative changes in pupil size based on mean values of consecutive data sequences" (Ludtke et al., 1998). Calculation of the PUI was adapted from Ludtke et al. (1998): first, the pupil size data was low-pass filtered by calculating the mean of 160 consecutive data points (0.64 s). Next, the differences between four neighboring means were calculated and their absolute values were summed up, yielding one PUI value per fMRI volume which was convolved with the canonical HRF and used in a separate GLM. This procedure was also applied to the entire time course, and the resulting segment values were then again summed up to obtain a single, total PUI value for each run of every subject. In order to test for differences in the above mentioned physiological parameters between the two lighting conditions, paired *t*-tests or nonparametric alternatives such as the Wilcoxon signed ranks test (if the data showed a non-Gaussian distribution based on Kolmogorov-Smirnoff tests for normality) were applied in subjects who fulfilled the inclusion criteria for both runs (N = 19).

fMRI

Participants were scanned in a 3T MRI Scanner (MR750, GE, Milwaukee, USA) using a 32-channel head coil, covering 40 slices (AC-PC-orientation, 96 × 96 matrix, 2 × 2 mm^2 voxel size, 2.5 mm slice thickness, 0.5 mm slice gap, echo planar imaging [EPI], TR 2.56 s, TE 30 ms, acceleration factor 2). Two-hundred-ninety volumes were recorded per run, of which the first four volumes (i.e. 10.24 s) were discarded due to T1 non-equilibrium effects, leaving 286 volumes for analysis.

FMRI data preprocessing and analysis was performed using Matlab (version 2015a, MathWorks, Natick, USA) and SPM8 (Statistical Parametric Mapping Software, Wellcome Department of Imaging Neuroscience, London, UK, http://www.fil.ion.ucl.ac.uk/SPM). Preprocessing steps included slice time correction, realignment to the mean volume (rigid body transformation), spatial normalization to the Montreal Neurological Institute (MNI) EPI template, resampling to a voxel resolution of 2 × 2 × 2 mm^3, and 3D smoothing using an isotropic Gaussian Kernel (full width at half maximum: 6 × 6 × 6 mm^3) for use in the first level GLMs. In addition, the slice time corrected and realigned data were normalized to a 4 × 4 × 4 mm^3 resolution, and masks for cerebrospinal fluid (CSF) and white matter (WM) as defined in SPM8 were used to extract voxel-wise WM and CSF signal time courses. Next, a principal component analysis was applied to these signal time courses from the lower resolution images to identify the first three principal components of both compartments (explaining 39.1–66.0% of the variance in the

data) for later use as nuisance regressors (CompCor correction; Behzadi et al., 2007). In order to account for signal changes caused by movement of the subject, six movement parameters were extracted from the rigid body realignment step. Runs with head movements larger than 2 mm between successive volumes were excluded. In order to assess whether the extent of movement differed between the two conditions, the following steps were performed: first, the absolute values of the between-volume differentials for the three translation and three rotation parameters (see Power et al., 2012) were summed across volumes, resulting in one total translation value and one total rotation value per run. After dividing these scores by the number of volumes, a paired *t*-test was applied to test for differences between the lighting conditions for the translation and rotation scores, respectively. To minimize motion-related artifacts, we additionally applied motion scrubbing using FSL (version 4.1, fsl_motion_outliers tool, http://www.fmri.ox.ac.uk), which yields a matrix with separate columns for each volume that contains a motion outlier.

The three WM regressors, three CSF regressors, six motion regressors, the absolute first order derivatives of these 12 regressors, as well as the confound matrix from the motion scrubbing step were included as nuisance regressors in all further GLM analyses. These nuisance regressors were also used in a separate first level GLM to obtain residual images (error term of the GLM). From these residual images, mean time courses of all voxels within a few selected seed regions were extracted, including bilateral thalamus and posterior cingulate cortex (PCC), the posterior midline hub of the DMN. The thalamus and PCC seeds were selected based on the Automated Anatomical Labeling (AAL) atlas by Tzourio-Mazoyer et al. (2002), in line with previous work of ourselves and others (e.g. Horovitz et al., 2009). As the left and right thalamus time-series and the left and right PCC time-series were highly correlated (mean correlation coefficient of thalamus = 0.73, mean correlation coefficient of PCC = 0.83), we report the analyses for the time-series of the left regions only. After band-pass filtering (0.01–0.1 Hz), these seed time courses were entered into separate GLMs performed on the residual images, yielding voxel-wise first level beta estimates.

Three separate first level analyses (high-pass filter cutoff: 250 s) were carried out, in which i) the pupil size regressor, ii) the pupil change regressor, iii) and the volume-wise PUI were entered. For the pupil size and pupil change model, the volume-wise proportion of blink/eye closure-related missing data was included as a first parametric modulation to a regressor consisting of volume times only (which was later removed from the model). The pupil size or pupil change regressor was then added as a second parametric modulation to this blink/eye closure regressor. This ensured an automatic orthogonalization of the second to the first parametric modulation, providing control for the potentially confounding effect of blinks/eye closures on the pupil size or change data.

In each GLM, we additionally included the temporal and dispersion derivatives of the canonical HRF. The temporal derivative allows the timing of the HRF peak response to vary, and the dispersion derivative allows the width of the HRF response to vary (Ashburner et al., 2014). We included these two derivatives to account for potentially different BOLD response characteristics of subcortical regions (Handwerker et al., 2004; Wall et al., 2009) and to achieve a better comparability with the findings observed by Murphy et al. (2014), who used a similar approach.

Simple *t*-tests against zero on the first level contrasts were performed for statistical inference on the group level. Clusters were sampled at uncorrected $p = 0.001$. Subsequently, a cluster-based multiple test correction procedure was performed, with significance defined as cluster p-values < 0.05 after correction for family-wise error (FWE). For the pupil size or pupil change plus temporal and dispersion derivatives models, full-factorial analyses of variance (ANOVA) were additionally performed. In order to address potential effects of pupil-based vigilance measures on pupil size, pupil change and the functional connectivity analyses (thalamus and PCC seeds), the total PUI score and average pupil diameter per run were entered as covariates in second level analyses. Moreover, separate psychophysiological interaction (PPI) analyses with thalamus and PCC as a seed region and volume-wise PUI, pupil size and pupil change as experimental vector were performed to examine potential interaction effects. Finally, to test for differences between the light and dark conditions, we conducted second level paired *t*-tests in those subjects who met analysis criteria in both runs ($N = 19$).

Replication sample

We additionally applied the same preprocessing and analysis steps as described above to the fMRI and pupil size data from a group of 36 healthy subjects (mean age: 25.0 ± 3.2 years, range: 19–33 years, 17 female), which was collected in a second study without any sleep restriction (referred to as "replication sample"). This study involved a 7.5-minute rs-fMRI/eye tracking session with identical instructions and luminance settings as in the light condition of the original sample (including the same red fixation dot). Participants were scanned in the same 3T scanner (with the same 32-channel head coil), using a multi-echo sequence with three echo times. For the replication analysis, we focused on the second echo time (TE 28.7–28.9 ms,[1] 36 slices, AC-PC-orientation, 64×64 matrix, 2×2 mm^2 voxel size, 3.0 mm slice thickness, 0.4 mm slice gap, TR 2.56 s, acceleration factor 2). One-hundred-eighty-four volumes were recorded per run, of which the first four volumes (i.e. 10.24 s) were discarded due to T1 non-equilibrium effects, leaving 180 volumes for analysis. Except for one individual, all subjects in the replication sample met analysis criteria ($N = 35$).

For spectral analysis of the pupil fluctuations, the 7.5-minute rs-fMRI run was divided into five segments of 90 s and analyzed as described above. To achieve a better comparability, the pupil size and pupil change first level analyses of the light condition in the original sample (referred to as "original sample") were repeated with the first 7.5 min of the 12-minute rs-fMRI recording only (in order to exclude potential differences due to a longer recording session). The first level contrast images were evaluated in the same manner as described before. Moreover, we conducted an independent samples *t*-test together with the corresponding contrast images from the replication sample. This test yielded two contrasts, showing which pupil-BOLD correlations were more pronounced in the light condition of the original sample compared to the (light condition of the) replication sample, and vice versa.

Due to the different durations of the resting state sessions in the original samples (~12 min, 286 volumes) and the replication sample (~7.5 min, 180 volumes), we computed a relative PUI score for both lighting conditions and the replication sample by dividing the total PUI score per run by the number of volumes. An independent samples *t*-test was conducted to test for differences in relative PUI scores between the two conditions. It should be noted that the KSS questionnaire was not applied in the replication sample. Therefore, all analyses including the KSS could only be applied to the light and dark conditions of the original sample.

Results

Self-report measures

In line with the sleep restriction protocol, subjects reported less sleep in the sleep restriction night compared to the preceding nights (mean sleep duration during sleep restriction night: 6 h 7.5 min; preceding nights: 7 h 49.1 min; $t_{(33)} = 10.29$, $p < 0.001$). Average bed time did not differ between the sleep restriction night (average bed time: 0:52 A.M.) and the preceding nights (average bed time:

[1] The echo times varied slightly due to slice orientation, with a standard deviation of 0.13 ms for this second echo time.

0:31 A.M.; $t_{(32)} = 1.63$, $p = 0.11$). Interestingly, subjects reported to fall asleep comparably later ($t_{(32)} = 2.15$, $p < 0.05$) on the sleep restriction night than the preceding nights (average time of falling asleep during sleep restriction night: 1:06 A.M.; preceding nights: 0:33 A.M.).

There was a significant difference in the KSS-score assessed before the start of the run and at the end of the run in both lighting conditions (dark: $t_{(29)} = -2.89$, $p < 0.05$; light: $t_{(30)} = -5.34$, $p < 0.001$), with higher sleepiness-scores after each run was over. No significant differences were present between lighting conditions, although subjects tended to show a slightly higher difference score in the light condition ($t_{(16)} = 1.74$, $p = 0.10$; see Supplementary Fig. S1).

Pupil data

The total PUI scores did not differ significantly between lighting conditions (dark: mean of relative PUI = 787.12, standard deviation [SD] = 303.67; light: mean of relative PUI = 861.59 (SD = 267.03), $t_{(18)} = 1.37$, $p = 0.19$). The average pupil size was significantly smaller in the light condition compared to the dark condition ($t_{(18)} = 4.46$, $p < 0.001$). Neither average blink duration nor the proportion of blink/eye closure-related missing data per run differed significantly between the lighting conditions (dark: mean blink duration = 223.2 ms (SD = 136.6 ms); light: mean blink duration = 194.3 ms (SD = 79.6 ms); Wilcoxon signed ranks test: $Z = -0.72$, $p = 0.47$; dark: mean proportion of missing data = 0.06; light: mean proportion of missing data = 0.05; Wilcoxon signed ranks test: $Z = -0.24$, $p = 0.81$). Furthermore, there was no significant difference in the number of eye closures > 1 s between the two lighting conditions (Wilcoxon signed ranks test: $Z = -0.11$, $p = 0.26$).

Supplementary Fig. S1 shows the relative PUI, average pupil size and proportion of missing data per run across lighting conditions for *all* subjects (including subjects that did not fulfill the inclusion criteria for data analysis). Supplementary Fig. S2 provides an overview of the spectral characteristics of pupil fluctuations (in line with previous work; Yellin et al., 2015).

Neural correlates of pupil size

Comparison of the fMRI motion parameters revealed no differences between lighting conditions (paired *t*-test: translation parameters: $t_{(18)} = 0.63$, $p = 0.54$; rotation parameters: $t_{(18)} = 0.48$, $p = 0.64$). In both lighting conditions, positive correlations between the BOLD signal and pupil size were observed in thalamus, caudate nucleus and cerebellum (Fig. 1A and B, Table 1 and Table 2). Negatively correlated activity located to the visual cortex and sensorimotor areas, as well as to the precuneus, cuneus, posterior insula, and superior temporal gyri. In the light condition, we additionally observed negative correlations in the amygdala and parahippocampal gyrus. To ensure that we did not miss clusters positively correlated with pupil size, we shifted the pupil size vector forward and backward by 1 s in both conditions. This yielded highly similar maps with the same clusters. The paired t-test did not reveal any significant differences between the two lighting conditions. Re-running the analyses with all subjects included yielded highly similar, albeit more robust activity patterns (see Supplementary Fig. S3).

Analysis of the temporal and dispersion derivative regressor revealed additional correlations in multiple brain regions across lighting conditions: dACC, anterior insula, prefrontal and parietal regions, and thalamus showed a positive correlation to the temporal derivative and a negative correlation to the dispersion derivative (see Supplementary Fig. S4 and Supplementary Table S4). At the same time, most of these regions did not have a significant correlation to the canonical HRF of the pupil size regressor. Visual and sensorimotor regions showed opposite correlations with the temporal and dispersion derivatives (Supplementary Fig. S4, Supplementary Table S4).

Neural correlates of pupil change

Analysis of the first order derivative of the pupil size time course (pupil change) revealed a whole network of regions with positively correlated BOLD activity in both lighting conditions, including ACC, thalamus, bilateral anterior insula, frontal regions (superior, middle, medial, inferior frontal gyri), inferior parietal lobules, precuneus, superior and middle temporal regions, caudate nucleus, cerebellum and brainstem (Fig. 2A and B, Table 3 and Table 4). Again, anti-correlated activity was found in visual and sensorimotor regions. For the light condition, we additionally observed negatively correlated activity in a cluster comprising amygdala, hippocampus and parahippocampal gyrus. The paired *t*-test revealed no significant differences between the two lighting conditions. Re-running the analyses with all subjects included again revealed very similar and more robust activity patterns (see Supplementary Fig. S5).

The analyses of the temporal derivative of the pupil change regressor (i.e., reflecting change points in pupil size) consistently revealed positive correlations primarily in the bilateral thalamus (Fig. 3A and B, Table 5 and Table 6). Negatively correlated activity was observed in visual and sensorimotor regions. Rerunning these analyses with all subjects included showed the same clusters of activity (Supplementary Fig. S6). No significant differences were observed between the dark and light condition for this pupil change point regressor.

Additional analyses: volume-wise PUI, covariates and PPI analyses

For the volume-wise PUI regressor, there was no consistently correlated activity in both lighting conditions. In the dark condition, positively correlated activity was observed in cuneus, superior occipital and calcarine gyrus, and in the light condition in cuneus (non-overlapping with the cuneus cluster in the dark condition) and precuneus. No negative correlations were observed in any of the two lighting conditions.

The total PUI and average pupil size over the whole run were entered as covariates on the second level for the pupil size, pupil change and the seed analyses of thalamus and PCC; there were no consistent correlations across lighting conditions for any of the covariates. (For an overview of observed clusters in the contrasts, please see Supplementary Tables S5–6).

The same applied to the PPI analyses of the thalamus or PCC with volume-wise PUI, pupil size or pupil change; also here no consistent correlations were observed across conditions (For an overview of observed clusters in the contrasts, please see Supplementary Tables S8–9).

Replication sample

Comparison of the fMRI motion parameters between the dark condition and the replication sample (rep. sam.) revealed a significant difference for the rotation parameters ($t_{(57)} = 2.21$, $p < 0.05$) and a trend for difference for the translation parameters ($t_{(57)} = 2.00$, $p = 0.051$). In the light condition, both translation and rotation values were significantly higher compared to the replication sample (rotation: $t_{(54)} = 2.21$, $p < 0.05$; translation: $t_{(54)} = 2.21$, $p < 0.05$), indicating that the sleep-restricted subjects in the original sample tended to show a comparably higher amount of head movements. Comparison of the relative PUI scores revealed a significantly smaller PUI score in the replication sample compared to both conditions of the original sample (dark vs rep. sam.: $t_{(56)} = 10.98$, $p < 0.001$; light vs. rep. sam.: $t_{(55)} = 13.93$, $p < 0.001$). Furthermore, average pupil size was significantly smaller in the replication sample compared to both lighting conditions (dark vs rep. sam.: $t_{(56)} = 5.02$, $p < 0.001$; light vs rep. sam.: $t_{(55)} = 3.20$, $p < 0.01$). Comparisons of the proportion of blink/eye closure-related missing data and average blink duration per run between original and replication sample did not yield any significant differences (Mann-Whitney *U* tests:

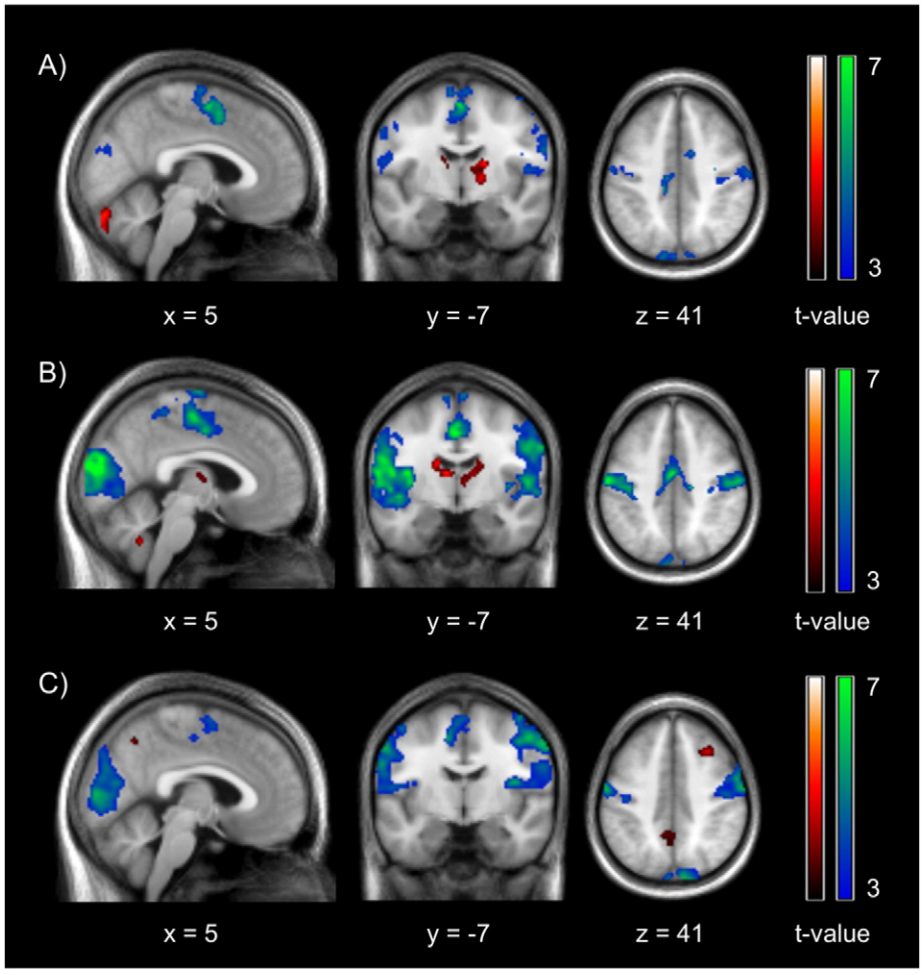

Fig. 1. Neural correlates of pupil *size* in the dark condition (A), light condition (B) and the replication sample (C). The positive contrast (hot colors) reflects regions with BOLD activity that is positively correlated to the pupil size time course, i.e. brain areas that are more active when pupil size is large and less active when pupil size is small during the resting state. The negative contrast (cool colors) reflects the reverse pattern. Both positive and negative statistical maps were sampled at uncorrected $p < 0.001$ and clusters were thresholded at a cluster-wise $p_{FWE} < 0.05$ (cluster extension threshold set to $k = 90$). [x y z] coordinates refer to the MNI coordinates of the respective slices. See Table 1, Table 2 & Supplementary Table S11 for further information on cluster extents and peak voxel coordinates.

proportion of missing data dark vs. rep. sam.: $Z = 0.52$, $p = 0.60$; proportion of missing data light vs. rep. sam.: $Z = 0.95$, $p = 0.34$; blink duration dark vs. rep. sam.: $Z = 1.06$, $p = 0.29$; blink duration light vs. rep. sam.: $Z = 0.46$, $p = 0.65$). Subjects in the replication sample showed a significantly smaller number of eye closures longer than 1 s compared to both conditions of the original sample (Mann-Whitney *U* tests: dark vs. rep. sam.: $Z = -3.39$, $p < 0.05$; light vs. rep. sam.: $Z = -2.90$, $p < 0.05$). For an overview over PUI, average pupil

Table 1
Regions correlated to pupil *size* in the dark condition.

	Cluster		Voxel			
	p_{corr}	k	t_{peak}	x	y	z
Positive						
Cerebellum crus I (R), cerebellum crus II (R), cerebellum crus I (L), cerebellum crus II (L)	<0.001	1279	6.86	20	−82	−38
Caudate nucleus (L), thalamus (L)	0.003	174	5.56	−10	−4	20
Thalamus (R), caudate nucleus (R)	0.014	133	5.08	18	−8	14
Negative						
Supplementary motor area (L), supplementary motor area (R), middle cingulate gyrus (L), precuneus (L)	<0.001	1245	6.79	0	−6	58
Postcentral gyrus (R), Rolandic operculum (R), precentral gyrus (R), insula (R)	<0.001	1287	6.48	18	−14	40
Superior occipital gyrus (L), cuneus (L), calcarine gyrus (L), inferior occipital gyrus (L), middle occipital gyrus (L)	<0.001	1299	6.01	−12	−84	30
Lingual gyrus (R), calcarine gyrus (R), cuneus (R)	<0.001	313	5.86	22	−80	0
Superior temporal gyrus (L), superior temporal pole (L), Rolandic operculum (L), insula (L)	<0.001	268	5.82	−50	4	−4
Postcentral gyrus (R), precentral gyrus (L)	<0.001	1157	5.72	−54	−14	24
Lingual gyrus (L), fusiform gyrus (L), cerebellum (L)	<0.001	472	5.35	−22	−58	−12
Cuneus (R), superior occipital gyrus (R)	<0.001	249	5.20	20	−74	26
Inferior occipital gyrus (R), inferior temporal gyrus (R), fusiform gyrus (R)	<0.001	241	5.03	34	−80	−14

Note: Table refers to Fig. 1A. Reported clusters survived cluster-wise family-wise error correction for multiple comparisons ($p_{FWE} < 0.05$) at a cluster extension threshold of $k = 90$. Only contributions from regions above $5\%_{cluster}$ are listed. R = right; L = left; p_{corr} stands for whole brain corrected cluster p-values, k for the cluster size, t_{peak} for the t-value of the peak-voxel, [x y z] coordinates are in MNI-space.

Table 2
Regions correlated to pupil *size* in the light condition.

	Cluster		Voxel			
	p_{corr}	k	t_{peak}	x	y	z
Positive						
Caudate nucleus (R), thalamus (R), caudate nucleus (L), putamen (L)	<0.001	634	7.76	−22	6	8
Cerebellum crus I (L), cerebellum (L), cerebellum crus II (L)	<0.001	794	7.51	−34	−50	−34
Cerebellum (L), cerebellar vermis, cerebellum (R)	0.015	138	6.34	−2	−54	−38
Cerebellum crus I (R), cerebellum (R), cerebellum crus II (R)	<0.001	764	5.83	34	−50	−34
Negative						
Calcarine gyrus (L), lingual gyrus (R), calcarine gyrus (R), cuneus (L), lingual gyrus (L), superior occipital gyrus (L), cuneus (R)	<0.001	7775	9.27	4	−90	16
Postcentral (L), superior temporal gyrus (L), insula (L), Rolandic operculum (L), supplementary motor area (R)	<0.001	7781	7.84	−36	−12	16
Postcentral gyrus (R), precentral gyrus (R), superior temporal gyrus (R), Rolandic operculum (R), insula (R)	<0.001	4490	7.28	38	−18	14
Precuneus (R), paracentral lobule (R)	0.002	203	6.44	10	−44	56
Superior temporal pole (R), parahippocampal gyrus (R), amygdala (R), middle temporal pole (R)	0.014	140	6.00	34	6	−26
Superior temporal pole (L), middle temporal pole (L), parahippocampal gyrus (L)	0.005	169	5.85	−26	6	−30

Note: Table refers to Fig. 1B. Reported clusters survived cluster-wise family-wise error correction for multiple comparisons ($p_{FWE} < 0.05$) at a cluster extension threshold of k = 90. Only contributions from regions above $5\%_{cluster}$ are listed. R = right; L = left; p_{corr} stands for whole brain corrected cluster p-values, k for the cluster size, t_{peak} for the t-value of the peak-voxel, [x y z] coordinates are in MNI-space.

size and proportion of missing data across conditions and groups, see Supplementary Fig. S1.

The pattern of pupil-BOLD correlations observed in the replication sample was very similar to the one observed in the original sample: for the pupil *size* regressor, negative correlations were again found in visual and sensorimotor areas, as well as posterior insula and middle cingulate gyrus (Fig. 1C, Supplementary Table S11). The positive contrast revealed a slightly different pattern compared to the original sample,

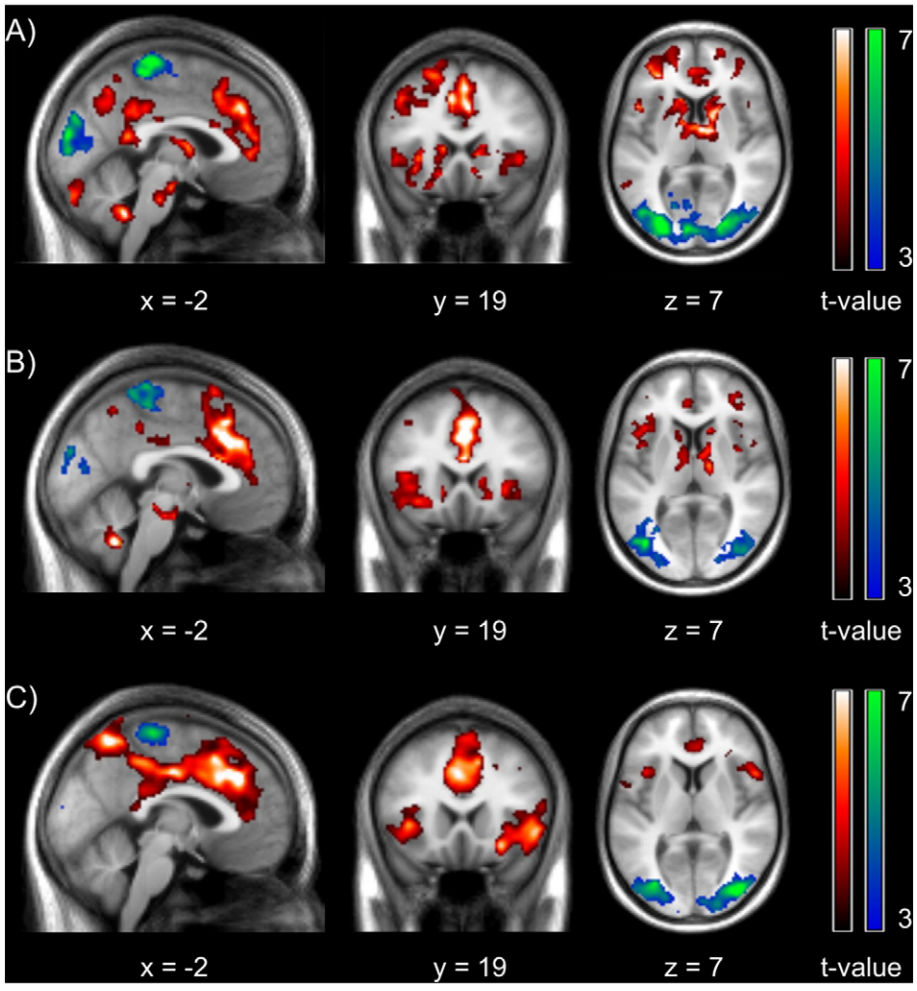

Fig. 2. Neural correlates of pupil change in the dark condition (A), light condition (B) and the replication sample (C). The positive contrast (hot colors) reflects regions with BOLD activity that is positively correlated to the pupil change time course (first order derivative of pupil size vector), i.e. brain areas that become more active during spontaneous pupil dilations and less active during pupil constrictions (resting state). The negative contrast (cool colors) reflects the reverse pattern. All maps were sampled at uncorrected $p < 0.001$ and clusters were thresholded at a cluster-wise $p_{FWE} < 0.05$ (cluster extension threshold set to k = 110). [x y z] coordinates refer to the MNI coordinates of the respective slices. See Table 3, Table 4 & Supplementary Table S12 for further information on cluster extents and peak voxel coordinates.

Table 3
Regions correlated to pupil *change* in the dark condition.

	Cluster		Voxel			
	p_{corr}	k	t_{peak}	x	y	z
Positive						
Caudate nucleus (R), inferior frontal gyrus, pars orbitalis (L), caudate nucleus (L), thalamus (R), putamen (L), brainstem[a]	<0.001	3462	10.66	16	4	12
Middle frontal gyrus (L), superior frontal gyrus (L), medial frontal gyrus (L), anterior cingulate gyrus (L), anterior cingulate gyrus (R)	<0.001	5910	9.50	−4	34	32
Cerebellum (R), cerebellum (L), cerebellar vermis	<0.001	372	8.05	0	−50	−38
Angular gyrus (L), inferior parietal lobule (L), middle occipital gyrus (L), supramarginal gyrus (L), middle temporal gyrus (L)	<0.001	1590	7.53	−40	−66	38
Precuneus (L), posterior cingulate gyrus (L), precuneus (R), middle cingulate gyrus (R), middle cingulate gyrus (L)	<0.001	1439	6.74	2	−38	34
Cerebellum crus I (R), cerebellum crus II (R), cerebellum crus II (L), cerebellum crus I (L)	<0.001	1143	6.60	−8	−86	−26
Middle frontal gyrus (R)	<0.001	367	6.45	36	44	10
Inferior parietal lobule (R), supramarginal gyrus (R)	<0.001	312	6.03	60	−42	44
cerebellum crus I (R), cerebellum (R)	0.001	205	5.65	30	−66	−36
Insula (R), inferior frontal gyrus, pars opercularis (R)	<0.001	346	5.48	34	12	−16
Middle temporal gyrus (L), inferior temporal gyrus (L)	0.023	122	4.93	−58	−38	−14
Precuneus (R), precuneus (L)	0.039	108	4.90	0	−54	56
Superior frontal gyrus (R), superior frontal gyrus, pars orbitalis (R), medial frontal gyrus (R)	0.002	186	4.59	20	60	8
Negative						
Middle occipital gyrus (L), superior occipital gyrus (L), lingual gyrus (L), fusiform gyrus (L), cuneus (L), calcarine gyrus (L), cuneus (R), middle occipital gyrus (R), superior occipital gyrus (R), inferior occipital gyrus (L)	<0.001	9910	10.46	−28	−84	8
Paracentral lobule (L), paracentral lobule (R), supplementary motor area (R), precuneus (L)	<0.001	842	8.75	2	−30	68
Postcentral gyrus (L), precentral gyrus (L)	<0.001	2289	8.43	−38	−28	56
Postcentral gyrus (R), precentral gyrus (R)	<0.001	660	6.67	54	−20	50

Note: Table refers to Fig. 2A. Reported clusters survived cluster-wise family-wise error correction for multiple comparisons ($p_{FWE} < 0.05$) at a cluster extension threshold of k = 100. Only contributions from regions above $5\%_{cluster}$ are listed. R = right; L = left; p_{corr} stands for whole brain corrected cluster p-values, k for the cluster size, t_{peak} for the t-value of the peak-voxel, [x y z] coordinates are in MNI-space.
[a] Peak voxel coordinates of brainstem cluster: [x y z] = [−2 −24 30].

with clusters in (superior and middle) frontal regions and precuneus, but no significant correlations in thalamus and caudate nucleus as observed in the original sample. For the pupil size regressor, the independent samples *t*-test between the light condition of the original sample and replication sample (original sample > replication sample) yielded one significant cluster in superior occipital gyrus, superior parietal gyrus and angular gyrus ($p_{corr} = 0.002$, k = 236, $t_{peak} = 4.89$, [x y z] = [22 −58 42]). The reverse contrast did not yield any significant clusters.

The pupil *change* analysis similarly replicated positive correlations in dACC, middle cingulate gyrus, bilateral anterior insula, frontal regions (middle, medial, inferior frontal gyri), inferior parietal lobules, superior temporal regions and supplementary motor areas (Fig. 2C, Supplementary Table S12). Negative correlations with the pupil change regressor

Table 4
Regions correlated to pupil *change* in the light condition.

	Cluster		Voxel			
	p_{corr}	k	t_{peak}	x	y	z
Positive						
Anterior cingulate gyrus (L), middle cingulate gyrus (R), anterior cingulate gyrus (R), supplementary motor area (L), medial frontal gyrus (L), supplementary motor area (R), middle cingulate gyrus (L)	<0.001	2593	10.03	0	22	34
Cerebellum crus I (R), cerebellum (R), cerebellum (L), cerebellar vermis, cerebellum crus II (R)	<0.001	1460	9.83	−4	−56	−38
Middle frontal gyrus (R), inferior frontal gyrus, pars triangularis	<0.001	932	8.51	32	44	16
Caudate nucleus (R), thalamus (R), pallidum (R), brainstem[a]	<0.001	762	7.82	14	8	16
Insula (R), putamen (R)	<0.001	748	6.36	30	18	0
Cerebellum crus I (L), cerebellum (L)	<0.001	682	6.17	−40	−52	−34
Middle cingulate gyrus (R), middle cingulate gyrus (L), precuneus (R)	0.008	161	6.08	10	−38	42
Middle cingulate gyrus (R), middle cingulate gyrus (L)	0.003	194	5.92	4	−20	32
Insula (L), inferior frontal gyrus, pars triangularis (L), inferior frontal gyrus, pars orbitalis (L), caudate nucleus (L), thalamus (L)	<0.001	1629	5.92	−14	10	14
Supramarginal gyrus (R), inferior parietal lobule (R), angular gyrus (R)	<0.001	723	5.88	68	−36	28
Precuneus (R), precuneus (L)	<0.001	256	5.48	5	−56	54
Middle frontal gyrus (L), superior frontal gyrus (L), inferior frontal gyrus, pars triangularis (L)	<0.001	625	5.17	−18	50	20
Superior frontal gyrus (R), supplementary motor area (R)	0.002	209	5.01	26	6	64
Supramarginal gyrus (L), superior temporal gyrus (L), middle temporal gyrus (L)	0.036	118	4.37	−56	−52	30
Negative						
Hippocampus (L), parahippocampal gyrus (L), amygdala (L)	0.001	223	8.89	−20	−14	−22
Superior occipital gyrus (R), cuneus (R), middle occipital gyrus (R), inferior occipital gyrus (R), calcarine gyrus (R), middle temporal gyrus (R), cuneus (L)	<0.001	2159	8.56	44	−78	0
Postcentral gyrus (L), postcentral gyrus (R), Paracentral lobule (R), paracentral lobule (L), precentral gyrus (L)	<0.001	3638	8.42	8	−34	68
Middle occipital gyrus (L), superior occipital gyrus (L), inferior occipital gyrus (L), cuneus (L)	<0.001	2106	8.08	−40	−74	6
Parahippocampal gyrus (R), hippocampus (R), amygdala (R)	0.013	148	6.29	28	−4	−28
Lingual gyrus (L), calcarine gyrus (L)	0.004	186	5.44	−20	−66	−2

Note: Table refers to Fig. 2B. Reported clusters survived cluster-wise family-wise error correction for multiple comparisons ($p_{FWE} < 0.05$) at a cluster extension threshold of k = 110. Only contributions from regions above $5\%_{cluster}$ are listed. R = right; L = left; p_{corr} stands for whole brain corrected cluster p-values, k for the cluster size, t_{peak} for the t-value of the peak-voxel, [x y z] coordinates are in MNI-space.
[a] Peak voxel coordinates of brainstem cluster: [x y z] = [0 −20 −20].

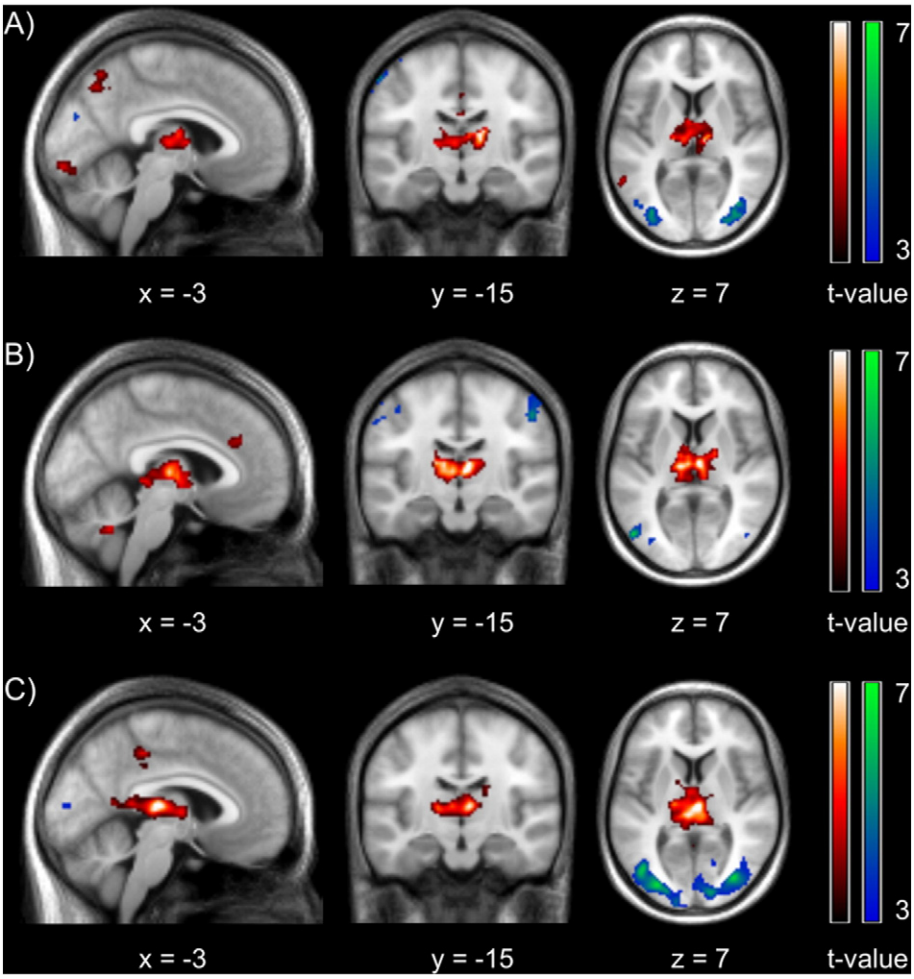

Fig. 3. Neural correlates of the temporal derivative regressor for pupil *change* in the dark condition (A), light condition (B) and the replication sample (C). The positive contrast (hot colors) reflects regions which exhibit increased BOLD activity at the onset of pupil dilations and decreased activity at the onset of pupil constrictions (resting state). The negative contrast (cool colors) reflects the reverse pattern. All maps were sampled at uncorrected $p < 0.001$ and clusters were thresholded at a cluster-wise $p_{FWE} < 0.05$ (cluster extension threshold set to $k = 110$). [x y z] coordinates refer to the MNI coordinates of the respective slices. See Table 5, Table 6 & Supplementary Table S13 for further information on cluster extents and peak voxel coordinates.

were again observed in the visual cortex and sensorimotor areas. In contrast to the original sample, we neither observed a positive correlation in thalamus (as observed in both lighting conditions) nor a negative correlation in hippocampus/parahippocampal gyrus (as observed in the light condition) in the replication sample. Still, the independent samples t-test for the pupil change regressor only yielded a cluster in cerebellum ($p_{corr} = 0.04$, $k = 131$, $t_{peak} = 4.94$, [x y z] = [22 −76 −26]) for the contrast light condition of the original sample > replication sample. No significant clusters were found in the reverse contrast.

In line with the findings from the original sample, the pupil change point regressor (the temporal derivative of pupil change) again yielded positively correlated activity in thalamus, in addition to other regions (Fig. 3C, Supplementary Table S13). Negatively correlated activity was again found in visual areas. The independent samples t-tests between

Table 5
Regions correlated to the temporal derivative of pupil change in the *dark* condition.

	Cluster		Voxel			
	p_{corr}	k	t_{peak}	x	y	z
Positive						
Thalamus (R), thalamus (L)	<0.001	730	7.90	14	−16	12
Calcarine gyrus (L)	0.001	187	4.95	−2	−90	−12
Middle temporal gyrus (L), supramarginal gyrus (L)	0.036	98	4.92	−58	−52	8
Middle cingulate gyrus (R), middle cingulate gyrus (L)	0.004	154	4.82	0	−20	40
Precuneus (L)	0.030	102	4.64	−2	−66	54
Negative						
Middle occipital gyrus (L), superior occipital gyrus (L), fusiform gyrus (L), superior occipital gyrus (R), middle occipital gyrus (R), inferior occipital gyrus (R), inferior occipital gyrus (L), cuneus (R)	<0.001	3568	9.23	−20	−82	32
Postcentral gyrus (L), precentral gyrus (L)	0.001	204	5.70	−62	−12	34

Note: Table refers to Fig. 3A. Reported clusters survived cluster-wise family-wise error correction for multiple comparisons ($p_{FWE} < 0.05$) at a cluster extension threshold of $k = 90$. Only contributions from regions above $5\%_{cluster}$ are listed. R = right; L = left; p_{corr} stands for whole brain corrected cluster p-values, k for the cluster size, t_{peak} for the t-value of the peak-voxel, [x y z] coordinates are in MNI-space.

Table 6
Regions correlated to the temporal derivative of pupil change in the *light* condition.

	Cluster		Voxel			
	p_{corr}	k	t_{peak}	x	y	z
Positive						
Thalamus (L), thalamus (R)	<0.001	1311	9.39	6	−16	8
Cerebellar vermis, cerebellum (L)	0.006	145	6.37	0	−58	−32
Superior frontal gyrus, pars orbitalis (L), medial frontal gyrus (L), middle frontal gyrus, pars orbitalis (L), rectus (L)	0.016	120	5.98	−16	64	−8
Anterior cingulate gyrus (R), anterior cingulate gyrus (L), middle cingulate gyrus (R), medial frontal gyrus (L)	<0.001	276	5.98	12	36	24
Angular gyrus (L), supramarginal gyrus (L), middle temporal gyrus (L)	0.012	128	4.84	−58	−58	32
Posterior cingulate gyrus (L), posterior cingulate gyrus (R), precuneus (L)	0.006	144	4.65	−2	−46	14
Negative						
Middle occipital gyrus (L), fusiform gyrus (L), inferior occipital gyrus (L), superior occipital gyrus (L), middle temporal gyrus (L)	<0.001	1539	8.15	−40	−78	−10
Postcentral gyrus (R), precentral gyrus (R)	<0.001	690	7.96	46	−38	58
Postcentral gyrus (L), superior parietal gyrus (L), inferior parietal lobule (L)	<0.001	731	7.63	−28	−40	54
Superior occipital gyrus (R), cuneus (R), middle occipital gyrus (R)	<0.001	355	6.50	20	−80	30
Superior parietal gyrus (R), inferior parietal lobule (R)	<0.001	379	6.48	24	−60	50
Inferior occipital gyrus (R), inferior temporal gyrus (R), middle occipital gyrus (R), Middle temporal gyrus (R)	<0.001	252	5.08	32	−80	−8
Postcentral gyrus (L), precentral gyrus (L)	0.002	180	4.36	−48	−22	42

Note: Table refers to Fig. 3B. Reported clusters survived cluster-wise family-wise error correction for multiple comparisons ($p_{FWE} < 0.05$) at a cluster extension threshold of k = 100. Only contributions from regions above $5\%_{cluster}$ are listed. R = right; L = left; p_{corr} stands for whole brain corrected cluster p-values, k for the cluster size, t_{peak} for the t-value of the peak-voxel, [x y z] coordinates are in MNI-space.

the original and replication sample for the pupil change point regressor revealed one large cluster comprising inferior, middle and superior occipital gyrus, lingual gyrus, fusiform gyrus, as well as cuneus ($p_{corr} < 0.001$, k = 6621, $t_{peak} = 6.18$, [x y z] = [−18 −90 12]) for the contrast light condition of the original sample > replication sample. The reverse contrast showed a cluster in middle/inferior frontal gyrus ($p_{corr} = 0.008$, k = 170, $t_{peak} = 4.83$, [x y z] = [−38 36 16]).

As in the original sample, we did not find any consistent correlations to the volume-wise PUI regressor in the replication sample. The covariate analyses with the total PUI score and mean pupil size did not reveal any consistently significant clusters for any of the regressors (pupil size, pupil change, thalamus seed, PCC seed; see Supplementary Table S7). The same applied to the PPI analyses. Here, no consistent pattern of clusters was found for any of the PPI combinations (thalamus or PCC as a seed region and volume-wise PUI, pupil size or pupil change as experimental vector; for individual results see Supplementary Table S10).

Discussion

We observed that an increase in pupil size was associated with increased activity in dACC (extending into rostral ACC and supplementary motor area) and bilateral anterior insula, dorsolateral prefrontal cortex, precuneus and inferior parietal lobules, among others. The dACC and bilateral anterior insula are components of the salience network (Heine et al., 2012) that is involved in orientation to salient stimuli (Menon and Uddin, 2010), conflict and error monitoring (Botvinick et al., 2004; Kerns et al., 2004; Menon et al., 2001), and evaluation of performance-related cost (Aston-Jones and Cohen, 2005). Furthermore, the salience network (particularly insula) has been suggested to map dynamic changes in arousal states, and enhanced activity of the dACC has been associated with the occurrence of sympathetic arousal responses (such as anticipatory skin conductance responses, blood pressure and heart rate), supporting the notion that the dACC modulates autonomic arousal according to situational requirements (Critchley, 2005). Interestingly, Sadaghiani et al. (2010) reported a robust positive correlation between spontaneous fluctuations in salience network activity and global field power of alpha oscillations (an established EEG marker of tonic alertness) during eyes-closed resting state. Based on this finding, the authors concluded that the salience network seems to play an important role in the maintenance of tonic alertness. Our data show a highly similar map in correlation with spontaneous pupil dilations, suggesting that pupil fluctuations or pupillary unrest indices indeed reflect transient changes in tonic alertness.

In our original sample (i.e. in the sleep-restricted subject group), we also found a positive correlation with pupil size increases in the brainstem and in the thalamus. Central arousal and alertness are mediated by the ARAS, which involves noradrenergic projections from the LC through the thalamus to numerous cortical areas (Aston-Jones et al., 1991; Critchley, 2005; Saper et al., 2005). The observed brainstem and thalamus clusters may reflect these relay stations of the ARAS (Naidich et al., 2009). Also, strong anatomical and functional connections have been shown to exist between the anterior thalamic nucleus and the dACC (Child and Benarroch, 2013; Liu et al., 2012). In our analytical approach, we supposed (in line with previous research) that due to signal transmission features, the neuronal events that trigger pupil size changes occur about 1 s earlier. By convolving this presumed neuronal regressor with the HRF, we assumed that the detected central neuronal sources operate simultaneously. Therefore, one possible interpretation of the observed positive pupil change-BOLD correlations is that ARAS-controlled arousal leads to both pupil size changes and concurrent thalamo-cingulate and eventually, full salience network activation to adapt the organism to increased arousal. In line with the idea of ascending activation from brainstem via thalamus to the cortex, thalamus activity was also positively correlated to the temporal derivative of pupil change, indicating that activity in thalamus was associated with the onset of pupil dilations. Not easily distinguishable, however, is viscerceptive monitoring activity following sympathetic tone changes - particularly the insular cortex holds such functions, as demonstrated in neuroimaging work studying blood pressure and heart rate viscerception (Craig, 2002; King et al., 1999; Williamson et al., 1999).

In addition, we found positive correlations with pupil size *increases* in regions belonging to the central executive network (CEN), including dorsolateral prefrontal cortex and posterior parietal cortex. The CEN has been linked to working memory, decision-making (Menon and Uddin, 2010), cognitive processing of external sensory input (Heine et al., 2012), as well as exogenously triggered initiation of control and adapting after errors (Dosenbach et al., 2007). At the same time, it is sometimes interpreted as constituting a unitary task activation-related network together with the salience network (Menon and Uddin, 2010). Before the start of each session, the subjects in our study (including the replication sample) received the instruction to not fall asleep and to keep their gaze on the fixation point. Besides representing ascending activation from brainstem via thalamus to dACC, the positive correlation with pupil size increase could also reflect a counter-regulatory pattern that prevents subjects from falling asleep and enables e.g. a continuous fixation. This could be achieved through repeated

stimulation of the brainstem/ARAS during periods of low vigilance/drowsiness, causing simultaneous pupil dilations. In line with this notion, it has been shown that activity in the frontoparietal network is correlated with pupil dilation during focused attention (Alnaes et al., 2014; Siegle et al., 2003), and increased noradrenergic signal transmission has been suggested to directly enhance cognitive control mechanisms in the prefrontal cortex, reinforcing cognitive control following a transient decrease in performance (Arnsten et al., 1996; Aston-Jones and Cohen, 2005).

Remarkably, activation of frontoparietal areas has not been described in experiments where participants were either allowed to sleep (Olbrich et al., 2009) or not specifically discouraged from doing so (Marx et al., 2004; Marx et al., 2003; Wiesmann et al., 2006). Our findings more generally provide evidence that the sleepiness-related pupil fluctuations may at least partly result from subjects' recurrent efforts of staying awake or maintaining fixation.

The positive correlation between thalamus and pupil dilation could not be replicated in the replication sample. However, we did find that in both lighting conditions and in the replication sample, bilateral thalamus was associated with the pupil change point regressor. Furthermore, the neural correlates of the pupil change regressor did not differ significantly between the original and the replication sample. Therefore, this result indicates either a failure to replicate or a potential effect of sleep restriction. This may involve different activity levels in thalamus in association with pupil dilations or increased top-down signaling from dACC to the thalamus and brainstem in order to counteract higher levels of drowsiness induced by the sleep restriction, which would be in line with the higher PUI values observed in the original sample.

Finally, we also found positive correlations with pupil dilations in parts of the DMN (including medial prefrontal cortex, PCC, precuneus and inferior parietal lobules). The DMN has been primarily associated with self-referential processing and attention to internal stimuli, and its connectivity has been shown to be reduced by sleep deprivation (Ong et al., 2015; Sämann et al., 2010) and during light sleep (Sämann et al., 2011). Our observation that the correlation of both CEN and DMN with pupil size increase was more pronounced (yet not significantly different) in the dark condition could implicate that darkness-promoted drowsiness leads to counteracting arousal reactions - possibly mediated by the CEN - that restores DMN connectivity to some degree.

A decrease in pupil size was associated with increased activity in regions belonging to the visual and sensorimotor system. In the light condition of the original sample, we also observed anti-correlated activity in parahippocampal and hippocampal regions. These correlations are in line with previous findings: Yellin et al. (2015) similarly used simultaneous pupillometry during rs-fMRI and also found a negative correlation between activity of sensorimotor areas and pupil size. Similar maps of brain regions (including hippocampal and parahippocampal regions) have been reported for spontaneous eye closures during rs-fMRI (Ong et al., 2015) and continuous visuomotor tasks (Poudel et al., 2014), as well as for cued eye closures (Marx et al., 2004; Marx et al., 2003; Ong et al., 2015; Poudel et al., 2010). Furthermore, Sadaghiani et al. (2010) observed that visual and sensorimotor areas showed a negative correlation with global field power of alpha and beta oscillations (EEG marker of tonic alertness) during eyes-closed resting state.

In line with previous work (Marx et al., 2004; Marx et al., 2003; Ong et al., 2015), we interpret the observed activation of visual areas during pupil constrictions as indicators of internally-focused processing and possibly, mental imagery during periods of increasing drowsiness. Given the involvement of the arousal/ARAS system as described above, the deactivation of these areas during pupil dilations might reflect a suppression of such interoceptive processes when subjects return to more alerted states, associated with a re-established focused attention to the external environment (i.e., to the fixation point). In any case, the statistical map for pupil constrictions is again highly similar to the map for reduction in alpha power (Sadaghiani et al., 2010), which supports the notion that pupil fluctuations constitute a marker for transient changes in tonic alertness.

In contrast, for the pupil *size* regressor, positive correlations were only found within minor clusters including thalamus, caudate nucleus and cerebellum (original sample), as well as frontal and parietal regions (replication sample). This analysis revealed much more wide-spread deactivation in regions belonging to the visual and sensorimotor system, as well as precuneus, cuneus, posterior insula, middle cingulate gyrus and superior temporal gyri, in accordance with observations by Yellin et al. (2015). Interestingly, the insula showed both positively correlated activity to pupil dilations and anti-correlated activity to pupil size. This finding supports previous findings emphasizing the heterogeneous connectivity and function of the insula: the anterior insula has been shown to be mainly connected with limbic and paralimbic regions including the ACC, and is suggested to be involved in high-level cognitive processes such as task switching, inhibition or error processing, as well as affective processing (Uddin, 2015). In contrast, the posterior insula is associated with sensorimotor processes and strongly connected with posterior temporal, parietal, and frontal areas including somatosensory, motor, and premotor cortices (Alcauter et al., 2015; Cerliani et al., 2012; Uddin, 2015). Our results match these previous findings: the insula cluster in the negative contrast of pupil size, which includes large clusters belonging to the sensorimotor system, localizes to the posterior division of the insula. The insula cluster in the positive contrast of pupil change, which includes strong co-activation of the dACC, localizes to the anterior subdivision.

In contrast to Yellin et al. (2015), we did not find a positive correlation between pupil size and DMN activity (including medial prefrontal cortex, inferior parietal lobules and precuneus), although some of the regions we observed in the positive contrast of the replication sample might possibly be interpreted as being part of the DMN. At the same time, we observed several DMN regions in the contrast of *increase* in pupil size as mentioned above. We further evaluated whether the DMN's connectivity would depend on the subject's overall drowsiness levels. For this purpose, we included the total PUI score and average pupil diameter per run as covariates in the PCC seed second level analyses and additionally conducted psychophysiological interaction analyses for the PCC seed with volume-wise PUI, pupil size and pupil change as experimental vector. Here, none of the analyses revealed consistent effects across conditions.

It should be noted that the inclusion of the temporal and dispersion derivatives into the GLM with the pupil *size* regressor yielded a map of brain regions that was comparable to the positive contrast of the pupil *change* analysis. Murphy et al. (2014) also included these derivatives and also observed a correlation between pupil size and activity in dACC and insula. Our analyses support the notion that it is not the pupil size per se, but the *increase* in pupil size that is associated with an increase in activity within a circumscribed set of brain areas relevant for arousal and saliency.

None of our analyses revealed any major differences between the two lighting conditions, indicating that the possible occurrence of light-induced pupil fluctuations did not have a large effect at the neural level. In the present study, we used a light sleep restriction procedure to ensure a certain level of drowsiness and variability in vigilance. By applying the same analysis pipelines to a dataset from a basically identical experiment with no sleep restriction, it could be shown that subjects who were allowed to sleep normally showed very similar pupil-BOLD correlations. It should be kept in mind that the present study was not specifically designed to assess sleep restriction-related differences: since we used an additional sample of subjects from a separate study, the sleep restriction procedure was not randomized across subjects. We only used the sleep restriction procedure to increase variance in pupil fluctuations; our data simultaneously show that this was both successful and unnecessary. After all, the well-rested subjects of the replication sample had much smaller PUI values but similar neural correlates of pupil change and change points. If the goal of the study

had been to experimentally compare the effects of sleep restriction versus normal sleep on pupil fluctuations, objective readouts to verify an experimental manipulation (e.g., actigraphy or polysomnography) would have been warranted.

Previous studies using eye video recording included tonic changes in the distance between the eyelids for the quantification of the subjects' drowsiness levels (Poudel et al., 2014; Poudel et al., 2012). In this context, it can be observed that very drowsy subjects often show droopy eyelids and/or slow eyelid closures which both involve a partial occlusion of the pupil that can cause artifacts in the pupil size data. The eye tracking system that was used in the present study features a so-called ellipse fitting mode, in which the system fits an ellipse to the pupil area, giving an accurate estimate for pupil size even when the pupil is occluded by the eyelids to a certain degree. Only for extremely droopy eyelids (e.g., causing an occlusion of roughly >50% of the pupil area), the ellipse fit becomes error-prone (manifest in abrupt jumps in the pupil size and eye gaze data). In the present study, this was only observed in the two subjects in the dark condition who actually fell asleep during the resting state recording and who therefore had been excluded from our analyses. However, future studies that address more intense sleep deprivation procedures (such as partial or total sleep deprivation) could have higher incidences of such extremely droopy eyelids covering more than half of the pupil size. In this case, it is advisable to include additional eyelid video recording to allow for analysis of these events.

Finally, in order to investigate whether the pupil-based vigilance measures exert a modulating effect on the pupil size/change-BOLD correlations and on the functional connectivity of thalamus, several covariate and PPI analyses were performed. Inclusion of the average pupil size and total PUI score as covariate in the pupil size, pupil change and thalamus connectivity analyses did not reveal any consistent effects across conditions. Similarly, the PPI analyses with thalamus as a seed region and volume-wise PUI, pupil size and pupil change as experimental vector did not reveal consistent correlations across conditions.

Conclusion

Spontaneous drifts in vigilance challenge the validity of resting state findings and might pose a severe confound when drawing comparisons between healthy controls and patients with hypo- or hyper-arousal symptomatology. Simultaneous pupillometry enables experimental control for such spontaneous vigilance changes by providing an objective readout of slow pupil fluctuations and an indirect index for activity of the LC, the brainstem's noradrenergic arousal center. Our findings show that increases in pupil size are correlated with activity of specific brain areas, including the salience network, thalamus and frontoparietal regions, whereas reductions in pupil size are associated with increased activity in visual and sensorimotor regions. Pupillometry appears an effective way to control for changes in tonic alertness during rs-fMRI with a less complicated setup than EEG, a higher sensitivity than eye blink analyses and an established link to a well-defined neurobiological system.

Funding/acknowledgements

VS acknowledges financial support by the Bavarian Academy of Sciences and Humanities and MS acknowledges financial support by the Graduate School of Systemic Neurosciences (LMU Munich). All authors would like to thank Ines Eidner for her technical support and the anonymous reviewers for their contributions.

Appendix A. Supplementary data

Supplementary data to this article can be found online at http://dx.doi.org/10.1016/j.neuroimage.2016.06.011.

References

Akerstedt, T., Gillberg, M., 1990. Subjective and objective sleepiness in the active individual. Int. J. Neurosci. 52 (1–2), 29–37.
Alcauter, S., Lin, W., Keith Smith, J., Gilmore, J.H., Gao, W., 2015. Consistent anterior-posterior segregation of the insula during the first 2 years of life. Cereb. Cortex 25 (5), 1176–1187. http://dx.doi.org/10.1093/cercor/bht312.
Alnaes, D., Sneve, M.H., Espeseth, T., Endestad, T., van de Pavert, S.H., Laeng, B., 2014. Pupil size signals mental effort deployed during multiple object tracking and predicts brain activity in the dorsal attention network and the locus coeruleus. J. Vis. 14 (4), 1–20. http://dx.doi.org/10.1167/14.4.1.
Arnsten, A.F., Steere, J.C., Hunt, R.D., 1996. The contribution of alpha 2-noradrenergic mechanisms of prefrontal cortical cognitive function. Potential significance for attention-deficit hyperactivity disorder. Arch. Gen. Psychiatry 53 (5), 448–455.
Ashburner, J., Barnes, G., Chen, C., Daunizeau, J., Flandin, G., Friston, K., Kiebel, S., Kilner, J., Litvak, V., Moran, R., et al., 2014. SPM12 Manual. Wellcome Trust Centre for Neuroimaging, London (UK).
Aston-Jones, G., Cohen, J.D., 2005. An integrative theory of locus coeruleus-norepinephrine function: adaptive gain and optimal performance. Annu. Rev. Neurosci. 28, 403–450. http://dx.doi.org/10.1146/annurev.neuro.28.061604.135709.
Aston-Jones, G., Chiang, C., Alexinsky, T., 1991. Discharge of noradrenergic locus coeruleus neurons in behaving rats and monkeys suggests a role in vigilance. Prog. Brain Res. 88, 501–520.
Barbato, G., De Padova, V., Paolillo, A.R., Arpaia, L., Russo, E., Ficca, G., 2007. Increased spontaneous eye blink rate following prolonged wakefulness. Physiol. Behav. 90 (1), 151–154. http://dx.doi.org/10.1016/j.physbeh.2006.09.023.
Behzadi, Y., Restom, K., Liau, J., Liu, T.T., 2007. A component based noise correction method (CompCor) for BOLD and perfusion based fMRI. NeuroImage 37 (1), 90–101. http://dx.doi.org/10.1016/j.neuroimage.2007.04.042.
Berridge, C.W., Waterhouse, B.D., 2003. The locus coeruleus–noradrenergic system: modulation of behavioral state and state-dependent cognitive processes. Brain Res. Rev. 42 (1), 33–84. http://dx.doi.org/10.1016/s0165-0173(03)00143-7.
Bianciardi, M., Fukunaga, M., van Gelderen, P., Horovitz, S.G., de Zwart, J.A., Duyn, J.H., 2009. Modulation of spontaneous fMRI activity in human visual cortex by behavioral state. NeuroImage 45 (1), 160–168. http://dx.doi.org/10.1016/j.neuroimage.2008.10.034.
Botvinick, M.M., Cohen, J.D., Carter, C.S., 2004. Conflict monitoring and anterior cingulate cortex: an update. Trends Cogn. Sci. 8 (12), 539–546. http://dx.doi.org/10.1016/j.tics.2004.10.003.
Cerliani, L., Thomas, R.M., Jbabdi, S., Siero, J.C., Nanetti, L., Crippa, A., Gazzola, V., D'Arceuil, H., Keysers, C., 2012. Probabilistic tractography recovers a rostrocaudal trajectory of connectivity variability in the human insular cortex. Hum. Brain Mapp. 33 (9), 2005–2034. http://dx.doi.org/10.1002/hbm.21338.
Child, N.D., Benarroch, E.E., 2013. Anterior nucleus of the thalamus: functional organization and clinical implications. Neurology 81 (21), 1869–1876. http://dx.doi.org/10.1212/01.wnl.0000436078.95856.56.
Craig, A.D., 2002. How do you feel? Interoception: the sense of the physiological condition of the body. Nat. Rev. Neurosci. 3 (8), 655–666. http://dx.doi.org/10.1038/nrn894.
Critchley, H.D., 2005. Neural mechanisms of autonomic, affective, and cognitive integration. J. Comp. Neurol. 493 (1), 154–166. http://dx.doi.org/10.1002/cne.20749.
Curcio, G., Casagrande, M., Bertini, M., 2001. Sleepiness: evaluating and quantifying methods. Int. J. Psychophysiol. 41 (3), 251–263.
Dosenbach, N.U., Fair, D.A., Miezin, F.M., Cohen, A.L., Wenger, K.K., Dosenbach, R.A., Fox, M.D., Snyder, A.Z., Vincent, J.L., Raichle, M.E., et al., 2007. Distinct brain networks for adaptive and stable task control in humans. Proc. Natl. Acad. Sci. U. S. A. 104 (26), 11073–11078. http://dx.doi.org/10.1073/pnas.0704320104.
Handwerker, D.A., Ollinger, J.M., D'Esposito, M., 2004. Variation of BOLD hemodynamic responses across subjects and brain regions and their effects on statistical analyses. NeuroImage 21 (4), 1639–1651. http://dx.doi.org/10.1016/j.neuroimage.2003.11.029.
Heine, L., Soddu, A., Gomez, F., Vanhaudenhuyse, A., Tshibanda, L., Thonnard, M., Charland-Verville, V., Kirsch, M., Laureys, S., Demertzi, A., 2012. Resting state networks and consciousness: alterations of multiple resting state network connectivity in physiological, pharmacological, and pathological consciousness states. Front. Psychol. 3, 295. http://dx.doi.org/10.3389/fpsyg.2012.00295.
Henson, D.B., Emuh, T., 2010. Monitoring vigilance during perimetry by using pupillography. Invest. Ophthalmol. Vis. Sci. 51 (7), 3540–3543. http://dx.doi.org/10.1167/iovs.09-4413.
Horovitz, S.G., Braun, A.R., Carr, W.S., Picchioni, D., Balkin, T.J., Fukunaga, M., Duyn, J.H., 2009. Decoupling of the brain's default mode network during deep sleep. Proc. Natl. Acad. Sci. U. S. A. 106 (27), 11376–11381. http://dx.doi.org/10.1073/pnas.0901435106.
Kaufmann, C., Wehrle, R., Wetter, T.C., Holsboer, F., Auer, D.P., Pollmacher, T., Czisch, M., 2006. Brain activation and hypothalamic functional connectivity during human non-rapid eye movement sleep: an EEG/fMRI study. Brain 129 (Pt 3), 655–667. http://dx.doi.org/10.1093/brain/awh686.
Kerns, J.G., Cohen, J.D., MacDonald 3rd, A.W., Cho, R.Y., Stenger, V.A., Carter, C.S., 2004. Anterior cingulate conflict monitoring and adjustments in control. Science 303 (5660), 1023–1026. http://dx.doi.org/10.1126/science.1089910.
King, A.B., Menon, R.S., Hachinski, V., Cechetto, D.F., 1999. Human forebrain activation by visceral stimuli. J. Comp. Neurol. 413 (4), 572–582.
Liu, Z., de Zwart, J.A., Yao, B., van Gelderen, P., Kuo, L.W., Duyn, J.H., 2012. Finding thalamic BOLD correlates to posterior alpha EEG. NeuroImage 63 (3), 1060–1069. http://dx.doi.org/10.1016/j.neuroimage.2012.08.025.
Loewenfeld, I.E., 1993. The Pupil. Anatomy, Physiology and Clinical Application. Wayne State University Press, Detroit.

Longtin, A., Milton, J.G., 1989. Insight into the transfer function, gain, and oscillation onset for the pupil light reflex using nonlinear delay-differential equations. Biol. Cybern. 61 (1), 51–58.
Longtin, A., Milton, J.G., Bos, J.E., Mackey, M.C., 1990. Noise and critical behavior of the pupil light reflex at oscillation onset. Phys. Rev. A 41 (12), 6992–7005.
Lowenstein, O., Feinberg, R., Loewenfeld, I.E., 1963. Pupillary movements during acute and chronic fatigue - a new test for the objective evaluation of tiredness. Investig. Ophthalmol. 2 (2), 138–157.
Ludtke, H., Wilhelm, B., Adler, M., Schaeffel, F., Wilhelm, H., 1998. Mathematical procedures in data recording and processing of pupillary fatigue waves. Vis. Res. 38 (19), 2889–2896.
Marx, E., Stephan, T., Nolte, A., Deutschlander, A., Seelos, K.C., Dieterich, M., Brandt, T., 2003. Eye closure in darkness animates sensory systems. NeuroImage 19 (3), 924–934.
Marx, E., Deutschlander, A., Stephan, T., Dieterich, M., Wiesmann, M., Brandt, T., 2004. Eyes open and eyes closed as rest conditions: impact on brain activation patterns. NeuroImage 21 (4), 1818–1824. http://dx.doi.org/10.1016/j.neuroimage.2003.12.026.
Menon, V., Uddin, L.Q., 2010. Saliency, switching, attention and control: a network model of insula function. Brain Struct. Funct. 214 (5–6), 655–667. http://dx.doi.org/10.1007/s00429-010-0262-0.
Menon, V., Adleman, N.E., White, C.D., Glover, G.H., Reiss, A.L., 2001. Error-related brain activation during a Go/NoGo response inhibition task. Hum. Brain Mapp. 12 (3), 131–143.
Mohanty, A., Gitelman, D.R., Small, D.M., Mesulam, M.M., 2008. The spatial attention network interacts with limbic and monoaminergic systems to modulate motivation-induced attention shifts. Cereb. Cortex 18 (11), 2604–2613. http://dx.doi.org/10.1093/cercor/bhn021.
Muppidi, S., Adams-Huet, B., Tajzoy, E., Scribner, M., Blazek, P., Spaeth, E.B., Frohman, E., Davis, S., Vernino, S., 2013. Dynamic pupillometry as an autonomic testing tool. Clin. Auton. Res. 23 (6), 297–303. http://dx.doi.org/10.1007/s10286-013-0209-7.
Murphy, P.R., O'Connell, R.G., O'Sullivan, M., Robertson, I.H., Balsters, J.H., 2014. Pupil diameter covaries with BOLD activity in human locus coeruleus. Hum. Brain Mapp. 35 (8), 4140–4154. http://dx.doi.org/10.1002/hbm.22466.
Naidich, T.P., Duvernoy, H.M., Delman, B.N., Sorensen, A.G., Kollias, S.S., Haacke, E.M., 2009. Duvernoy's Atlas of the Human Brain Stem and Cerebellum: High-field MRI, Surface Anatomy, Internal Structure, Vascularization and 3D Sectional Anatomy. Springer, Vienna (AT).
Olbrich, S., Mulert, C., Karch, S., Trenner, M., Leicht, G., Pogarell, O., Hegerl, U., 2009. EEG-vigilance and BOLD effect during simultaneous EEG/fMRI measurement. NeuroImage 45 (2), 319–332. http://dx.doi.org/10.1016/j.neuroimage.2008.11.014.
Ong, J.L., Kong, D., Chia, T.T., Tandi, J., Thomas Yeo, B.T., Chee, M.W., 2015. Co-activated yet disconnected-neural correlates of eye closures when trying to stay awake. NeuroImage 118, 553–562. http://dx.doi.org/10.1016/j.neuroimage.2015.03.085.
Poudel, G.R., Jones, R.D., Innes, C.R., Watts, R., Davidson, P.R., Bones, P.J., 2010. Measurement of BOLD changes due to cued eye-closure and stopping during a continuous visuomotor task via model-based and model-free approaches. IEEE Trans. Neural. Syst. Rehabil. Eng. 18 (5), 479–488. http://dx.doi.org/10.1109/tnsre.2010.2050782.
Poudel, G.R., Innes, C.R., Jones, R.D., 2012. Cerebral perfusion differences between drowsy and nondrowsy individuals after acute sleep restriction. Sleep 35 (8), 1085–1096. http://dx.doi.org/10.5665/sleep.1994.
Poudel, G.R., Innes, C.R., Bones, P.J., Watts, R., Jones, R.D., 2014. Losing the struggle to stay awake: divergent thalamic and cortical activity during microsleeps. Hum. Brain Mapp. 35 (1), 257–269. http://dx.doi.org/10.1002/hbm.22178.
Power, J.D., Barnes, K.A., Snyder, A.Z., Schlaggar, B.L., Petersen, S.E., 2012. Spurious but systematic correlations in functional connectivity MRI networks arise from subject motion. NeuroImage 59 (3), 2142–2154. http://dx.doi.org/10.1016/j.neuroimage.2011.10.018.
Rajkowski, J., Kubiak, P., Aston-Jones, G., 1993. Correlations between locus coeruleus (LC) neural activity, pupil diameter and behavior in monkey support a role of LC in attention. Soc. Neurosci. Abstr. 19 (1–3), 974.
Ranzijn, R., Lack, L., 1997. The pupillary light reflex cannot be used to measure sleepiness. Psychophysiology 34 (1), 17–22.
Regen, F., Dorn, H., Danker-Hopfe, H., 2013. Association between pupillary unrest index and waking electroencephalogram activity in sleep-deprived healthy adults. Sleep Med. 14 (9), 902–912. http://dx.doi.org/10.1016/j.sleep.2013.02.003.
Sadaghiani, S., D'Esposito, M., 2015. Functional characterization of the cingulo-opercular network in the maintenance of tonic alertness. Cereb. Cortex 25 (9), 2763–2773. http://dx.doi.org/10.1093/cercor/bhu072.
Sadaghiani, S., Scheeringa, R., Lehongre, K., Morillon, B., Giraud, A.L., Kleinschmidt, A., 2010. Intrinsic connectivity networks, alpha oscillations, and tonic alertness: a simultaneous electroencephalography/functional magnetic resonance imaging study. J. Neurosci. 30 (30), 10243–10250. http://dx.doi.org/10.1523/jneurosci.1004-10.2010.
Sämann, P.G., Tully, C., Spoormaker, V.I., Wetter, T.C., Holsboer, F., Wehrle, R., Czisch, M., 2010. Increased sleep pressure reduces resting state functional connectivity. Magma 23 (5–6), 375–389. http://dx.doi.org/10.1007/s10334-010-0213-z.
Sämann, P.G., Wehrle, R., Hoehn, D., Spoormaker, V.I., Peters, H., Tully, C., Holsboer, F., Czisch, M., 2011. Development of the brain's default mode network from wakefulness to slow wave sleep. Cereb. Cortex 21 (9), 2082–2093. http://dx.doi.org/10.1093/cercor/bhq295.
Saper, C.B., Scammell, T.E., Lu, J., 2005. Hypothalamic regulation of sleep and circadian rhythms. Nature 437 (7063), 1257–1263. http://dx.doi.org/10.1038/nature04284.
Shahid, A., Shen, J., Shapiro, C.M., 2010. Measurements of sleepiness and fatigue. J. Psychosom. Res. 69 (1), 81–89. http://dx.doi.org/10.1016/j.jpsychores.2010.04.001.
Sheth, S.A., Mian, M.K., Patel, S.R., Asaad, W.F., Williams, Z.M., Dougherty, D.D., Bush, G., Eskandar, E.N., 2012. Human dorsal anterior cingulate cortex neurons mediate ongoing behavioural adaptation. Nature 488 (7410), 218–221. http://dx.doi.org/10.1038/nature11239.
Siegle, G.J., Steinhauer, S.R., Stenger, V.A., Konecky, R., Carter, C.S., 2003. Use of concurrent pupil dilation assessment to inform interpretation and analysis of fMRI data. NeuroImage 20 (1), 114–124.
Spoormaker, V.I., Schröter, M.S., Gleiser, P.M., Andrade, K.C., Dresler, M., Wehrle, R., Sämann, P.G., Czisch, M., 2010. Development of a large-scale functional brain network during human non-rapid eye movement sleep. J. Neurosci. 30 (34), 11379–11387. http://dx.doi.org/10.1523/jneurosci.2015-10.2010.
Szabadi, E., 2012. Modulation of physiological reflexes by pain: role of the locus coeruleus. Front. Integr. Neurosci. 6, 94. http://dx.doi.org/10.3389/fnint.2012.00094.
Szabadi, E., 2013. Functional neuroanatomy of the central noradrenergic system. J. Psychopharmacol. 27 (8), 659–693. http://dx.doi.org/10.1177/0269881113490326.
Tagliazucchi, E., Laufs, H., 2014. Decoding wakefulness levels from typical fMRI resting-state data reveals reliable drifts between wakefulness and sleep. Neuron 82 (3), 695–708. http://dx.doi.org/10.1016/j.neuron.2014.03.020.
Tagliazucchi, E., von Wegner, F., Morzelewski, A., Brodbeck, V., Borisov, S., Jahnke, K., Laufs, H., 2013. Large-scale brain functional modularity is reflected in slow electroencephalographic rhythms across the human non-rapid eye movement sleep cycle. NeuroImage 70, 327–339. http://dx.doi.org/10.1016/j.neuroimage.2012.12.073.
Tzourio-Mazoyer, N., Landeau, B., Papathanassiou, D., Crivello, F., Etard, O., Delcroix, N., Mazoyer, B., Joliot, M., 2002. Automated anatomical labeling of activations in SPM using a macroscopic anatomical parcellation of the MNI MRI single-subject brain. NeuroImage 15 (1), 273–289. http://dx.doi.org/10.1006/nimg.2001.0978.
Uddin, L.Q., 2015. Salience processing and insular cortical function and dysfunction. Nat. Rev. Neurosci. 16 (1), 55–61. http://dx.doi.org/10.1038/nrn3857.
Wall, M.B., Walker, R., Smith, A.T., 2009. Functional imaging of the human superior colliculus: an optimised approach. NeuroImage 47 (4), 1620–1627. http://dx.doi.org/10.1016/j.neuroimage.2009.05.094.
Warga, M., Ludtke, H., Wilhelm, H., Wilhelm, B., 2009. How do spontaneous pupillary oscillations in light relate to light intensity? Vis. Res. 49 (3), 295–300. http://dx.doi.org/10.1016/j.visres.2008.09.019.
Wierda, S.M., van Rijn, H., Taatgen, N.A., Martens, S., 2012. Pupil dilation deconvolution reveals the dynamics of attention at high temporal resolution. Proc. Natl. Acad. Sci. U. S. A. 109 (22), 8456–8460. http://dx.doi.org/10.1073/pnas.1201858109.
Wiesmann, M., Kopietz, R., Albrecht, J., Linn, J., Reime, U., Kara, E., Pollatos, O., Sakar, V., Anzinger, A., Fesl, G., et al., 2006. Eye closure in darkness animates olfactory and gustatory cortical areas. NeuroImage 32 (1), 293–300. http://dx.doi.org/10.1016/j.neuroimage.2006.03.022.
Wilhelm, H., Ludtke, H., Wilhelm, B., 1998. Pupillographic sleepiness testing in hypersomniacs and normals. Graefes Arch. Clin. Exp. Ophthalmol. 236 (10), 725–729.
Wilhelm, B., Giedke, H., Ludtke, H., Bittner, E., Hofmann, A., Wilhelm, H., 2001. Daytime variations in central nervous system activation measured by a pupillographic sleepiness test. J. Sleep Res. 10 (1), 1–7.
Williamson, J.W., McColl, R., Mathews, D., Ginsburg, M., Mitchell, J.H., 1999. Activation of the insular cortex is affected by the intensity of exercise. J. Appl. Physiol. 87 (3), 1213–1219.
Yellin, D., Berkovich-Ohana, A., Malach, R., 2015. Coupling between pupil fluctuations and resting-state fMRI uncovers a slow build-up of antagonistic responses in the human cortex. NeuroImage 106, 414–427. http://dx.doi.org/10.1016/j.neuroimage.2014.11.034.

3 Disentangling reward anticipation with simultaneous pupillometry/ fMRI

3.1 Summary

The aim of the second study was to assess whether the link between pupil dilations and SN activity previously observed during the resting state would also extend to task-evoked (positive) emotional arousal. For this purpose, we examined the pupil dynamics of 46 healthy subjects within a well-established reward anticipation paradigm, which required subjects to quickly respond to a target cue in order to receive a reward. A cue preceding the target stimulus for 6 s indicated the experimental condition (chance to win a monetary reward, a non-monetary reward, or no reward), and our analyses were focused on the BOLD correlates of the pupil size and pupil change time courses within this reward anticipation window.

As expected, we found that cues indicating the possibility to win a reward evoked an increase in pupil size, the magnitude of which predicted response time to the target stimulus. Similar to our observations in the resting state study, we found that these pupil dilations were coupled with increased activity of the SN. Furthermore, we observed that activity in the VS was inversely related to the pupil size time course, indicating an early onset of activation in line with reward prediction updating. Increased pupil size immediately before the required motor response was associated with activity in the ventral attention network.

The findings from our second study further support a role of the SN in performance optimization via the dynamic regulation of arousal levels. In addition, our second study suggests that pupillometry can be used to disentangle different phases of reward anticipation, with relevance for anhedonia symptomatology.

3.2 Reference

This work was carried out under the supervision of Victor Spoormaker; M.S. and V.S. designed research and wrote the manuscript; the data was collected within the framework of the BeCOME study; M.S. and V.S. analyzed the data; L.L., M.C. and P.S. critically revised the manuscript.

The paper was published in *Neuroimage* under the following reference:

Schneider M, Leuchs L, Czisch M, Samann PG, Spoormaker VI. 2018. Disentangling reward anticipation with simultaneous pupillometry / fMRI. *Neuroimage*. 178:11-22. DOI: 10.1016/j.neuroimage.2018.04.078

NeuroImage 178 (2018) 11–22

Contents lists available at ScienceDirect

NeuroImage

journal homepage: www.elsevier.com/locate/neuroimage

Disentangling reward anticipation with simultaneous pupillometry / fMRI

Max Schneider, Laura Leuchs, Michael Czisch, Philipp G. Sämann, Victor I. Spoormaker *

Max Planck Institute of Psychiatry, 80804, Munich, Germany

ARTICLE INFO

Keywords:
Reward
Salience network
dACC
Arousal
Pupil size

ABSTRACT

The reward system may provide an interesting intermediate phenotype for anhedonia in affective disorders. Reward anticipation is characterized by an increase in arousal, and previous studies have linked the anterior cingulate cortex (ACC) to arousal responses such as dilation of the pupil. Here, we examined pupil dynamics during a reward anticipation task in forty-six healthy human subjects and evaluated its neural correlates using functional magnetic resonance imaging (fMRI). Pupil size showed a strong increase during monetary reward anticipation, a moderate increase during verbal reward anticipation and a decrease during control trials. For fMRI analyses, average pupil size and pupil change were computed in 1-s time bins during the anticipation phase. Activity in the ventral striatum was inversely related to the pupil size time course, indicating an early onset of activation and a role in reward prediction processing. Pupil dilations were linked to increased activity in the salience network (dorsal ACC and bilateral insula), which likely triggers an increase in arousal to enhance task performance. Finally, increased pupil size preceding the required motor response was associated with activity in the ventral attention network. In sum, pupillometry provides an effective tool for disentangling different phases of reward anticipation, with relevance for affective symptomatology.

Introduction

Abnormalities in the processing of rewarding stimuli constitute a core symptom in various psychiatric disorders, including major depressive disorder (MDD), bipolar disorder and schizophrenia (American Psychiatric Association, 2013). For instance, reduced reward responsiveness (also referred to as anhedonia) in MDD has been linked to symptom severity (Vrieze et al., 2014), longer time to remission (McMakin et al., 2012) and poorer treatment outcome (Spijker et al., 2001). Previous studies employing reward learning paradigms have revealed that in comparison to healthy controls, MDD patients show reduced reward learning that was associated with self-reported anhedonic symptoms (Pizzagalli et al., 2008; Vrieze et al., 2013).

Reward processing involves two distinct temporal components: the anticipation of a positive stimulus and its pleasure-related consummation (Berridge, 1999). The reward anticipation phase has been suggested to involve a positive arousal response that is related to approach behavior (Knutson and Greer, 2008) and has been linked to motivation, attention and motor-preparation processes as well as goal-directed activity (Berridge et al., 2009; Klein, 1987; Sherdell et al., 2012; Whitton et al., 2015). Also, these processes are not necessarily bound solely to hedonic stimuli, but can become associated with reward-*predicting* cues as well, for example through a Pavlovian or instructed conditioning procedure (Sherdell et al., 2012). Interestingly, there is initial evidence that deficits in reward anticipation rather than reward consummation drive the reward-related abnormalities observed in depressive patients (Dichter, 2010; Sherdell et al., 2012) and individuals at risk for MDD (Olino et al., 2014).

Although the two reward processing components are strongly coupled, functional magnetic resonance imaging (fMRI) studies in humans have revealed that reward anticipation and consummation are in fact associated with the activity of distinct brain regions. For instance, previous studies have shown that reward anticipation involves increased activity in the ventral striatum (VS), ACC, bilateral anterior insula, inferior parietal lobule and brainstem, whereas the medial prefrontal cortex (mPFC), medial orbitofrontal cortex, and amygdala are more strongly activated during reward consummation (Knutson et al., 2001, 2003; Liu et al., 2011; Samanez-Larkin et al., 2007).

A recent study employing pupil size recordings in macaque monkeys by Rudebeck et al. (2014) could show that the reward anticipation phase is characterized by a sustained increase in pupil size, reflecting an increase in autonomic arousal. After lesions in the subgenual (and in some animals more dorsal) parts of the ACC, the macaque monkeys showed a failure to sustain this increased arousal during reward anticipation

* Corresponding author. Max Planck Institute of Psychiatry, Department of Translational Research in Psychiatry, Kraepelinstr. 2-10, 80804, Munich, Germany.
E-mail address: spoormaker@psych.mpg.de (V.I. Spoormaker).

https://doi.org/10.1016/j.neuroimage.2018.04.078
Received 19 December 2017; Received in revised form 28 March 2018; Accepted 30 April 2018
Available online 5 May 2018

(Rudebeck et al., 2014). The initial pupil dilation at onset of the reward cue was not affected, which would suggest that the actual prediction update was not affected by the lesion – and that pupillometry may be helpful to dissect different processes during the reward anticipation phase. Furthermore, its use in macaque monkeys and human subjects makes it a promising translational tool, which can be readily employed as a readout during simultaneous fMRI.

To date, relatively few fMRI studies have incorporated pupillometry during reward tasks (Bijleveld et al., 2009; Chiew and Braver, 2013, 2014; O'Doherty et al., 2003; Takarada and Nozaki, 2017), even though it provides a sensitive readout in addition to behavioral responses and an objective experimental control. To our best knowledge, the neural correlates of pupil dilations during reward anticipation are unknown. In previous fMRI/pupillometry studies, we were able to show that pupil dilations are strongly linked to activity in dorsal ACC (dACC) and bilateral insula (also referred to as the salience network) during both resting state and fear learning (Leuchs et al., 2016; Schneider et al., 2016).

This coupling of the salience network, particularly dACC, with spontaneous and fear-induced pupil dilations is in line with the observation that the dACC, as well as the lateral orbitofrontal cortex, are major input regions to the locus coerueleus (LC), the brainstem's noradrenergic arousal center (Aston-Jones and Cohen, 2005). In one human pupillometry/fMRI study employing neuromelanin-sensitive imaging, the LC and dACC were found to correlate with pupil size fluctuations during rest (Murphy et al., 2014). Moreover, spontaneous pupil fluctuations increase with increasing sleepiness (referred to as “pupillary unrest”; Lowenstein et al., 1963; Wilhelm et al., 1998), which in mildly sleep deprived subjects resulted in more pronounced correlations to the thalamus in addition to the dACC and insula (Schneider et al., 2016). Among others, activity in the dACC has been associated with the occurrence of sympathetic arousal reactions (e.g. skin conductance responses and increases in heart rate) and the insular cortices have been suggested to track changes in arousal states (Critchley, 2005; Critchley et al., 2000; Fredrikson et al., 1998). Based on this, we proposed that the pupil/salience network correlation observed in our previous studies may reflect fluctuations in arousal levels, and specifically in emotional arousal. This would make pupil dilation a primary readout for reward anticipation, akin to fear learning (Leuchs et al., 2016).

Here, we recorded the pupil size of healthy subjects while they performed a reward anticipation task inside the MRI scanner. We hypothesized that the reward-predicting stimuli would be associated with an increase in pupil size. Furthermore, in order to investigate the blood oxygen level dependent (BOLD) correlates of reward anticipation- (and consummation-) related pupil dynamics, we determined the pupil size and pupil change (first order derivative of pupil size) time course within the reward anticipation phase. We hypothesized that reward anticipation-related *changes* in pupil size would be associated with activity of the salience network.

Methods

Subjects

Forty-six healthy subjects (range: 20–41 years, mean [M] age = 28.02, standard deviation [SD] = 4.17, 25 female) participated in the study, as part of a larger in-house study (Biological Classification of Mental Disorders). All subjects were right-handed, non-smokers and had normal or contact lens corrected vision. Prior to participation, a general medical interview and an anatomical MRI screening were conducted to exclude subjects with present or past psychiatric and neurological disorders, structural brain abnormalities, as well as current use of psychotropic medication. The study protocol was in accordance with the Declaration of Helsinki and was approved by a local ethics committee. Subjects provided their written informed consent after the study protocol had been fully explained and were reimbursed for their participation.

Reward task

The reward task was largely adopted from Knutson et al. (2001) and modified for pupillometric recordings by using isoluminant stimuli. All stimuli were presented using Presentation Software (Neurobehavioral Systems Inc., Berkeley, California, USA) in a central position on a monitor located at the end of the scanner bore, and could be seen by the subjects through a first surface reflecting mirror that was attached to the head coil. The Shine toolbox (Willenbockel et al., 2010) was used in order to edit the three reward-predicting stimuli such that their mean luminance matched to the grey background (RGB-code: 153, 153, 153) on which all stimuli were presented (mean luminance across stimuli: M = 152.90, SD = 0.025).

At the beginning of each trial, a fixation cross was presented for a variable interval between 3 and 10 s. Next, one of three quadratic gabor patch stimuli featuring different stripe orientations (see Fig. 1) appeared for 6 s (reward anticipation phase). The presented stimulus either signaled the possibility to gain money (tilted stripes), to receive a non-monetary/“verbal” reward (vertical stripes), or no response requirement (control stimulus; horizontal stripes). In both reward conditions, the reward anticipation phase was followed by a brief flash of light (target stimulus; duration of 100 ms), to which subjects had to respond as fast as possible by pressing a button. In monetary reward trials, participants won 1 € if they pressed the button fast enough. This was indicated by a green euro symbol that was subsequently presented for 1.5 s. In the non-monetary reward trials, subjects could not win money for fast responding, but were nevertheless instructed to react as fast as possible in order to receive a green checkmark symbol (serving as a form of non-monetary/verbal reward). In both conditions, a red cross served as feedback for responses that were too slow. An adaptive algorithm ensured that participant would succeed on approximately 50% of his or her responses across the session, typically resulting in a total monetary reward of around 5 to 6 € (M = 5.67 €, SD = 1.24 €). The algorithm automatically adjusted the width of the response time window: For instance, if subjects responded fast enough, the response time window that defined button presses as sufficiently fast (vs. too slow) would get narrower, such that subjects would have to respond comparably faster in the next trial to continue getting rewards.

Compared to previous reward anticipation paradigms which involved a text-based feedback (e.g. “fast response!” vs. “slow response!”), we decided to use single digits/symbols (“€”, “✓”,“X”) as feedback stimuli in order to avoid saccades caused by reading, thus minimizing artifacts related to eye movement in the pupil data. The red and green color used for the feedback stimuli were matched to the luminance of the grey background (RGB-codes: 112, 176, 142 [green], 248, 111, 120 [red]). The respective feedback stimulus was then followed by a number indicating the subject's cumulative total at that point (e.g. “3€” following the third successful monetary reward trial), which was presented for 1.5 s. The control trials did not involve any light flash, therefore no response was required and neither a feedback stimulus nor a number indicating the cumulative total was presented.

The duration of a single trial was on average 14.41 s (SD = 3.25 s). The task involved 10 trials for each condition (i.e. 30 trials in total), lasting approximately 7.5 min. The three conditions were presented in a pseudo-randomized order, with no more than two subsequent trials of the same condition.

Procedure

Before performing the task inside the scanner, subjects received an instruction about the reward task in front of a computer outside the scanner. For this purpose, subjects were first familiarized with the three different gabor patch stimuli and informed about the corresponding conditions (i.e., tilted stripes = monetary reward trial, vertical stripes = non-monetary reward trial, and horizontal stripes = no reward trial), as well as the light flash/button press and feedback procedure. To

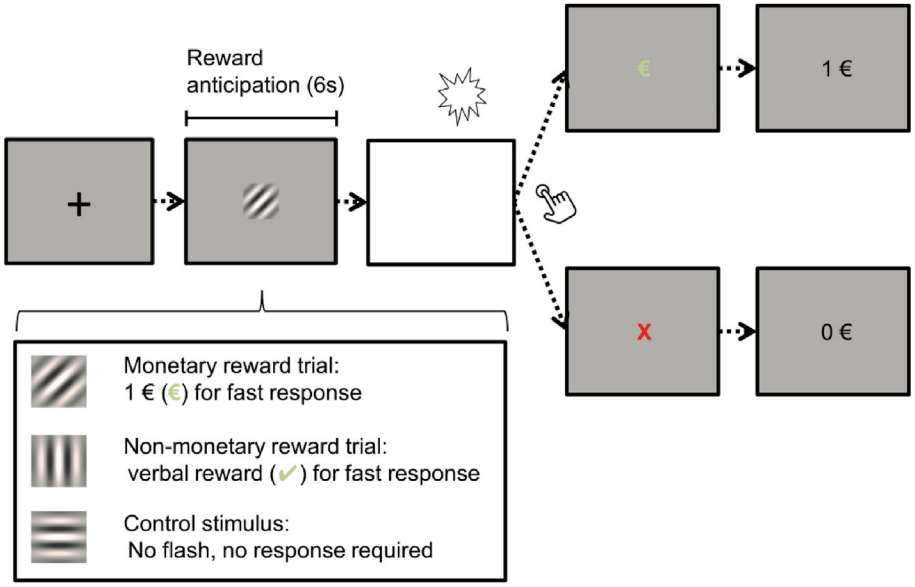

Fig. 1. Trial sequence. Subjects had to respond as fast as possible to a flash of light by pressing a button. The experiment involved three conditions, indicated by gabor patch stimuli presented for 6 s (reward anticipation phase): In monetary reward trials (tilted stripes), fast responses were rewarded with 1 €, indicated by a green euro symbol. In the non-monetary reward trials (vertical stripes), subjects could not gain 1 €, but were nevertheless instructed to react as fast as possible in order to receive a green checkmark symbol (verbal reward). Thresholds for a fast response time were adapted such that the subject would succeed in about 50% of trials. In both reward conditions, a red cross served as feedback for responses that were too slow. In the control trials (horizontal stripes), no flash appeared, therefore no response was required and no feedback was given.

make sure that subjects were aware of the instructed contingencies, they completed a 2-min training of the task outside the scanner without eye tracking (involving two trials per condition, the procedure of which was identical to the task inside the MR environment). After making sure that subjects had fully understood the task and clarification of potentially remaining questions, subjects were positioned in the scanner.

Behavioral data

To assess whether subjects showed faster responses for the monetary compared to the non-monetary reward condition (Knutson et al., 2001), we computed and tested the average reaction times across respective trials for each individual.

Pupillometry

Recording & preprocessing

For pupil size recordings, an MR-compatible eye tracker (EyeLink 1000 Plus; SR Research, Osgoode, ON, Canada) was placed at the end of the scanner bore and below the presentation monitor, such that the subject's right eye could be tracked via the head coil mirror. Pupil size was recorded in arbitrary units at a sampling rate of 250 Hz. In order to calibrate the eye gaze position on the monitor, a standard nine-point calibration procedure was conducted. Post-processing of the pupil data was performed in Matlab (version 2012a, MathWorks, Natick, USA). Here, eye blinks in the pupil data (resulting in zero-values) were replaced by interpolating values for the period from 100 ms before blink onset to 100 ms after blink offset. Blinks that occurred shortly after each other (<100 ms) were combined and treated as one single blink. To remove post-eye-blink-related artifacts, we semi-automatically adapted the standard interpolation window from 100 ms after blink offset to 200 ms after blink offset if necessary. After this procedure, the data were visually inspected to ensure that all artifacts had been successfully removed. No further manual corrections had to be applied. Finally, pupil data were smoothed by computing the mean of a 200 ms sliding window and z-transformed to control for variability in average pupil size across subjects.

Control for gaze shifts and eye blinks

In order to exclude subjects with suboptimal data quality, datasets with more than 15% blink/eye closure-related missing pupil values over the whole run (N = 7) were excluded, leaving 39 subjects for further pupil size-related analyses. Additionally, single trials containing more than 50% of interpolated data points were discarded (M = 0.31% of trials per subject, SD = 0.01%; see also Siegle et al., 2003; Visser et al., 2016; Visser et al., 2013). Since strong shifts in gaze can impair pupil detection, we also determined the gaze shift per trial for each subject. For this purpose, we first determined the median of the horizontal (x) and vertical (y) gaze data (within the 6 s anticipation time window) across all trials per subject, yielding a pair of coordinates that roughly indicates the center of the screen for each subject. Next, we computed the average standard deviations of the x (sd_x) and y gaze (sd_y) shift across all anticipation trials of all subjects (M(sd_x) = 92.50, SD(sd_x) = 55.77; M(sd_y) = 64.75, SD(sd_y) = 72.25), and defined a rectangular window of 3.3 standard deviations around each subject's center coordinates. If the subjects' gaze remained outside this window for longer than 1 s, the trial was discarded (see Supplementary Fig. S1 for an illustration of the gaze control analysis for one representative subject), akin to previous work (Leuchs et al., 2016; see Supplementary Fig. S1 for an illustration of the gaze control analysis for one representative subject). Based on this criterion, a total of 13 control trials, 27 non-monetary and 35 monetary reward trials (out of 39*10 = 390 trials per condition) had to be discarded in 23 subjects.

Quantification of the pupil response

Since we observed that the pupillometry-based discrimination between the three reward-predicting stimuli reached its maximum shortly before stimulus offset (i.e., just before presentation of the light flash in the reward conditions), we first calculated the pupil response for each trial by subtracting the pre-stimulus baseline (defined as average over the last 0.5 s before stimulus onset) from the maximum pupil size between 5 s and 6 s after stimulus onset (Fig. 2A).

In addition, to consider the temporal dynamics of the pupil-BOLD correlations during reward anticipation, a similar approach as used in previous work was employed (see Schneider et al., 2016). For this purpose, the 6 s reward anticipation time window was first divided into six 1-s time bins for each stimulus type. Next, average pupil size was computed for each bin by taking the mean over all pupil data points per bin (each 1-s bin contained 250 pupil data points). For reward trials, this procedure typically yielded a step-wise increase in average pupil values over time bins (Fig. 2C, top). Since previous findings showed a robust (positive) correlation of salience network activity with the *slope* of changes in pupil size rather than with pupil size per se (Schneider et al., 2016), we also determined the average pupil change per bin (Fig. 2C,

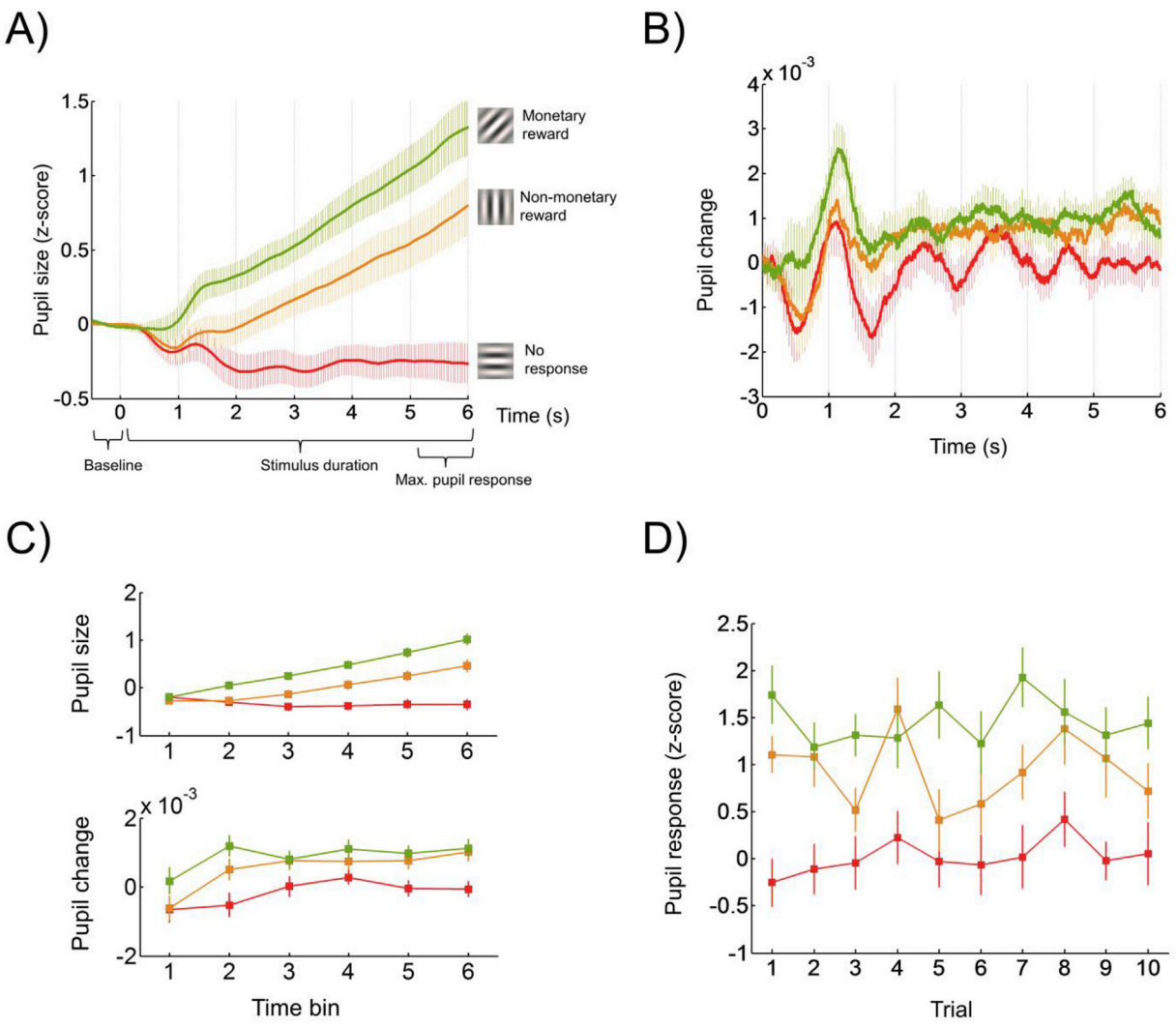

Fig. 2. Pupil size during reward anticipation. A) Pupil diameter (z-scores) in response to the three stimulus types during the reward anticipation phase (average across all subjects and trials). B) Pupil change (first order derivative of pupil size) during the three stimulus types, averaged across all trials from all subjects. C) Mean pupil size (top) and mean pupil change (bottom) per 1-s time bin, averaged across all trials from all subjects. D) Trial-wise pupil response magnitudes to the three stimulus types, averaged across all subjects. Trial-wise pupil response magnitudes were calculated by subtracting the pre-stimulus baseline (average over the last 0.5 s of the fixation cross period, i.e. 0.5 s before stimulus onset) from the maximum pupil dilation between 5 s and 6 s after stimulus onset (time window of interest, see Fig. 2A). Vertical bars indicate 95% confidence intervals.

bottom). To this end, we first computed the first order derivative of the pupil data vector (yielding the change in pupil size between consecutive pupil data points, with positive values reflecting pupil dilation and negative values reflecting pupil constriction, see Fig. 2B) and then calculated the mean of this pupil change vector per 1-s bin. This procedure yielded six pupil size and pupil change values for each of the ten reward anticipation periods within the three stimulus types.

Finally, pupil responses to the *feedback* stimuli were computed by subtracting the minimum pupil size during the light reflex-related pupil constriction from the maximum pupil size between 1 s and 2 s after feedback stimulus onset (Supplementary Fig. S2).

Pupil & response time

For exploring potential correlations between pupil size/change and (button-press) response time, we considered the trial-wise pupil response magnitude as well as the maximum, standard deviation and last value of the six mean pupil size/change values per trial (one per second). Next, we computed correlation coefficients between these trial-wise pupil readouts and reaction time within subjects, and tested the detected correlations for statistical significance using Wilcoxon signed rank tests.

fMRI

Preprocessing

Participants were scanned in a 3 T MRI Scanner (MR750, GE, Milwaukee, USA) using a 32-channel head coil, covering 40 slices (AC-PC-orientation, 96 × 96 matrix, 2.5 mm slice thickness, 0.5 mm slice gap, resulting voxel size 2 × 2 × 3 mm^3, echo planar imaging [EPI], TR 2.5 s, TE 30 ms, acceleration factor 2). The reward task comprised a total of 182 vol, of which the first four volumes (i.e. 10 s) were discarded to avoid non steady-state effects.

Preprocessing and analysis of the fMRI data was performed with Matlab (version 2012a, MathWorks, Natick, USA) and SPM8 (Statistical Parametric Mapping Software, Wellcome Department of Imaging Neuroscience, London, UK, http://www.fil.ion.ucl.ac.uk/SPM). Preprocessing involved slice time correction, motion correction through rigid body realignment to the mean volume, spatial normalization to the Montreal Neurological Institute (MNI) EPI template and resampling to a voxel resolution of 2 × 2 × 2 mm^3 using XYZ interpolation, as well as spatial smoothing using an isotropic Gaussian Kernel (full width at half maximum: 6 × 6 × 6 mm^3). In addition, the slice time corrected and

realigned data were normalized and resliced to a $4 \times 4 \times 4\,mm^3$ resolution in order to extract voxel-wise white matter (WM) and cerebrospinal fluid (CSF) signal time courses, using the a priori defined masks in SPM8. We then applied a principal component analysis to these time courses in order to identify the first three principal components per compartments (explaining 39.1–66.0% of the variance in the data), which were later used as nuisance regressors (CompCor correction; Behzadi et al., 2007). To account for motion-related signal changes, six motion regressors were extracted from the rigid body realignment step. Runs containing head movements larger than 2 mm between successive volumes were excluded. The three WM regressors, three CSF regressors, six motion regressors, as well as the absolute first order derivatives of these 12 regressors were included as nuisance regressors in all further general linear model (GLM) analyses.

Reward anticipation GLMs

Temporal dynamics of pupil size/pupil change. Separate first level GLMs were conducted for the binned pupil size and pupil change regressors. In both cases, the SPM design matrix involved three regressors (one per stimulus type) including the onset times of the six time bins (each modelled as an event of 1 s duration). To each regressor, the corresponding pupil values (i.e., either mean pupil size or mean pupil change of each 1 s bin) were entered as parametric modulations (see Supplementary Fig. S2A). We determined the average correlation to all pupil size/change regressors across stimulus types ([0 +1 0 +1 0 +1]), as well as the correlations to the individual pupil size/change regressor per stimulus type ([control stimulus: [0 +1 0 0 0 0], non-monetary reward: [0 0 0 +1 0 0], monetary reward: [0 0 0 0 0 +1]).

Pupil response magnitude. In order to both assess whether we would be able to replicate the results from the previously described GLMs and to provide a better comparability with previous work (Leuchs et al., 2016), we additionally modelled the reward anticipation periods as single events of 6 s duration. One single pupil response magnitude value (maximum pupil size between 5 s and 6 s minus baseline; see section "2.5 Pupillometry") was entered as parametric modulation to each stimulus event. Since this approach involved a design matrix that was very similar to the pupil size/change model (Supplementary Fig. S2B), the same first level contrasts as described above were used. In addition, stimulus contrasts were created, involving the contrasts "(monetary and non-monetary) reward stimuli > control stimulus" ([−2 0 +1 0 +1 0]) and "monetary reward > non-monetary reward stimulus" ([0 0 −1 0 +1 0]).

Reward consummation GLM

Finally, to reveal brain activity related to reward consummation, another GLM with separate regressors for the presentation times of the two reward ("€", "✓") and the negative feedback ("X") stimuli (modelled as events of 1.5 s duration) was set up, including the feedback-related pupil responses as parametric modulations. First level contrasts involved the differential contrasts "reward feedback stimuli > negative feedback stimulus" ([−2 0 +1 0 +1 0]) and "monetary reward feedback stimulus > non-monetary reward feedback stimulus" ([0 0 −1 0 +1 0]), as well as the positive correlation to all feedback stimulus-related pupil responses ([0 +1 0 +1 0 +1]).

Second level analyses

Second level GLMs were estimated using the above specified contrast images of the first level analyses of all subjects, and tested using one sample t-tests against zero (contrasts [+1] and [−1]). Furthermore, to investigate potential differences regarding the pupil-BOLD correlations between individual stimulus types, paired t-tests were conducted on the respective first level contrasts. After collecting clusters at uncorrected $p_{voxel} < 0.001$, statistical inference was based on whole-brain family-wise error (FWE) corrected cluster p-values, with $p_{cluster.FWE} < 0.05$ accepted as significance criterion.

Results

Response times

Subjects showed faster responses for the monetary compared to the non-monetary reward trials ($t_{(38)} = 2.54$, $p < .05$; monetary reward trial: $M = 235.79$ ms, $SD = 28.55$ ms; non-monetary reward trial: $M = 245.48$ ms, $SD = 35.99$ ms).

Pupillometry

Reward anticipation

Fig. 2A shows the mean pupil response to the three stimulus types during the reward anticipation phase, averaged across all trials from all subjects. Subjects exhibited a strong and continuous increase in pupil size in response to the monetary reward stimulus, reaching its maximum just before the light flash. The non-monetary reward stimulus similarly triggered a continuous increase in pupil size during this 6 s time window, which was less pronounced and did not reach the same magnitude as observed for the monetary reward stimulus. In contrast to both reward stimuli, the control stimulus did not cause a dilation of the pupil, but instead triggered a slight initial constriction of the pupil during the first 2 s, which remained small in size the following 4 s.

As mentioned earlier, we also computed the first order derivative of the pupil data vector, yielding a vector that describes the direction and magnitude of change in pupil size between consecutive data points. Fig. 2B shows the mean pupil change during presentation of the three stimulus types, averaged across all trials from all subjects. Pupil change was highest approximately 1 s after stimulus onset (i.e., corresponding to the second time bin in Fig. 2C bottom) and remained at a high level for both reward stimulus types. It is noteworthy that there was a lot of inter-individual variability in the mean pupil change vector over all trials (see Supplementary Fig. S4).

Fig. 2C shows the mean pupil size and mean pupil change for successive time bins of 1 s per stimulus type, averaged across all trials from all subjects. As expected, the binned pupil size (top) and pupil change (bottom) time courses showed a very similar pattern as described above for Fig. 2A and B.

Fig. 2D illustrates the pupil response magnitudes (computed as described in the section "2.5 Pupillometry") to the three stimulus types over trials, averaged across all subjects. The differences in pupil response magnitudes between stimulus types were apparent throughout the entire experiment. A repeated measures ANOVA including the mean pupil responses, averaged across all trials from all subjects, revealed a significant effect of stimulus type ($F_{(2,76)} = 124.60$, $p < .001$). Post-hoc t-tests yielded a significantly higher pupil response in the monetary ($M = 1.31$, $SD = 0.55$) vs. non-monetary reward condition ($M = 0.83$, $SD = 0.57$; $t_{(38)} = 5.99$, $p < .001$), as well as in the non-monetary reward vs. control condition ($M = 0.01$, $SD = 0.37$; $t_{(38)} = 10.00$, $p < .001$).

Testing for correlations between trial-wise pupil readouts and response times yielded the following results: For both monetary and non-monetary reward trials, the Wilcoxon signed rank tests yielded weak but significant, negative correlations for the last pupil size value before the flash (monetary: $M = -0.14$, $SD = 0.39$, $z = -2.32$, $p < .05$; non-monetary: $M = -0.15$, $SD = 0.36$, $z = -2.34$, $p < .05$), as well as the last pupil change value before the flash (monetary: $M = -0.19$, $SD = 0.40$, $z = -2.61$, $p < .05$; non-monetary: $M = -0.17$, $SD = 0.33$, $z = -2.85$, $p < .05$), indicating that larger pupil size and stronger increase in pupil size shortly before the flash were associated with faster responses.

Reward consummation

Supplementary Fig. S2 shows the mean pupil response to the three

feedback stimulus types, averaged across all trials from all subjects. After recovering from the constriction caused by the pupillary light reflex to the light flash, pupil size slowly decreased in a similar way across feedback stimulus types. A repeated measures ANOVA including the feedback-associated pupil responses (computed as described in section "2.5 Pupillometry"; averaged across all trials from all subjects) revealed a significant effect of stimulus type ($F_{(2,76)} = 11.80$, $p < .001$). Post-hoc t-tests yielded a significantly stronger pupil response to the negative feedback ($M = 3.24$, $SD = 0.91$) compared to both the non-monetary ($M = 2.98$, $SD = 0.99$; $t_{(38)} = 4.48$, $p < .001$) and monetary reward feedback ($M = 3.05$, $SD = 1.01$; $t_{(38)} = 3.51$, $p < .05$). No significant difference was observed between the monetary and non-monetary reward feedback-related pupil responses.

fMRI

fMRI reward anticipation stimulus contrasts

The contrast "reward stimuli > control stimulus" ([−2 0 +1 0 +1 0], design matrix see Supplementary Fig. S3B) revealed bilateral activity in the inferior frontal gyrus, middle cingulate gyrus, supplementary motor area (SMA), inferior parietal lobules, inferior/middle occipital cortex, insula, thalamus, caudate nucleus/VS, brainstem (peak voxel coordinates: [x y z] = [−4 −26 −22]) and cerebellum (Fig. 3A). The reverse contrast "control stimulus > reward stimuli" ([+2 0 −1 0 −1 0]) revealed significant, bilateral clusters of activation in middle/posterior cingulate gyrus, precuneus, medial frontal regions, middle occipital gyrus, angular gyrus and temporal regions. These clusters also survived voxel-wise FWE correction for multiple comparisons ($p_{FWE} < 0.05$), see Supplementary Fig. S6 and Table S1A.

The contrast "monetary reward stimulus > non-monetary reward stimulus" ([0 0 −1 0 +1 0]) revealed activation in bilateral clusters covering middle cingulate gyrus, SMA, insula, inferior/middle occipital gyrus, thalamus and cerebellum (Fig. 3B and Table S1B). The reverse contrast "non-monetary reward stimulus > monetary reward stimulus" ([0 0 +1 0 −1 0]) showed clusters in left angular gyrus, left inferior parietal lobule and bilateral precuneus.

Neural correlates of reward anticipation-related pupil dynamics

Temporal dynamics of pupil size. The GLM of the mean pupil size values per 1-s time bins revealed significantly correlated activity in several contrasts: First, the contrast including the mean pupil size values across stimulus types ([0 +1 0 +1 0 +1]) showed significant activity in bilateral inferior frontal gyrus, right middle frontal gyrus and right superior temporal pole/middle temporal gyrus (Fig. 4A and Supplementary Table S2A). The negative contrast ([0 −1 0 −1 0 −1]) revealed corresponding deactivation in clusters including bilateral cuneus, SMA, superior/middle occipital gyrus, as well as in a cluster comprising bilateral caudate nucleus, putamen and globus pallidus (including VS). It should be noted that the mean pupil size values were typically lowest at stimulus onset and increased throughout stimulus duration (see Fig. 2C top), meaning that the negative correlation of this pupil size time-course with the striatal cluster implies a mirrored time-course for this cluster (i.e., highest activity at stimulus-onset).

Second, in order to assess the extent to which the various stimulus types contributed to the observed pupil size-BOLD correlations, we additionally investigated the contrasts which only included the monetary reward-related ([0 0 0 0 0 +1], see Supplementary Fig. S3), non-monetary reward-related ([0 0 0 +1 0 0]) and control stimulus-related average pupil size values ([0 +1 0 0 0 0]). The monetary reward contrast revealed very similar clusters as the contrast across stimulus types, involving positively correlated activity in bilateral inferior/middle frontal gyrus and bilateral middle temporal gyrus, as well as negatively correlated activity in bilateral SMA, superior/middle occipital gyrus and VS (Fig. 4B and Table S2B). Regarding the non-monetary reward-related pupil size correlations, activation was restricted to the right inferior/middle frontal gyrus, and deactivation was mainly confined to bilateral SMA (Fig. 4C and Table S2C). The pupil size-BOLD correlations were least pronounced in the control stimulus contrast (Fig. 4D and Table S2D), which only showed activation in a cluster within the right inferior frontal gyrus, but no significant deactivation.

For an overview of the paired *t*-test results, see Supplementary Table S3. Interestingly, the paired *t*-test of the control > monetary reward

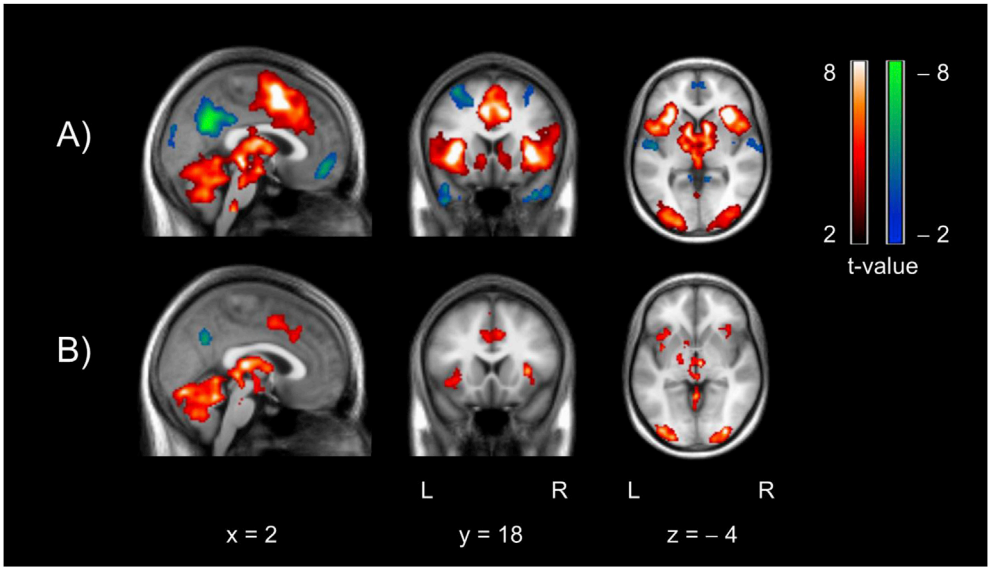

Fig. 3. Activity associated with the stimulus contrast "reward stimuli > control stimulus" (A) and "monetary reward > non-monetary reward stimulus" (B). In A), hot colors reflect brain areas that showed increased activity during both monetary and non-monetary reward stimulus presentations compared to control stimulus trials. Statistical maps were sampled at uncorrected $p < .001$ and clusters were thresholded at a cluster-wise $p_{FWE} < .05$ (resulting in an effective cluster extension threshold of $k = 100$ for display purposes). Supplementary Fig. S6 shows the same contrasts after applying *voxel*-wise FWE correction for multiple comparisons ($p_{FWE} < 0.05$). See Supplementary Table S1A for further information on cluster extents and peak voxel coordinates. In B), hot colors illustrate brain regions that showed stronger activity during monetary compared to non-monetary reward stimulus presentations. Cool colors reflect the reverse pattern, respectively. Statistical maps were sampled at uncorrected $p < .001$ and clusters were thresholded at a cluster-wise $p_{FWE} < .05$ (resulting in an effective cluster extension threshold of $k = 100$ for display purposes). See Supplementary Table S1B for further information on cluster extents and peak voxel coordinates. Coordinates [mm] refer to MNI space.

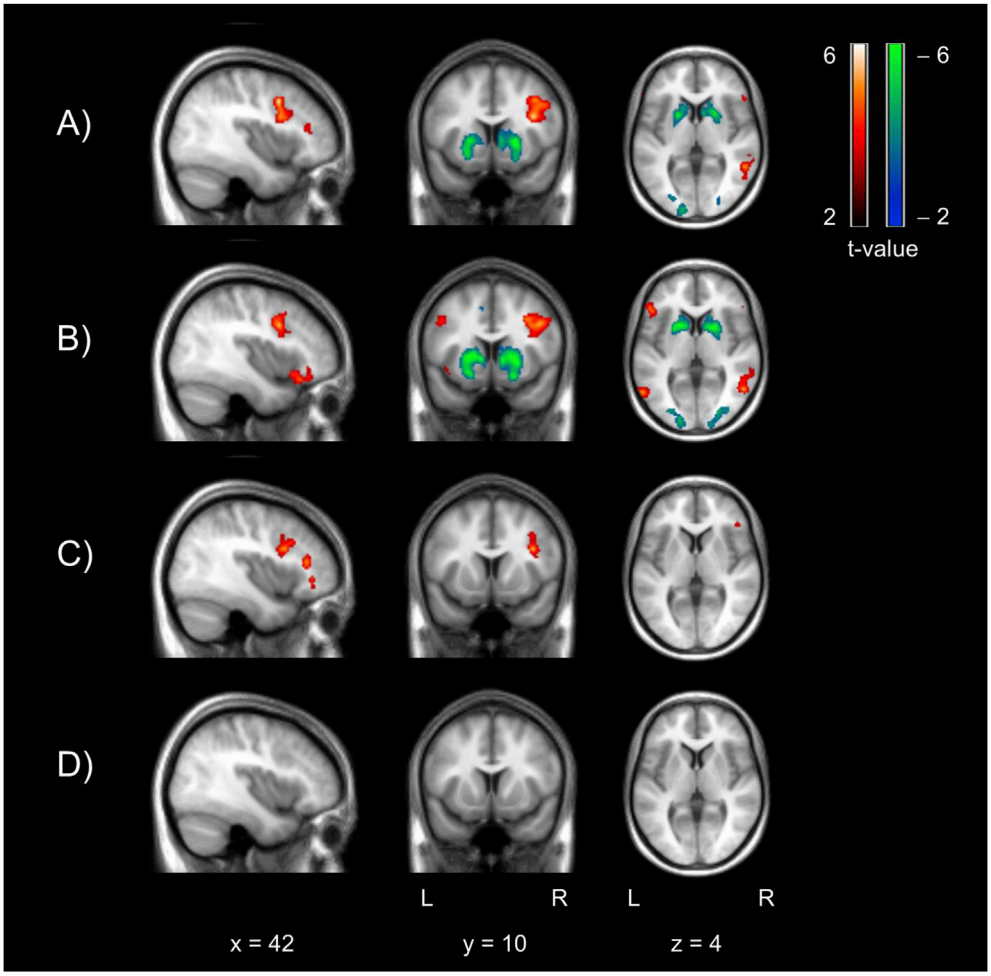

Fig. 4. Neural correlates of reward anticipation-related pupil size. The 6 s reward anticipation time window was divided into time bins of 1 s, and average pupil size was computed for each bin, typically yielding a step-wise increase in average pupil size over time bins during reward trials (see Fig. 2B top). Figure A) shows the BOLD correlates of average pupil size across all stimulus types, while B) to D) separately illustrate activity correlated to average pupil size during monetary reward (B), non-monetary reward (C), and control stimulus trials (D), respectively. Hot colors show brain regions with activity that was positively correlated to the pupil size time course, i.e., regions showing a peak of activity towards the end of reward anticipation, while cool colors depict negative correlations, i.e., regions with strongest activity at the beginning of stimulus presentation. Statistical maps were sampled at uncorrected $p < .001$ and clusters were thresholded at a cluster-wise $p_{FWE} < .05$ (resulting in an effective cluster extension threshold of $k = 100$ for display purposes). Coordinates [mm] refer to MNI space. See Supplementary Tables 2A – D for further information on cluster extents and peak voxel coordinates.

stimulus-associated pupil-BOLD correlations yielded significant striatal activation. This is because we observed negative pupil-BOLD correlation in the striatum during monetary reward trials as mentioned before, and no significant correlations during control trials.

Temporal dynamics of pupil change. The contrast of the parametric modulation including the mean pupil change values (1-s time bins) across all stimulus types ([0 +1 0 +1 0 +1]) revealed positively correlated, activity in bilateral anterior/middle cingulate gyrus, inferior frontal gyrus, SMA, supramarginal gyrus, insula, temporal regions and thalamus (Fig. 5A and Supplementary Table S4A). Negatively correlated activity was located bilaterally in middle/posterior cingulate gyrus, precuneus, inferior parietal lobules, angular gyrus and occipital cortex. The contrast of this modulation to monetary reward-related pupil change only ([0 0 0 0 0 +1]) revealed significant, bilateral activation in middle cingulate gyrus, SMA, supramarginal gyrus and thalamus, as well as deactivation in left angular gyrus and right occipital cortex (Fig. 5B and Table S4B). In the non-monetary reward contrast ([0 0 0 +1 0 0]), positive pupil change-BOLD correlations were located bilaterally in inferior frontal gyrus, calcarine gyrus, lingual gyrus, middle temporal gyrus, insula, thalamus and left caudate nucleus (Fig. 5C and Table S4C). No significant negative correlations were apparent in this contrast. The control stimulus contrast ([0 +1 0 0 0 0]) only yielded negatively correlated activity in visual regions, including bilateral middle occipital gyrus and fusiform gyrus, but no positive correlations (Fig. 5D and Table S4D). Paired t-tests between the stimulus type-specific pupil change-BOLD correlations primarily revealed activation in visual cortices, for an overview see Supplementary Table S5.

Temporal dynamics: additional analyses. To further investigate the temporal dynamics of brain activity related to pupil size/change, we additionally extracted reward anticipation-related BOLD signal time courses from several regions of interest (ROIs): dACC, right insula, mPFC, thalamus, VS and inferior frontal junction (IFJ), see also the Supplementary Material section "1.3 Temporal dynamics: Additional analyses" for more details on the methods. These analyses revealed that regions show a similar BOLD signal time course as suggested by their individual correlation with the temporal pupil dynamics regressors. For instance, the VS shows an early peak of activity followed by a prolonged decrease in activity, while the IFJ shows comparably late activation. In contrast, the activation of dACC and insula seems to occur somewhere in between (Supplementary Fig. S7).

Another approach to investigate these temporal dynamics of reward anticipation is to subdivide the 6 s time window into smaller time windows and to compare brain activity associated with each window (Supplementary Material section "1.3 Temporal dynamics: Additional analyses"). When contrasting the early, middle and late phases of monetary reward stimulus presentation using time bins from 0–2 s, 2–4 s and 4–6 s following stimulus onset, we found a similar sequence of brain activation as suggested by the pupil-BOLD correlations (Supplementary Fig. S8). The VS shows increased activity in the early phase compared to the middle and late phase of reward anticipation. In contrast, dACC and insula activation is strongest during the middle phase, while IFJ activity peaks in the late phase of reward anticipation.

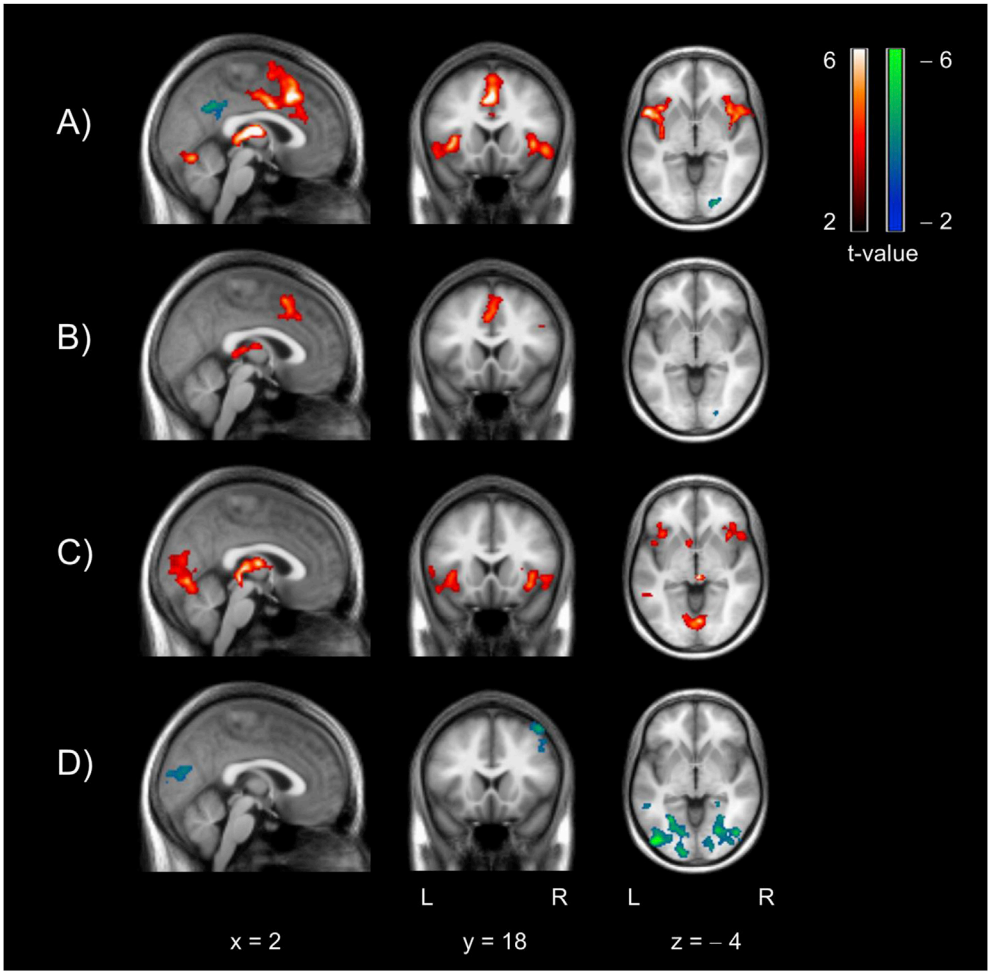

Fig. 5. Neural correlates of reward anticipation-related pupil change. Here, the average pupil change (i.e., the first order derivative of pupil size) was computed for time bins of 1 s within the reward anticipation time window. The resulting time course showed a strong pupil dilation after 1–2 s following reward stimulus onset (see Fig. 2B bottom). A) shows the BOLD correlates of average pupil change across all stimulus types, while B) to D) separately illustrate activity correlated to average pupil change during monetary reward (B), non-monetary reward (C), and control stimulus trials (D), respectively. Hot colors show brain regions with activity that was positively correlated to the pupil change time course, while cool colors depict regions with negatively correlated activity. Statistical maps were sampled at uncorrected $p < .001$ and clusters were thresholded at a cluster-wise $p_{FWE} < .05$ (resulting in an effective cluster extension threshold of $k = 100$ for display purposes). Coordinates [mm] refer to MNI space. See Supplementary Tables S4A – D for further information on cluster extents and peak voxel coordinates.

Pupil response magnitude. The positive contrast including all pupil response magnitudes (from baseline to the last second of the stimulus) across stimulus types ([0 +1 0 +1 0 +1]) revealed activation in bilateral middle cingulate gyrus, SMA, supramarginal gyrus, superior temporal gyrus, rolandic operculum, insula, as well as activation in a striatal cluster comprising left caudate nucleus, putamen and globus pallidus (Fig. 6A and Supplementary Table S6A). The negative contrast yielded bilateral clusters in medial frontal gyrus, middle/posterior cingulate gyrus, precuneus, superior parietal gyrus, inferior parietal lobules, angular gyrus and middle occipital gyrus.

The contrast only including the monetary reward-related pupil response magnitudes ([0 0 0 0 0 +1]) yielded similar, albeit slightly weaker activation in middle cingulate gyrus, SMA, inferior frontal gyrus, rolandic operculum and insula (Fig. 6B and Table S6B). No significant deactivation was observed in this contrast. The contrast of the non-monetary reward-related pupil response magnitudes ([0 0 0 +1 0 0]) revealed deactivation in bilateral precuneus, as well as right angular gyrus and right middle occipital gyrus, but no significant activation (Fig. 6C and Table S6C). The control stimulus-related pupil response magnitude ([0 +1 0 0 0 0]) was positively correlated to bilateral activity in anterior/middle cingulate gyrus, SMA, rolandic operculum and insula (Fig. 6D and Table S6D). Negatively correlated activity was observed bilaterally in inferior parietal lobules, angular gyrus and middle occipital gyrus.

Paired t-tests between the control stimulus and reward stimulus-associated pupil-BOLD correlations revealed stronger activation within right inferior parietal lobule and angular gyrus in both the monetary and non-monetary reward contrast. For an overview see Supplementary Table S7.

Neural correlates of reward feedback

Analysis of the feedback stimulus presentations (i.e. reward outcome phase) revealed stimulus/task effects that were in line with previous work, see Supplementary Fig. S9 and Tables S8A – B. Contrasts of the pupil responses to the feedback stimuli did not reveal any significant correlations.

Discussion

Our results show that subjects responded with a strong and continuous increase in pupil size to a stimulus that signaled the possibility to earn a monetary reward, providing first evidence that pupil dilation tracks reward anticipation-related increases in autonomic arousal in humans. We also observed weaker pupil dilations during presentation of the stimulus that signaled the possibility to receive a verbal reward, probably reflecting the subjects' comparably reduced effort during trials in which no monetary gain was possible. In both reward conditions, large pupil size and strong pupil dilation during the last second of reward anticipation were associated with faster response times, suggesting that increased arousal shortly before the light flash had a positive effect on task performance. In contrast, trials in which no response was required and no reward could be achieved involved a constriction of the pupil, indicating a decrease in the subjects' arousal levels (or in other words, increased relaxation).

Analysis of BOLD activity linked to reward anticipation yielded similar neural correlates as reported in previous studies (Haber and Knutson, 2010; Knutson et al., 2001). Compared to control trials, presentation of the two reward-predicting cues evoked a strong bilateral brain activation pattern including dACC and insula (salience network),

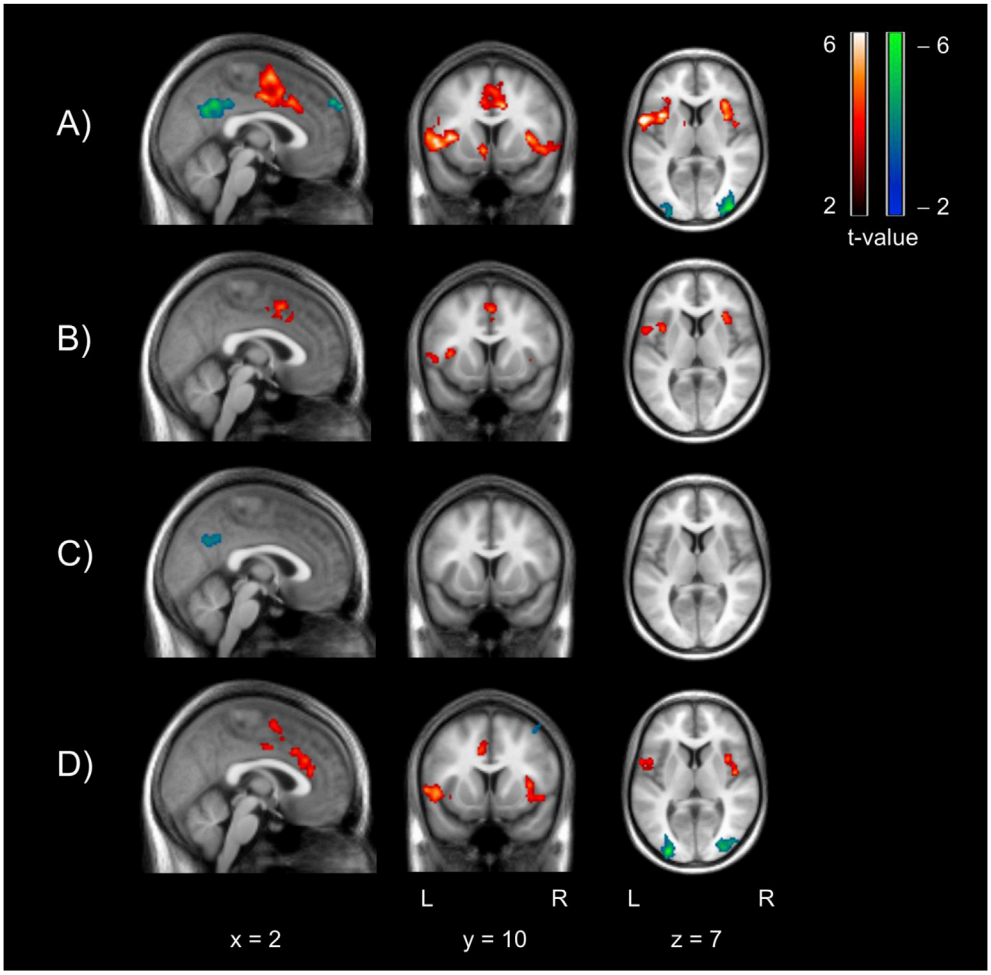

Fig. 6. Neural correlates of pupil response magnitude. In this GLM, pupil response magnitudes (maximum pupil size during last second of reward anticipation minus baseline value, see Fig. 2A) were entered as parametric modulations to the onset times of the three stimulus types (modelled as events of 6 s duration, see Supplementary Fig. S3B). Fig. 6A) shows the BOLD correlates of pupil response magnitudes across all stimulus types, while B) to D) separately illustrate activity correlated to pupil response magnitudes during monetary reward (B), non-monetary reward (C), and control stimulus trials (D), respectively. Hot colors reflect brain regions with BOLD activity that is positively correlated to pupil response magnitude, while colors depict regions with negatively correlated activity. Statistical maps were sampled at uncorrected $p < .001$ and clusters were thresholded at a cluster-wise $p_{FWE} < .05$ (resulting in an effective cluster extension threshold of $k = 100$ for display purposes). Coordinates [mm] refer to MNI space. See Supplementary Tables S6A – D for further information on cluster extents and peak voxel coordinates.

SMA, thalamus, VS and brainstem. In contrast, control trials involved increased activity in areas belonging to the default mode network (DMN), including mPFC, precuneus, angular gyrus and inferior parietal lobules.

In order to further disentangle the reward anticipation phase, we computed the average pupil size and average pupil change for consecutive time bins spanning 1 s and determined the BOLD correlates of the resulting pupil size and change regressors, respectively. The pupil data and its neural correlates both revealed three rather different phases of reward anticipation: First, activity in the VS was inversely related to the pupil size time course, indicating an early activation of the VS right after stimulus onset (when pupil size was at its trough) and a subsequent decline of activity over the course of the reward anticipation time window. Previous neuroimaging studies in human subjects have shown that during reward learning, the VS shifts its response from the time of reward presentation to the onset time of reward-predicting cues, an activity pattern that is well described by prediction error models (Garrison et al., 2013; McClure et al., 2003; O'Doherty et al., 2003). In the present study, subjects completed a short training of the task before performing the task inside the scanner, ensuring that subjects had learnt the reward contingencies before fMRI recordings started. Therefore, the early response in the VS just after stimulus onset (when pupil size was small) is likely to reflect reward prediction signaling.

Second, the pupil change time course showed a group mean peak in the second time bin of reward trials, indicating a strong increase in pupil size 1–2 s after onset of the reward-predicting stimulus. In line with a previous resting state fMRI/pupillometry study (Schneider et al., 2016), we found that such a pupil change regressor was positively correlated with activity in the salience network (including dACC, bilateral insula), suggesting that the these regions showed increased activity during periods of high pupil dilation magnitude. Negatively correlated activity was found in regions belonging to the DMN, which typically show deactivation during goal-directed tasks (Raichle, 2015; Shulman et al., 1997). It is worth mentioning that even though a peak of the group mean was observed within the first 2 s, the pupil dilation (change) time-course showed much inter-individual variability with frequent later dilations during reward anticipation (see Supplementary Fig. S4 for some representative examples). Therefore, a pupillometric dissection of reward anticipation only partially overlaps with a temporal dissection of reward anticipation (e.g., contrasting the early, middle and late phases in bins from 0–2 s, 2–4 s and 4–6 s), at least regarding the neural correlates (Supplementary Fig. S8). The correlation between pupil dilation and the salience network could also be reproduced when applying a slightly different analysis approach as used in a previous fear conditioning study (Leuchs et al., 2016), including one single pupil response magnitude value obtained by computing the difference between the maximum pupil value during the last second of reward anticipation and the baseline pupil value.

The insular cortex has been suggested to represent the input component of the salience network (Medford and Critchley, 2010), and is most likely involved in the integration of internal arousal states with appraisal of external emotional stimuli (Critchley, 2005). In line with this, Rothkirch et al. (2014) revealed that reward-related responses in anterior insula (and ACC) were attention-dependent, likely reflecting a more conscious evaluation of sensory information with respect to motivational value. Increased dACC activity has previously been linked to the

occurrence of autonomic arousal responses such as pupil dilation and skin conductance responses (Critchley, 2005; Joshi et al., 2016), giving rise to the notion that the dACC is involved in the modulation of arousal levels according to situational requirements. In addition, the dACC shows strong interactions with the SMA and has been associated with motor response preparation, promoting a role of the dACC as output component within the salience network (Asemi et al., 2015; Paus, 2001; Sheth et al., 2012). Based on these findings, it seems plausible that the integration of a motivational salience signal (generated in the VS) and current arousal state within the insular cortex is followed by an activation of dACC that initiates an adjustment of arousal levels required for optimal task performance.

We assume that this modulation of arousal is likely to be mediated by projections from dACC to LC, triggering increased noradrenergic activity and the observed pupil dilation, as LC activity is known to be modulated by dACC via reciprocal connections (Aston-Jones and Cohen, 2005). A recent study by Joshi et al. (2016) in macaque monkeys provided evidence that pupil-related modulations of neuronal activity in ACC occasionally show an earlier timing compared to LC, indicating a signal transmission from ACC to the LC. Given the broad evidence that the dACC/salience network is strongly involved in the detection of salient stimuli (Menon and Uddin, 2010), performance monitoring (Botvinick et al., 2004) as well as adjustments in pupil-linked arousal (Ebitz and Platt, 2015; Joshi et al., 2016), we are inclined to interpret the pupil-BOLD correlations observed in the present study to result from top-down projections from dACC to LC. However, we cannot exclude that the observed correlations in the dACC could also result from a reverse signal transmission, that is, LC projecting to dACC.

Finally, at the group level, the "increasing arousal" phase was followed by a phase in which pupil size remained large. Activity in regions belonging to the ventral attention network (including IFJ and temporoparietal junction [TPJ]) was positively correlated to the pupil size time course, implying that these regions showed a peak of activity towards the end of the reward anticipation trial. Previous studies have linked these regions to continuous maintenance of attentional focus, also referred to as preparatory or vigilant attention (Langner and Eickhoff, 2013; Petersen and Posner, 2012; Robertson and Garavan, 2004). More precisely, the IFJ has been suggested to mediate the detection of action-relevant stimuli, as well as the mapping between the target stimulus and the instructed motor response (Chikazoe et al., 2009; Langner and Eickhoff, 2013). The TPJ is assumed to be involved in reorienting of attention (or in other words, refocusing) whenever attention drifts away from the task (Langner and Eickhoff, 2013; Weissman et al., 2006). Actually, the control over these attention-reorienting processes has been attributed to the dACC, based on its accepted role in performance/error monitoring (Langner and Eickhoff, 2013; Ridderinkhof et al., 2004; Weissman et al., 2006) which loops back to the above suggested dACC-centered second phase. Taken together, it seems that the final stage of reward anticipation is characterized by preparatory or vigilant attention, during which subjects – in a state of high arousal – await and prepare for the light flash/motor response.

Regarding the reward consummation period, we found a stronger pupil response to the negative feedback stimulus, that is, when subjects were informed that their response was too slow. A previous study (Preuschoff et al., 2011) provided evidence that outcome-related pupil responses do not signal reward per se, but surprise, irrespective of outcome valence (win or loss). Since our paradigm involved an adaptive algorithm which ensured a success rate of 50%, it seems likely that subjects may have been surprised when they received feedback that a rather fast response time (which was rewarded in a previous trial) did no longer lead to a reward. However, the reward consummation phase did not involve any significant pupil-BOLD correlations. This might be due to the rather short duration of the reward feedback stimulus presentation (1.5 s) and its short temporal distance to the light flash, which could have masked potential correlations.

Affective states are assumed to involve at least two independent dimensions: valence and arousal (Knutson et al., 2014; Russell, 1980). Previous neuroimaging studies on reward anticipation have occasionally included a loss condition in the paradigm to disentangle brain activity related to positive and negative valence. For instance, it has been shown that the nucleus accumbens responds only to gain (but not loss) anticipation with increased activity, whereas the insula shows similar increases in activity during both gain and loss anticipation (Knutson et al., 2008). Also, in a previous fear learning study, we were able to show that the pupil shows a similar response to stimuli that predicted administration of an electric shock to the wrist. Here too, pupil dilations were found to be positively correlated with dACC activity (Leuchs et al., 2016), supporting the notion of a valence-independent arousal response. Future studies could address the presumed valence-independency of pupil dilation by including an additional loss anticipation condition.

Finally, measuring pupil responses to reward-predicting stimuli might also turn out to be informative in a more clinical context. For instance, it is conceivable that pupil readouts could provide a biological marker for disturbed reward processing in psychiatric patients with anhedonia, who may show a reduced reward-related pupil dilation. Also, there is initial evidence that pupil dilation is sensitive to serotonin and norepinephrine reuptake inhibitors (SNRIs) like Venlafaxin (Siepmann et al., 2007). Therefore, in future studies, it would be an interesting venue to use pupillometry to track disease/treatment progress in patients with anhedonia symptomatology after the start of medication.

Methodological considerations

Previous single cell recordings in macaque monkeys and human fMRI experiments have revealed a strong link between LC activity and pupil size (Aston-Jones and Cohen, 2005; Joshi et al., 2016; Murphy et al., 2014). In the present study, however, we did not observe any significant pupil-BOLD correlations in the brainstem. The reason for this could be that whole-brain coverage fMRI recording as used in this study is not sensitive enough to detect the proposed correlation in the LC, which contains no more than 50,000 neurons (Mouton et al., 1994). Future studies could address this issue by employing brainstem fMRI (at higher field strength), taking into account recent suggestions regarding LC fMRI by Liu et al. (2017).

To assess whether reward anticipation-related pupil dilation and pupil-BOLD correlations were confounded by eye movements or blinks/eye closures, we also tested for differences in the extent of gaze shifts and blinks during the anticipation phase between the three conditions (see Supplementary Material sections "1.1 Additional analyses on eye movements" and "1.2 Additional analyses on eye blinks"). These analyses revealed that the conditions in fact differed in terms of gaze shifts and blink frequency. Controlling for gaze shifts within our GLMs did not influence the pupil-BOLD correlations (Supplementary Figures S10 – 12), however, controlling for eye blinks lead to several additional analyses.

First of all, we found that eye blinks were less frequent during reward trials, and generally occurred most frequently within the first 2 s of stimulus presentation, strongly decreasing in the following seconds (Supplementary Figures S13A – B). We controlled for these blink-related differences by including an additional blink regressor in the GLMs and excluding trials with excessive blinking (Supplementary Figures S14 – 16). We observed that a parametric modulation which quantified the extent of blinking per second was associated with activity in several regions that had been linked to pupil size/change in our previous analyses, abolishing the originally observed pupil change-BOLD correlations revealed by the second parametric modulation (which was orthogonal to the first). When comparing trials with eye blinks in the first 2 s to trials without any eye blinks in the first 2 s, we found that blinking was actually associated with *reduced* pupil dilation (Supplementary Fig. S13C), suggesting that increased pupil dilations (and increased correlations with the dACC and insula) are not due to blink-related pupil artifacts. Moreover, the GLM excluding trials with excessive blinking revealed a very similar map (however at a lower threshold due to fewer

trials).

To investigate whether the reduction of pupil-BOLD correlations after controlling for eye blinks was due to the specific task (i.e., task-induced blinking) or constituted a more general feature, we applied a very similar analysis pipeline to a resting state data set from a previous study (see Schneider et al., 2016). Here, controlling for blinking in an identical way did not have an impact on the pupil-BOLD correlations (Supplementary Fig. S17), confirming the notion of a stimulus-induced temporal coincidence between blinking and pupil dilation during reward anticipation. From the literature, it is well known that blink timing is related to explicit attentional breaks (Drew, 1951; Fukuda, 1994; Hall, 1945; Nakano et al., 2009; Stern et al., 1984), i.e. blinks typically occur immediately before and after a task to prevent temporal loss of critical visual information. In the present study, reduced blinking in the reward conditions and the declining blink rate over time presumably reflects a suppression of blinks towards the end of reward anticipation, preventing subjects from missing the light flash due to eye closure.

Another issue concerns whether neural correlates can be reliably modelled for changes in pupil size on a time scale of single seconds (as assumed for the temporal dynamics GLMs), given that the hemodynamic response function (HRF) is slow and prolonged. We compared the HRF-convolved pupil regressors from the temporal dynamics of pupil change model to the ones from the pupil response magnitude model, which modelled the reward anticipation time window as one single stimulus event of 6 s duration (instead of six stimulus events of 1 s duration). The regressors from the two models did show differences despite the "blurring" by the HRF (Supplementary Fig. S18). Although the "temporal dynamics"-associated fluctuations within trials often appeared to be rather small compared to the differences between trials, consideration of intra-trial pupil fluctuations appears to increase sensitivity, manifest in the statistical parametric maps. This notion is also supported by our observations from the ROI time course analyses and the GLM involving a temporal dissection of reward anticipation based on 2 s time bins, yielding brain activity related to early, middle and late phases of reward anticipation. Taken together, these findings suggest that it is possible to disentangle different phases of reward anticipation using combined fMRI/pupillometry, even though a precise per-second disentanglement might not be possible.

Finally, since the control trials in the present study did not require any motor response, one might argue that the pupil dilations we observed during the reward trials might simply relate to motor preparation processes. To investigate this issue, we conducted an additional experiment outside the MR scanner comprising an additional control stimulus that did require a motor response, which however was not followed by any reward or feedback stimulus (Supplementary Fig. S5). Presentation of this stimulus type did not evoke a comparable increase in pupil size as observed for the two reward stimuli. Therefore, despite an intrinsic coupling between reward anticipation and motor preparation, we can rule out that pupil dilations during reward anticipation are solely caused by motor preparation.

Conclusion

Pupil dilation during reward anticipation differentiates between reward conditions and appears to reflect anticipatory arousal, involving strongest magnitudes in response to a stimulus that predicts a monetary reward. These increases in pupil size during reward anticipation could not be explained by motor preparation-related processes alone. Activity in the VS was inversely related to pupil size time course, indicating an early onset of activity which is presumably linked to the signaling of the stimulus' motivational salience and reward prediction. Reward anticipation-related changes in pupil were associated with activity in the salience network (including dACC and insula), which seems to initiate an increase in arousal to ensure optimal task performance. Finally, increased pupil size preceding the occurrence of the target stimulus was associated with increased activity in regions of the ventral attention network, probably reflecting vigilant attention of subjects expecting the target stimulus.

In sum, pupillometry appears to be an effective tool for disentangling different phases of reward anticipation, involving reward prediction, modulation of arousal and attention-related processes. Such an additional window of access to reward anticipation may be useful for studying affective disorders such as unipolar and bipolar depression that are characterized by complex combinations of disturbances of the reward system, arousal and attention.

Acknowledgements

The authors would like to thank Ines Eidner and Anna Hetzel for their support in collecting the data.

Appendix A. Supplementary data

Supplementary data related to this article can be found at https://doi.org/10.1016/j.neuroimage.2018.04.078.

References

American Psychiatric Association, 2013. Diagnostic and Statistical Manual of Mental Disorders, fifth ed. American Psychiatric Association, Arlington, VA.

Asemi, A., Ramaseshan, K., Burgess, A., Diwadkar, V.A., Bressler, S.L., 2015. Dorsal anterior cingulate cortex modulates supplementary motor area in coordinated unimanual motor behavior. Front. Hum. Neurosci. 9, 309. https://doi.org/10.3389/fnhum.2015.00309.

Aston-Jones, G., Cohen, J.D., 2005. An integrative theory of locus coeruleus-norepinephrine function: adaptive gain and optimal performance. Annu. Rev. Neurosci. 28, 403–450. https://doi.org/10.1146/annurev.neuro.28.061604.135709.

Behzadi, Y., Restom, K., Liau, J., Liu, T.T., 2007. A component based noise correction method (CompCor) for BOLD and perfusion based fMRI. Neuroimage 37 (1), 90–101. https://doi.org/10.1016/j.neuroimage.2007.04.042.

Berridge, K.C., 1999. Pleasure, pain, desire, and dread: hidden core processes of emotion. Well-being Found. Hedonic Psychol. 525–557.

Berridge, K.C., Robinson, T.E., Aldridge, J.W., 2009. Dissecting components of reward: 'liking', 'wanting', and learning. Curr. Opin. Pharmacol. 9 (1), 65–73. https://doi.org/10.1016/j.coph.2008.12.014.

Bijleveld, E., Custers, R., Aarts, H., 2009. The unconscious eye opener: pupil dilation reveals strategic recruitment of resources upon presentation of subliminal reward cues. Psychol. Sci. 20 (11), 1313–1315. https://doi.org/10.1111/j.1467-9280.2009.02443.x.

Botvinick, M.M., Cohen, J.D., Carter, C.S., 2004. Conflict monitoring and anterior cingulate cortex: an update. Trends Cogn. Sci. 8 (12), 539–546. https://doi.org/10.1016/j.tics.2004.10.003.

Chiew, K.S., Braver, T.S., 2013. Temporal dynamics of motivation-cognitive control interactions revealed by high-resolution pupillometry. Front. Psychol. 4, 15. https://doi.org/10.3389/fpsyg.2013.00015.

Chiew, K.S., Braver, T.S., 2014. Dissociable influences of reward motivation and positive emotion on cognitive control. Cogn. Affect Behav. Neurosci. 14 (2), 509–529. https://doi.org/10.3758/s13415-014-0280-0.

Chikazoe, J., Jimura, K., Asari, T., Yamashita, K., Morimoto, H., Hirose, S., Miyashita, Y., Konishi, S., 2009. Functional dissociation in right inferior frontal cortex during performance of go/no-go task. Cereb. Cortex 19 (1), 146–152. https://doi.org/10.1093/cercor/bhn065.

Critchley, H.D., 2005. Neural mechanisms of autonomic, affective, and cognitive integration. J. Comp. Neurol. 493 (1), 154–166. https://doi.org/10.1002/cne.20749.

Critchley, H.D., Elliott, R., Mathias, C.J., Dolan, R.J., 2000. Neural activity relating to generation and representation of galvanic skin conductance responses: a functional magnetic resonance imaging study. J. Neurosci. 20 (8), 3033–3040.

Dichter, G.S., 2010. Anhedonia in unipolar major depressive disorder: a review. Open Psychiatry J. 4, 1–9.

Drew, G.C., 1951. Variations in reflex blink-rate during visual-motor tasks. Q. J. Exp. Psychol. 3 (2), 73–88. https://doi.org/10.1080/17470215108416776.

Ebitz, R.B., Platt, M.L., 2015. Neuronal activity in primate dorsal anterior cingulate cortex signals task conflict and predicts adjustments in pupil-linked arousal. Neuron 85 (3), 628–640. https://doi.org/10.1016/j.neuron.2014.12.053.

Fredrikson, M., Furmark, T., Olsson, M.T., Fischer, H., Andersson, J., Langstrom, B., 1998. Functional neuroanatomical correlates of electrodermal activity: a positron emission tomographic study. Psychophysiology 35 (2), 179–185.

Fukuda, K., 1994. Analysis of eyeblink activity during discriminative tasks. Percept. Mot. Ski. 79 (3 Pt 2), 1599–1608. https://doi.org/10.2466/pms.1994.79.3f.1599.

Garrison, J., Erdeniz, B., Done, J., 2013. Prediction error in reinforcement learning: a meta-analysis of neuroimaging studies. Neurosci. Biobehav Rev. 37 (7), 1297–1310. https://doi.org/10.1016/j.neubiorev.2013.03.023.

Haber, S.N., Knutson, B., 2010. The reward circuit: linking primate anatomy and human imaging. Neuropsychopharmacology 35 (1), 4–26. https://doi.org/10.1038/npp.2009.129.

Hall, A., 1945. The ORIGIN and PURPOSES of blinking. Br. J. Ophthalmol. 29 (9), 445–467.
Joshi, S., Li, Y., Kalwani, R.M., Gold, J.I., 2016. Relationships between pupil diameter and neuronal activity in the locus coeruleus, colliculi, and cingulate cortex. Neuron 89 (1), 221–234. https://doi.org/10.1016/j.neuron.2015.11.028.
Klein, D.F., 1987. Anhedonia and Affect Deficit States. Depression and Anhedonia. PMA Publishing, New York, pp. 1–14.
Knutson, B., Bhanji, J.P., Cooney, R.E., Atlas, L.Y., Gotlib, I.H., 2008. Neural responses to monetary incentives in major depression. Biol. Psychiatry 63 (7), 686–692. https://doi.org/10.1016/j.biopsych.2007.07.023.
Knutson, B., Fong, G.W., Adams, C.M., Varner, J.L., Hommer, D., 2001. Dissociation of reward anticipation and outcome with event-related fMRI. Neuroreport 12 (17), 3683–3687.
Knutson, B., Fong, G.W., Bennett, S.M., Adams, C.M., Hommer, D., 2003. A region of mesial prefrontal cortex tracks monetarily rewarding outcomes: characterization with rapid event-related fMRI. Neuroimage 18 (2), 263–272.
Knutson, B., Greer, S.M., 2008. Anticipatory affect: neural correlates and consequences for choice. Philos. Trans. R. Soc. Lond. B Biol. Sci. 363 (1511), 3771–3786. https://doi.org/10.1098/rstb.2008.0155.
Knutson, B., Katovich, K., Suri, G., 2014. Inferring affect from fMRI data. Trends Cogn. Sci. 18 (8), 422–428. https://doi.org/10.1016/j.tics.2014.04.006.
Langner, R., Eickhoff, S.B., 2013. Sustaining attention to simple tasks: a meta-analytic review of the neural mechanisms of vigilant attention. Psychol. Bull. 139 (4), 870–900. https://doi.org/10.1037/a0030694.
Leuchs, L., Schneider, M., Czisch, M., Spoormaker, V.I., 2016. Neural correlates of pupil dilation during human fear learning. Neuroimage 147, 186–197. https://doi.org/10.1016/j.neuroimage.2016.11.072.
Liu, K.Y., Marijatta, F., Hammerer, D., Acosta-Cabronero, J., Duzel, E., Howard, R.J., 2017. Magnetic resonance imaging of the human locus coeruleus: a systematic review. Neurosci. Biobehav Rev. https://doi.org/10.1016/j.neubiorev.2017.10.023.
Liu, X., Hairston, J., Schrier, M., Fan, J., 2011. Common and distinct networks underlying reward valence and processing stages: a meta-analysis of functional neuroimaging studies. Neurosci. Biobehav Rev. 35 (5), 1219–1236. https://doi.org/10.1016/j.neubiorev.2010.12.012.
Lowenstein, O., Feinberg, R., Loewenfeld, I.E., 1963. Pupillary movements during acute and chronic fatigue - a new test for the objective evaluation of tiredness. Investig. Ophthalmol. 2 (2), 138–157.
McClure, S.M., Berns, G.S., Montague, P.R., 2003. Temporal prediction errors in a passive learning task activate human striatum. Neuron 38 (2), 339–346.
McMakin, D.L., Olino, T.M., Porta, G., Dietz, L.J., Emslie, G., Clarke, G., Wagner, K.D., Asarnow, J.R., Ryan, N.D., Birmaher, B., et al., 2012. Anhedonia predicts poorer recovery among youth with selective serotonin reuptake inhibitor treatment-resistant depression. J. Am. Acad. Child. Adolesc. Psychiatry 51 (4), 404–411. https://doi.org/10.1016/j.jaac.2012.01.011.
Medford, N., Critchley, H.D., 2010. Conjoint activity of anterior insular and anterior cingulate cortex: awareness and response. Brain Struct. Funct. 214 (5–6), 535–549. https://doi.org/10.1007/s00429-010-0265-x.
Menon, V., Uddin, L.Q., 2010. Saliency, switching, attention and control: a network model of insula function. Brain Struct. Funct. 214 (5–6), 655–667. https://doi.org/10.1007/s00429-010-0262-0.
Mouton, P.R., Pakkenberg, B., Gundersen, H.J., Price, D.L., 1994. Absolute number and size of pigmented locus coeruleus neurons in young and aged individuals. J. Chem. Neuroanat. 7 (3), 185–190.
Murphy, P.R., O'Connell, R.G., O'Sullivan, M., Robertson, I.H., Balsters, J.H., 2014. Pupil diameter covaries with BOLD activity in human locus coeruleus. Hum. Brain Mapp. 35 (8), 4140–4154. https://doi.org/10.1002/hbm.22466.
Nakano, T., Yamamoto, Y., Kitajo, K., Takahashi, T., Kitazawa, S., 2009. Synchronization of spontaneous eyeblinks while viewing video stories. Proc. Biol. Sci. 276 (1673), 3635–3644. https://doi.org/10.1098/rspb.2009.0828.
O'Doherty, J.P., Dayan, P., Friston, K., Critchley, H., Dolan, R.J., 2003. Temporal difference models and reward-related learning in the human brain. Neuron 38 (2), 329–337.
Olino, T.M., McMakin, D.L., Morgan, J.K., Silk, J.S., Birmaher, B., Axelson, D.A., Williamson, D.E., Dahl, R.E., Ryan, N.D., Forbes, E.E., 2014. Reduced reward anticipation in youth at high-risk for unipolar depression: a preliminary study. Dev. Cogn. Neurosci. 8, 55–64. https://doi.org/10.1016/j.dcn.2013.11.005.
Paus, T., 2001. Primate anterior cingulate cortex: where motor control, drive and cognition interface. Nat. Rev. Neurosci. 2 (6), 417–424. https://doi.org/10.1038/35077500.
Petersen, S.E., Posner, M.I., 2012. The attention system of the human brain: 20 years after. Annu. Rev. Neurosci. 35, 73–89. https://doi.org/10.1146/annurev-neuro-062111-150525.
Pizzagalli, D.A., Iosifescu, D., Hallett, L.A., Ratner, K.G., Fava, M., 2008. Reduced hedonic capacity in major depressive disorder: evidence from a probabilistic reward task. J. Psychiatr. Res. 43 (1), 76–87. https://doi.org/10.1016/j.jpsychires.2008.03.001.
Preuschoff, K., t Hart, B.M., Einhauser, W., 2011. Pupil dilation signals surprise: evidence for Noradrenaline's role in decision making. Front. Neurosci. 5, 115. https://doi.org/10.3389/fnins.2011.00115.
Raichle, M.E., 2015. The brain's default mode network. Annu. Rev. Neurosci. 38, 433–447. https://doi.org/10.1146/annurev-neuro-071013-014030.
Ridderinkhof, K.R., Ullsperger, M., Crone, E.A., Nieuwenhuis, S., 2004. The role of the medial frontal cortex in cognitive control. Science 306 (5695), 443–447. https://doi.org/10.1126/science.1100301.
Robertson, I.H., Garavan, H., 2004. Vigilant Attention. The Cognitive Neurosciences, third ed. MIT Press, Cambridge, MA, pp. 631–640.
Rothkirch, M., Schmack, K., Deserno, L., Darmohray, D., Sterzer, P., 2014. Attentional modulation of reward processing in the human brain. Hum. Brain Mapp. 35 (7), 3036–3051. https://doi.org/10.1002/hbm.22383.
Rudebeck, P.H., Putnam, P.T., Daniels, T.E., Yang, T., Mitz, A.R., Rhodes, S.E., Murray, E.A., 2014. A role for primate subgenual cingulate cortex in sustaining autonomic arousal. Proc. Natl. Acad. Sci. U. S. A. 111 (14), 5391–5396. https://doi.org/10.1073/pnas.1317695111.
Russell, J.A., 1980. A circumplex model of affect. J. Pers. Soc. Psychol. 39 (6), 1161–1178. https://doi.org/10.1037/h0077714.
Samanez-Larkin, G.R., Gibbs, S.E., Khanna, K., Nielsen, L., Carstensen, L.L., Knutson, B., 2007. Anticipation of monetary gain but not loss in healthy older adults. Nat. Neurosci. 10 (6), 787–791. https://doi.org/10.1038/nn1894.
Schneider, M., Hathway, P., Leuchs, L., Samann, P.G., Czisch, M., Spoormaker, V.I., 2016. Spontaneous pupil dilations during the resting state are associated with activation of the salience network. Neuroimage 139, 189–201. https://doi.org/10.1016/j.neuroimage.2016.06.011.
Sherdell, L., Waugh, C.E., Gotlib, I.H., 2012. Anticipatory pleasure predicts motivation for reward in major depression. J. Abnorm Psychol. 121 (1), 51–60. https://doi.org/10.1037/a0024945.
Sheth, S.A., Mian, M.K., Patel, S.R., Asaad, W.F., Williams, Z.M., Dougherty, D.D., Bush, G., Eskandar, E.N., 2012. Human dorsal anterior cingulate cortex neurons mediate ongoing behavioural adaptation. Nature 488 (7410), 218–221. https://doi.org/10.1038/nature11239.
Shulman, G.L., Fiez, J.A., Corbetta, M., Buckner, R.L., Miezin, F.M., Raichle, M.E., Petersen, S.E., 1997. Common blood flow changes across visual tasks: II. Decreases in cerebral cortex. J. Cogn. Neurosci. 9 (5), 648–663. https://doi.org/10.1162/jocn.1997.9.5.648.
Siegle, G.J., Steinhauer, S.R., Stenger, V.A., Konecky, R., Carter, C.S., 2003. Use of concurrent pupil dilation assessment to inform interpretation and analysis of fMRI data. Neuroimage 20 (1), 114–124.
Siepmann, T., Ziemssen, T., Mueck-Weymann, M., Kirch, W., Siepmann, M., 2007. The effects of venlafaxine on autonomic functions in healthy volunteers. J. Clin. Psychopharmacol. 27 (6), 687–691. https://doi.org/10.1097/jcp.0b013e31815a255b.
Spijker, J., Bijl, R.V., de Graaf, R., Nolen, W.A., 2001. Determinants of poor 1-year outcome of DSM-III-R major depression in the general population: results of The Netherlands Mental Health Survey and Incidence Study (NEMESIS). Acta Psychiatr. Scand. 103 (2), 122–130.
Stern, J.A., Walrath, L.C., Goldstein, R., 1984. The endogenous eyeblink. Psychophysiology 21 (1), 22–33.
Takarada, Y., Nozaki, D., 2017. Pupil dilations induced by barely conscious reward goal-priming. Neuropsychologia 103, 69–76. https://doi.org/10.1016/j.neuropsychologia.2017.07.020.
Visser, R.M., de Haan, M.I., Beemsterboer, T., Haver, P., Kindt, M., Scholte, H.S., 2016. Quantifying learning-dependent changes in the brain: single-trial multivoxel pattern analysis requires slow event-related fMRI. Psychophysiology 53 (8), 1117–1127. https://doi.org/10.1111/psyp.12665.
Visser, R.M., Scholte, H.S., Beemsterboer, T., Kindt, M., 2013. Neural pattern similarity predicts long-term fear memory. Nat. Neurosci. 16 (4), 388–390. https://doi.org/10.1038/nn.3345.
Vrieze, E., Demyttenaere, K., Bruffaerts, R., Hermans, D., Pizzagalli, D.A., Sienaert, P., Hompes, T., de Boer, P., Schmidt, M., Claes, S., 2014. Dimensions in major depressive disorder and their relevance for treatment outcome. J. Affect Disord. 155, 35–41. https://doi.org/10.1016/j.jad.2013.10.020.
Vrieze, E., Pizzagalli, D.A., Demyttenaere, K., Hompes, T., Sienaert, P., de Boer, P., Schmidt, M., Claes, S., 2013. Reduced reward learning predicts outcome in major depressive disorder. Biol. Psychiatry 73 (7), 639–645. https://doi.org/10.1016/j.biopsych.2012.10.014.
Weissman, D.H., Roberts, K.C., Visscher, K.M., Woldorff, M.G., 2006. The neural bases of momentary lapses in attention. Nat. Neurosci. 9 (7), 971–978. https://doi.org/10.1038/nn1727.
Whitton, A.E., Treadway, M.T., Pizzagalli, D.A., 2015. Reward processing dysfunction in major depression, bipolar disorder and schizophrenia. Curr. Opin. Psychiatry 28 (1), 7–12. https://doi.org/10.1097/yco.0000000000000122.
Wilhelm, H., Ludtke, H., Wilhelm, B., 1998. Pupillographic sleepiness testing in hypersomniacs and normals. Graefes Arch. Clin. Exp. Ophthalmol. 236 (10), 725–729.
Willenbockel, V., Sadr, J., Fiset, D., Horne, G.O., Gosselin, F., Tanaka, J.W., 2010. Controlling low-level image properties: the SHINE toolbox. Behav. Res. Methods 42 (3), 671–684. https://doi.org/10.3758/brm.42.3.671.

4 Discussion

4.1 Pupil dilations: an index for salience network activation

As mentioned in the introduction, previous pupillometry studies reported that during periods of increasing drowsiness, pupil size declines while at the same time showing recurrent, spontaneous dilations (indicating waves of increased arousal), referred to as pupillary fatigue waves. Given its strong projections to the LC and involvement in performance monitoring/arousal modulation, our first hypothesis was that the activity of the dACC is correlated to spontaneous pupil dilations during the resting state. The results obtained within the resting state study confirm a positive correlation between dACC activity and spontaneous pupil dilations. In addition, we found positively correlated activity in bilateral anterior insula, which together with the dACC forms the SN. Also, in our sample of mildly sleep deprived subjects, positively correlated activity extended to the thalamus. Spontaneous pupil constrictions during the resting state were associated with increased activity in visual and sensorimotor areas.

At the start of this thesis, only two studies had addressed the neural correlates of pupil size fluctuations during the resting state (see section 1.5.1), yielding rather conflicting results. Our findings partially overlap with the observations by Murphy et al. (2014) and Yellin et al. (2015) to a certain degree: in line with these two previous studies, we found (positive) pupil-BOLD correlations in the dACC and (right) insula (see Murphy et al. 2014), as well as negative correlations in visual/sensorimotor regions (see Murphy et al. 2014; Yellin et al. 2015). Moreover, our results seem to complement both studies, providing a potential explanation for their deviating findings: in contrast to the research groups around Murphy and Yellin, we did not only assess the neural correlates of pupil size, but also considered pupil dilations and constrictions in our analyses by computing the first order derivative of pupil size. The resulting brain maps argue against a robust (positive) relationship between absolute pupil size and global brain activity, but strongly indicate that phasic changes in pupil size are associated with widespread brain activity, primarily in the SN. Interestingly, Murphy et al. also found correlated activity in the SN when analyzing the

neural correlates of pupil size (not change). However, Murphy et al. included the temporal and dispersion HRF derivatives in their general linear model (GLM), which can be added to the conventional canonical HRF in order to increase sensitivity, that is, to capture neural correlates despite unknown variations in timing and duration of the HRF. In addition, Murphy et al. only reported F-contrasts, not specifying whether the observed correlations in dACC and insula were positive or negative. When using a similar approach as Murphy et al., i.e. convolving the pupil size vector with the temporal HRF derivative, we found that this procedure yielded a regressor that was very similar (still not identical) to the pupil change regressor. Furthermore, we observed that the BOLD signal in dACC and insula did not significantly correlate with the canonical HRF-convolved pupil size regressor, but only showed a significant positive correlation to this temporal derivative-derived regressor (see Supplementary Figure S4). The temporal derivative is typically only included to allow for small differences in HRF onset, and is always analyzed in combination with the original regressor. One major issue concerning the interpretation of neural correlates (solely) associated with the temporal HRF derivative (but not with the canonical HRF) is that the temporal derivative HRF does not reflect any known neurophysiological signal. In other words, it is unlikely that there are brain regions which show a BOLD signal time course as described by the temporal HRF derivative, involving rapid successions of strongly increasing and decreasing activity. In sum, taking into account the derivative of pupil size (i.e. pupil change) yielded findings that were highly consistent across our studies, enabling a straightforward interpretation that fits with the neurophysiological properties of the BOLD response.

The second hypothesis of this thesis was that reward anticipation-related emotional arousal involves a dilation of the pupils, which again was expected to be associated with increased activity of the dACC (suggesting a role of the dACC in the generation of emotional arousal responses). We observed that the pupil response differed between reward conditions, involving a strong and continuous dilation to a cue that signaled the opportunity to gain a monetary reward (and a constriction to a control stimulus with no reward possibility). Furthermore, to our knowledge, we were the first group that investigated the neural correlates of pupil size/pupil dilations during reward anticipation. These analyses revealed that reward anticipation involves

three consecutive phases associated with distinct cognitive processes: 1) reward prediction, characterized by VS activation and small pupil size at the beginning of reward anticipation; 2) subsequent arousal-upregulation, indexed by a strong dilation of the pupils and increased activity of the dACC and bilateral insula (SN); 3) preparatory/vigilant attention, linked to large pupil size and increased activity of the ventral attention network just before the motor response.

Our fMRI results are in line with findings from numerous previous neuroimaging studies, primarily showing activation of the VS, medial prefrontal cortex (mPFC), ACC, OFC, insula and thalamus during monetary and (to a lesser degree) verbal reward anticipation (Knutson et al. 2001; Knutson et al. 2000). The VS has been proposed to constitute a central hub in the brain's reward circuitry and previous studies provided evidence that the VS is involved in a variety of reward prediction-related processes. For instance, the VS seems to process the motivational salience of reward-predicting stimuli, to track anticipated reward magnitude and probability/uncertainty (likely represented in different subcomponents of the VS; Haber and Knutson 2010), and to mobilize effort and allocate attention to reward-predictive cues (Whitton et al. 2015). Our observations of early VS activation support the previously reported roles in motivational salience signaling and reward prediction-associated processes. The ACC/mPFC has been suggested to track reward prediction errors and to form associations between reward and appropriate action (Alexander and Brown 2010; Haber and Knutson 2010; Knutson and Cooper 2005). Furthermore, based on its established role in conflict monitoring, the dACC (together with the dorsal PFC) has been proposed to play an important role in comparing different options, choosing the most valuable option, and translating the choice into a goal-directed action (Haber and Knutson 2010). By simultaneously recording pupil size as an index of autonomic arousal, we could show for the first time that the dACC (together with bilateral insula) is also involved in the regulation of reward anticipation-related arousal in humans. A similar link between ACC activity and reward-related increases in arousal (indexed by pupil dilation) has recently been shown in macaque monkeys: Rudebeck et al. (2014) could demonstrate that after lesions of the subgenual ACC (partly extending to the dACC), monkeys only showed an initial, brief pupil dilation to a reward-predicting cue, but failed to maintain an increased pupil size (i.e. a high level of arousal)

until the anticipated reward was delivered (see section 1.5.3, Figure 3). Our results largely extend this finding to humans, showing that reward anticipation-related pupil dilations involve increased activity in the dACC/SN.

4.2 Salience network: performance optimization through arousal modulation

In the resting state study, participants received the instruction to continuously fixate on a fixation dot, to think of nothing in particular, and not to fall asleep during the recording session. Maintaining fixation on a dot over 12 minutes while lying in a horizontal position in a weakly illuminated environment after a night of sleep restriction (together with the monotonous, ear plug-dampened sounds of the MRI scanner) is likely to promote sleepiness. Previous studies showed that the transition to a drowsy state involves a decrease in pupil size, reflecting a decrease in tonic LC activity. Declining tonic LC activity has been suggested to promote a disengagement from the external environment, eventually facilitating the transition to sleep (Aston-Jones and Cohen 2005b). In line with this, daytime sleepiness has been linked to an increased occurrence of task-unrelated, internally-focused mentation such as mind wandering and daydreaming (Carciofo et al. 2014). Mind wandering and daydreaming affect task performance by shifting attention away from the external environment. We found that a dilation of the pupils, either occurring spontaneously during the resting state or in response to a reward-predicting cue, was associated with activation of the SN.

The SN is assumed to play an important role for task performance, particularly by detecting conflicts and errors (Botvinick et al. 2004; Kerns et al. 2004). Our results strongly support the idea that the SN optimizes task performance by modulating arousal levels according to situational requirements: in the resting state, the transition to a drowsy state (likely accompanied by increased mind wandering/daydreaming) compromises attention to the fixation cross, creating a conflict. Therefore, the recurring pupil dilations observed during periods of increasing drowsiness are likely to reflect processes restoring external attention and inhibiting a transition to sleep. We propose that spontaneous decreases in arousal levels are first detected by the insula, which previously has been suggested to track changes in interoceptive states (Critchley 2005; Critchley

et al. 2000; Medford and Critchley 2010). Furthermore, we expect that the conflict between the current arousal state (drowsiness) and the arousal level required for continuous task performance is detected by the dACC. Since the dACC is a major input region to the LC and previously has been linked to the generation of sympathetic arousal responses (Critchley 2005; Critchley et al. 2000; Medford and Critchley 2010) we believe that the dACC subsequently sends a signal to the LC, initiating a compensatory upregulation of arousal levels.

Alternatively, SN activation during periods of pupil dilation could also result from a reverse signal transmission, that is, LC projecting to dACC. The LC is known to be part of the so-called ascending reticular activating system, which mediates arousal and involves projections from the LC through the thalamus to numerous cortical areas (Aston-Jones et al. 2001; Daube 1986; Saper et al. 2005). We found that activity in bilateral thalamus was associated with pupil change points, indicating that thalamic activation occurred immediately before the pupil started to dilate. On the one hand, as dACC activity correlated most strongly with the following pupil dilation, this finding appears to support a signal propagation from thalamus to dACC, which is difficult to reconcile with a cognitive view on pupil fluctuations. Such spread of arousal-related activity could originate from the LC.

On the other hand, other studies provided evidence that the thalamus (within a thalamo-cortical circuit) is strongly involved in performance monitoring and conflict-related cognitive control (Bellebaum et al. 2005; Blakemore et al. 1998; Diamond and Ahissar 2007; Ide and Li 2011; Mitchell et al. 2007; Seifert et al. 2011; Wagner et al. 2006). For instance, Seifert et al. (2011) investigated patients with focal thalamic lesions and healthy subjects using diffusion-based tractography as well as electrophysiological recordings during a flanker task. They found that the thalamus closely interacts with the anterior midcingulate cortex during performance monitoring, concluding that thalamo-cingulate interactions appear to be necessary for the generation of an error signal in the anterior midcingulate cortex. With regard to our study, this could indicate that the conflict between increasing drowsiness and task engagement might be first detected by the thalamus, which would trigger SN activation subsequently. Such an interpretation would again fit our cognitive “performance optimization” interpretation (although it remains unclear where the

performance monitoring-associated input to the thalamus would stem from). Similarly, a recent study in macaque monkeys provided evidence that pupil-linked modulations of ACC activity can both temporally precede and follow LC activation (Joshi et al. 2016). We primarily interpreted waves of pupil dilation during periods of decreasing tonic pupil size to reflect intentional efforts to stay awake/keep external attention, involving a neuronal signal that first emerges in the insula/dACC and then propagates (presumably via the thalamus) to the LC. Such an interpretation implies that animals should not display spontaneous waves of increased arousal under similar experimental conditions (i.e. if not rewarded for staying awake/keeping fixation). This notion is supported by earlier reports by Lowenstein and Loewenfeld (1964), stating that monkeys, "devoid of spontaneous thoughts or emotions which would keep them awake", do not show pupillary fatigue waves. Instead, "after a few minutes (…) the pupils become smaller, and soon the animal falls asleep" (p. 142). In sum, such a cognitive interpretation extends previous theories on the origin of the pupillary fatigue waves with a main focus on imbalance of the sympathetic and parasympathetic nervous system (e.g. Loewenfeld 1993; Warga et al. 2009; Wilhelm et al. 2001).

In the reward anticipation paradigm, responding quickly to a target stimulus in order to achieve a reward requires a certain level of autonomic arousal. Similar to keeping fixation in the resting state, this task is hampered once subjects become drowsy or distracted by interoceptive mentation. At the onset of the reward predicting cue, subjects' pupil size was typically rather small, indicating comparatively low arousal and LC activity. At the same time, we observed an early activation of the VS, likely reflecting a reward prediction signal, followed by activation of the SN and a strong increase in pupil size. We assume that the strong increase in pupil size following presentation of a cue that predicted the opportunity to win a monetary reward likely reflects an emotional arousal response. As described earlier, arousal is a key component of reward anticipation since it involves an increase in sympathetic activity and thus enables/facilitates reward approach behavior. In our paradigm, successful reward attainment required a fast motor response to a target stimulus occurring at the end of the reward anticipation time window. We found that pupil size preceding the target stimulus was negatively correlated with response time, confirming that high arousal (i.e. large pupil size) promotes fast responding. Again, our results

suggest that such a dynamic adjustment of arousal levels is initiated by the SN: the insula has been suggested to integrate internal arousal states with cognitive/evaluative and emotional information (Citron et al. 2014; Craig 2009; Critchley 2005). For instance, a study by Phillips et al. (2003) demonstrated that the bilateral anterior insula responds to both (non-painful) oesophageal stimulation and viewing of fearful faces and that insula activation was synergistically enhanced when the two stimuli were delivered simultaneously. Based on such findings, we propose that the insula plays a key role in integrating the momentary state of autonomic arousal and the reward prediction/motivational salience signal generated in the VS. Furthermore, we expect that the subsequent arousal response is triggered by the dACC via its projections to the LC. In addition, the dACC shows strong connections to the frontal motor system (especially to the SMA) and has been considered a major interface between cognitive and sensorimotor processing (Paus 2001), including a role in motor control by maintaining stimulus timing expectancy (Asemi et al. 2015). Joint activations of the (anterior) insula and ACC have been reported in numerous previous studies, which gave rise to the idea that the two structures work together as complementary limbic sensory and motor regions, in a similar way as the somatosensory and motor cortices (Craig 2009).

As mentioned earlier, decreasing tonic LC activity is assumed to promote a disengagement from the external environment, associated with drowsiness and increased occurrence of mind wandering/daydreaming. Previous studies showed that mind wandering and daydreaming are linked to increased activity in the DMN as well as secondary visual (especially lingual gyrus) and somatosensory regions (for a recent meta-analysis, see Fox et al. 2015). We found that spontaneous constrictions of the pupil and small pupil size during the resting state were associated with increased activity in secondary visual (including bilateral lingual gyrus) and somatosensory regions, supporting the notion that a decline in autonomic arousal/LC activity likely involves an increased occurrence of interoceptive mentation. In line with this notion, pupil dilations during reward anticipation were associated with an inhibition of DMN activity, suggesting that the state of increased emotional arousal while subjects were expecting the target stimulus involved a suppression of internal processes (likely facilitating a fast detection of the target stimulus).

However, we did not find a similar link for DMN activity in the resting state study. Although increased activity of visual and somatosensory regions has typically been attributed to a (wakeful) interoceptive state, activation of these regions has also been linked to hypnagogic hallucinations (i.e. dream-like mentation) occurring during sleep onset and microsleeps (Ong et al. 2015; Poudel et al. 2014). A recent study by Tagliazucchi and Laufs (2014) revealed that a large portion of subjects actually falls asleep during the resting state, implying that pupil constriction-related activations of visual and sensorimotor regions might also reflect microsleep-related hypnagogic hallucinations. Sleep deprivation and the transition to sleep has been shown to result in a decline in functional connectivity of the DMN (Ong et al. 2015; Sämann et al. 2010; Sämann et al. 2011), which might explain to some extent why we did not observe additional DMN activation during pupil constrictions in the resting state (however, we excluded subjects that fell asleep from our analyses).

Taken together, the two studies showed that pupillometry allows tracking spontaneous changes in vigilance/arousal as well as task-induced emotional arousal. Furthermore, while SN activity during the resting state appears to maintain task performance by restoring external attention and inhibiting sleep during periods of increased drowsiness, the SN-mediated upregulation of arousal during reward anticipation likely facilitates goal-directed motor responses (or more generally, reward approach behavior).

4.3 Pupillometry: an index for the LC-NA system?

We proposed that the SN dynamically adjusts arousal by modulating activity of the LC-NA system, implying that we should have found a pupil-BOLD correlation in the LC as well. We did observe pupil-correlated activity in brainstem clusters in proximity to the LC; however, as described in section 1.4.1, standard fMRI recordings are not suitable to reliably capture signals within small brainstem nuclei like the LC. We thus refrained from over-interpreting the observed correlations in the brainstem. Still, it should be noted that Murphy et al. (2014) previously found evidence for a correlation between pupil size and the BOLD signal in human LC by using special brainstem imaging techniques.

As described earlier, the pupil is innervated by a sympathetic and parasympathetic pathway, involving NA and ACh signaling, respectively. NA release activates the α1-adrenergic receptors of the dilator muscle, causing a dilation of the pupil. The constriction is mediated by ACh, activating the muscarinic receptors of the constrictor muscle and inhibiting NA activity in the dilator muscle. Resting pupil size generally mirrors the balance between the two systems and a dilation of the pupil can either reflect increased NA or decreased ACh input, or both. Previous studies provided evidence that the influences of different systems on the pupil may be disentangled by separately analyzing different phases/features of the pupillary light reflex (PLR; e.g. Fountoulakis et al. 1999; Loewenfeld 1993). Assessment of the PLR typically involves administration of a brief light flash, causing a constriction and re-dilation of the pupil, that is, a successive activation of the parasympathetic and sympathetic innervation of the iris. Since pupil constriction starts when ACh activity plus ACh-mediated blockade of NA activity overcome NA activity, the latency of constriction has been proposed to be a measure for the balance between ACh and NA activity. The amplitude of constriction is assumed to provide an absolute measure of ACh activity, since NA activity is already neutralized (Fountoulakis et al. 1999). Since the subsequent dilation of the pupil is triggered by NA release, recovery time (i.e. the duration of the re-dilation) has been suggested to provide a measure of NA activity (Bitsios et al. 1999; Fountoulakis et al. 1999; Loewenfeld 1993).

The distinct features of the PLR have previously been investigated to make inferences about the extent to which the two systems are affected in certain psychiatric disorders. For instance, Fountoulakis et al. (1999) found that depressive patients show shorter constriction latencies and concluded that depression is primarily characterized by NA hypoactivity (and to a lesser extent ACh hypoactivity). Several groups also investigated the effects of different antidepressant medications on the PLR readouts in patients and healthy controls. In sum, these studies showed that NA reuptake inhibitors potentiate the sympathetic input to the pupil (Bitsios et al. 1999; Kerr and Szabadi 1985; Shur and Checkley 1982; Theofilopoulos et al. 1995). For instance, Bitsios et al. (1999) found that venlafaxine administration (a selective serotonin and NA reuptake inhibitor [SSNRI]) involves an increased resting pupil diameter, a prolonged latency and decreased

amplitude of PLR-related pupil constriction, as well as a shortened recovery time. Venlafaxine is known to have negligible affinity for muscarinic ACh receptors, implying that the observed effects were not due to the blockade of ACh signaling. Furthermore, paroxetine (a selective serotonin reuptake inhibitor with little effect on NA re-uptake) did not have significant effects on the pupil. These results indicate that the pupil-dilating effects of Venlafaxine cannot be traced back to changes in serotonergic and ACh signaling, but result from an increase in NA levels due to the blockade of NA uptake.

Taken together, our interpretation that pupil dilations reflect increased firing of LC neurons/NA signaling is supported by converging evidence from electrophysiology, pharmacology, anatomy, and human imaging. Still, it should be noted that correlations of LC activity and pupil dilation might theoretically also result from a common input to the LC and EW (see section 1.4.2), possibly provided by the paragigantocellularis nucleus of the ventral medulla (Larsen and Waters 2018; Nieuwenhuis et al. 2011). Also, the rather long time lag between electrical stimulation of the LC and subsequent pupil dilations (approx. 500 ms in monkeys, 1 s in mice) might indicate an indirect LC-pupil pathway. For example, the superior colliculus (SC) in the midbrain is known to receive input from the LC and to project to the EW, where it may influence pupil dilation (Wang and Munoz, 2015). Furthermore, the SC has been shown to play an important role in initiating orienting behaviors to salient stimuli. Interestingly, a study by Wang et al. (2012) found that micro stimulation of the monkey SC evokes pupil dilations, suggesting that the SC is not only involved in shifts of gaze and attention, but also in pupil dilation as part of the orienting reflex. In a recent review on this issue, Larsen and Waters (2018) concluded the following: “Future manipulations of activity in only noradrenergic locus coeruleus neurons are necessary to determine whether noradrenergic neurons directly influence pupil size” (p. 3).

4.4 Outlook: pupillometry in psychiatry

As described in section 1.2.1, the RDoC initiative emphasizes the exploration of biomarkers and intermediate endophenotypes for improving diagnostic, prevention, and treatment of psychiatric disorders. Psychophysiological measurements are a promising strategy to explore

endophenotypes, and our results suggest that pupillometry could provide a helpful tool to investigate several RDoC domains/constructs: we found that both spontaneous pupil dilations during the resting state and reward anticipation-associated pupil dilations reflect activation of the SN. Furthermore, pupil size is known to index activity of the LC-NA system, which has a well-established role in the regulation of vigilance/arousal and which is involved in performance optimization (see section 1.3). Therefore, our results suggest that pupillometry-based assessments are relevant for at least two RDoC domains: arousal/regulatory systems (including the construct "sleep-wakefulness") and positive valence systems (especially the subconstruct "reward anticipation"). In addition, further work involving simultaneous pupillometry/fMRI in a human fear learning experiment revealed that pupil dilations (associated with SN activity) track fear learning, extending the use of pupillometric measurements to the "negative valence systems" RDoC domain (see Leuchs et al. 2016).

The SN has been proposed to be in a "hub" or "crossroads" position in the brain, interacting with regions involved in cognition, emotion, behavioral self-control, social behavior and theory of mind (Downar et al. 2016). Furthermore, the SN has been ascribed a central role in the detection of behaviorally relevant stimuli and the coordination of neural resources (Uddin 2015). Recent meta-analyses of structural and functional neuroimaging studies provide converging evidence that the SN constitutes a "common core" of brain regions affected across most psychiatric disorders. For instance, a voxel-based morphometry meta-analysis including 193 structural MRI studies (with more than 7000 patients in total) revealed a consistent pattern of gray matter volume reductions in multiple brain regions comprising the SN in schizophrenia, bipolar disorder, depression, addiction, obsessive-compulsive disorder, and anxiety (Goodkind et al. 2015). Interestingly, gray matter loss was exclusively restricted to the dACC and bilateral anterior insula when only non-psychotic disorders were included in the analysis. Another meta-analysis focusing on functional neuroimaging investigations of major depressive disorder (MDD) showed that the SN is selectively hyper-reactive to negative stimuli in MDD patients, supporting the notion of enhanced processing of negative information in depression (Hamilton et al. 2012). Several systematic reviews addressing the relationship between SN integrity and psychiatric diseases

suggest that functional imbalances within the SN are associated with deficient self-regulation of behavior, cognition and emotion, as for instance observed in depression, posttraumatic stress disorder (PTSD), and obsessive compulsive disorder (e.g. Downar et al. 2016; Peters et al. 2016). Furthermore, these reviews proposed that normalization of abnormalities in the SN may underlie the therapeutic effects of novel brain stimulation treatments.

Given the strong link between SN activation and pupil dilation observed in our studies, we propose that pupillometry provides a reliable method for assessing SN functioning, especially SN-mediated modulation of arousal. Based on the well-established implication of the LC-NA system and SN in stress-related disorders, pupillometry likely bears a potential for use as an assessment tool in clinical psychiatry. For instance, pupil size fluctuations during the resting state can be considered an objective index for daytime sleepiness/hypoarousal symptomatology. Moreover, pupil readouts could provide a biological marker for abnormal reward-related arousal regulation, which may underlie anhedonia, a core symptom of mood disorders. In line with this, initial evidence suggests that reward anticipation deficits in depression are related to abnormal dACC activation (Gorka et al. 2014; Knutson et al. 2008). Finally, distinct features of the PLR provide separate readouts for NA and ACh activity. For instance, recovery time of the PLR is sensitive to antidepressant medications that target the LC-NA system, such as SSNRIs like Venlafaxin (Siepmann et al. 2007). Therefore, pupillometry might also be helpful to track disease/treatment progress in patients with anhedonia symptomatology after the start of medication.

4.5 Methodological considerations

Our findings imply that pupillometry provides an economic and less complex alternative to fMRI and electroencephalography for investigations specifically addressing SN activity. Moreover, previous studies provide converging evidence that pupillometry tracks activity of the LC-NA system. As mentioned earlier, conventional whole-brain coverage fMRI recording as used in this study is not sensitive enough to detect potential correlations in the LC, which covers less than one voxel in the axial plane at standard voxel size settings. However, future research with a focus on

the link between LC activity and pupil size could circumvent this problem by applying brainstem fMRI (for a review of LC fMRI in humans, see Liu et al. 2017).

Resting state fMRI (rs-fMRI) has been extensively used for the identification of neuroimaging-based biomarkers in mental disorders. Numerous studies comparing brain activity and connectivity between psychiatric patients and healthy subjects report differences between the groups. These findings strongly rely on the assumption that resting state constitutes a homogenous state across different groups of subjects, implying that the observed group differences result from discrepancies in the brain architecture but not from differences in behavior. This assumption has been increasingly questioned over the last years. As mentioned before, Tagliazucchi and Laufs (2014) showed that a considerable portion of subjects falls asleep during the resting state, which has been associated with distinct changes in brain connectivity (Sämann et al. 2010; Spoormaker et al. 2010). Furthermore, our results indicate that even during wakefulness, subjects show alternating periods of increased and decreased arousal, as indexed by spontaneous pupil constrictions/low pupil size and pupil dilations/large pupil size. Arousal dysregulation is a common symptom among multiple psychiatric disorders such as depression, PTSD and anxiety disorders, manifest for instance in increased daytime sleepiness or constant hyperarousal. Group differences that are obtained by contrasting rs-fMRI data of patients and control subjects thus have a high risk of being confounded by differences in arousal/vigilance levels. Our findings suggest that pupillometry might be helpful to control for such differences. For instance, we assume that patients with hyperarousal symptoms are less likely to fall asleep or to drift into a state of drowsiness that is characterized by an increased prevalence of pupil constrictions and low pupil size, associated with increased activity in visual and somatosensory regions. Taken together, future studies should consider simultaneous pupillometry to improve the validity of rs-fMRI-based comparisons between patients and healthy subjects.

Furthermore, we proposed that the spontaneous, SN activation-associated pupil dilations during the resting state reflect intentional efforts to stay awake and keep fixation, implying a cognitive basis of pupillary fatigue waves. In order to test this hypothesis, future studies could compare pupil behavior during the resting state between two groups of healthy subjects, one

group receiving the instruction to stay awake and the other group being explicitly allowed to fall asleep. In line with our theory, we would expect subjects in the latter group to show significantly less spontaneous pupil dilations during a drowsiness-related decline of tonic pupil size, associated with less SN activation and a faster transition to/higher prevalence of sleep.

Regarding pupil size measurements within a task setting, we found that stimulus-induced pupil dilations were accompanied by changes in blinking behavior and that controlling for eye blinks had a significant impact on our pupil-BOLD correlations. For instance, the prevalence of eye blinks was much lower during presentation of the reward-predicting stimuli compared to control stimulus presentations and quickly decreased over the 6 s reward anticipation time window. Furthermore, controlling for eye blinks in our analyses partly abolished the originally observed pupil-BOLD correlations, leading to the initial suspicion that the neural correlates of pupil dilation may have been confounded by eye blinks. We performed multiple control analyses and in short, we found that the pupil-BOLD correlations could not be traced back to blink-related pupil artifacts. Instead, these additional analyses revealed a stimulus-induced temporal coincidence between blink suppression and pupil dilation. Still, we would like to suggest that future studies investigating neural correlates of pupil dynamics should be aware of the fact that presentations of salient stimuli might involve simultaneous changes in pupil size and blinking behavior, which need to be carefully disentangled and controlled for.

5 Conclusions

At the start of this thesis, only two studies had investigated the neural correlates of pupil size during the resting state and to our knowledge, no group had assessed the neural correlates of reward anticipation-related pupil dilations in humans before. Using simultaneous pupillometry and fMRI in healthy subjects, we found that dilations of the pupil, either occurring spontaneously during the resting state or in response to reward-predicting cues, were associated with activation of the SN. Furthermore, our results show that pupillometry is helpful to disentangle different processes and associated brain activations occurring during reward anticipation, involving reward prediction, arousal (up)regulation, and vigilant attention.

The consistent link between SN activity and pupil dilation observed in our studies complements the observations from the two previously existing pupillometry/rs-fMRI studies and may clarify their conflicting results. Moreover, our results replicate the findings from previous neuroimaging investigations of reward anticipation and extend these findings by providing evidence for a strong link between SN activity and emotional arousal. In addition, another study by our research group involving simultaneous pupillometry/fMRI in a human fear learning experiment revealed that SN activation-associated pupil dilations also track fear learning, indicating that pupil dilations reflect valence-independent arousal responses.

Based on its well-established role in performance monitoring and previous associations with autonomic arousal responses, we propose that the SN optimizes task performance by dynamically adjusting arousal levels, presumably via projections from dACC to LC. In the resting state, spontaneous activations of the SN appear to reflect a mechanism that restores attention to the fixation cross and inhibits a transition to sleep during periods of increased drowsiness (characterized by a decline of tonic pupil size), manifesting as spontaneous pupil dilations. Therefore, our findings provide first evidence that the dilation component of the pupillary fatigue waves in fact reflect intentional efforts to stay awake/keep external attention. Furthermore, we found that stronger pupil dilation during reward anticipation was associated with faster

responding to a target stimulus, suggesting that an upregulation of arousal initiated by the SN in response to a reward-predicting cue facilitates reward-directed behaviors.

Recent initiatives like the RDoC project emphasize the exploration of intermediate endophenotypes in order to advance diagnostics and eventually treatments in psychiatry, recommending psychophysiological measurements as a promising strategy. Previous studies have found a strong link between the LC-NA system and pupil size and our studies suggest that pupillometry additionally provides a reliable index for SN activity. Both systems are known to be strongly involved in the development and maintenance of stress-related disorders, and our findings point towards a potential application of pupillometry as an objective diagnostic tool in clinical psychiatry, for instance to assess arousal dysregulation, anhedonia symptomatology and responsiveness to SSNRI medication.

6 References

Alexander WH, Brown JW. 2010. Computational models of performance monitoring and cognitive control. Top Cogn Sci. 2(4):658-677. DOI: 10.1111/j.1756-8765.2010.01085.x

Allen RJ. 1983. Human Stress: Its Nature and Control. Minneapolis: Burgess.

Alnaes D, Sneve MH, Espeseth T, Endestad T, van de Pavert SH, Laeng B. 2014. Pupil size signals mental effort deployed during multiple object tracking and predicts brain activity in the dorsal attention network and the locus coeruleus. J Vis. 14(4):1-20. DOI: 10.1167/14.4.1

Asemi A, Ramaseshan K, Burgess A, Diwadkar VA, Bressler SL. 2015. Dorsal anterior cingulate cortex modulates supplementary motor area in coordinated unimanual motor behavior. Front Hum Neurosci. 9:309. DOI: 10.3389/fnhum.2015.00309

Aston-Jones G, Bloom FE. 1981. Norepinephrine-containing locus coeruleus neurons in behaving rats exhibit pronounced responses to non-noxious environmental stimuli. J Neurosci. 1(8):887-900.

Aston-Jones G, Chen S, Zhu Y, Oshinsky ML. 2001. A neural circuit for circadian regulation of arousal. Nat Neurosci. 4(7):732-738. DOI: 10.1038/89522

Aston-Jones G, Cohen JD. 2005a. Adaptive gain and the role of the locus coeruleus-norepinephrine system in optimal performance. J Comp Neurol. 493(1):99-110. DOI: 10.1002/cne.20723

Aston-Jones G, Cohen JD. 2005b. An integrative theory of locus coeruleus-norepinephrine function: adaptive gain and optimal performance. Annu Rev Neurosci. 28:403-450. DOI: 10.1146/annurev.neuro.28.061604.135709

Aston-Jones G, Rajkowski J, Kubiak P, Alexinsky T. 1994. Locus coeruleus neurons in monkey are selectively activated by attended cues in a vigilance task. J Neurosci. 14(7):4467-4480.

Beatty J, Lucero-Wagoner B. 2000. The pupillary system. In: Cacioppo JT, Tassinary LG, Berntson GG, editors. Handbook of psychophysiology. Hillsdale: Cambridge University Press. p. 142–162.

Beauchaine TP. 2009. The Role of Biomarkers and Endophenotypes in Prevention and Treatment of Psychopathological Disorders. Biomark Med. 3(1):1-3. DOI: 10.2217/17520363.3.1.1

Beissner F. 2015. Functional MRI of the Brainstem: Common Problems and their Solutions. Clin Neuroradiol. 25 Suppl 2:251-257. DOI: 10.1007/s00062-015-0404-0

Bellebaum C, Daum I, Koch B, Schwarz M, Hoffmann KP. 2005. The role of the human thalamus in processing corollary discharge. Brain. 128(Pt 5):1139-1154. DOI: 10.1093/brain/awh474

Bitsios P, Szabadi E, Bradshaw CM. 1999. Comparison of the effects of venlafaxine, paroxetine and desipramine on the pupillary light reflex in man. Psychopharmacology (Berl). 143(3):286-292.

Blakemore SJ, Rees G, Frith CD. 1998. How do we predict the consequences of our actions? A functional imaging study. Neuropsychologia. 36(6):521-529.

Botvinick MM, Cohen JD, Carter CS. 2004. Conflict monitoring and anterior cingulate cortex: an update. Trends Cogn Sci. 8(12):539-546. DOI: 10.1016/j.tics.2004.10.003

Bowrey HE, James MH, Aston-Jones G. 2017. New directions for the treatment of depression: Targeting the photic regulation of arousal and mood (PRAM) pathway. Depress Anxiety. 34(7):588-595. DOI: 10.1002/da.22635

Bremner JD, Krystal JH, Southwick SM, Charney DS. 1996. Noradrenergic mechanisms in stress and anxiety: II. Clinical studies. Synapse. 23(1):39-51.

Cannon WB. 1929. Bodily changes in pain, hunger, fear, and rage. New York: Appleton-Century-Crofts.

Carciofo R, Du F, Song N, Zhang K. 2014. Mind Wandering, Sleep Quality, Affect and Chronotype: An Exploratory Study. PLoS ONE. 9(3):e91285. DOI: 10.1371/journal.pone.0091285

Carmichael ST, Price JL. 1995a. Limbic connections of the orbital and medial prefrontal cortex in macaque monkeys. J Comp Neurol. 363(4):615-641. DOI: 10.1002/cne.903630408

Carmichael ST, Price JL. 1995b. Sensory and premotor connections of the orbital and medial prefrontal cortex of macaque monkeys. J Comp Neurol. 363(4):642-664. DOI: 10.1002/cne.903630409

Carter CS, Braver TS, Barch DM, Botvinick MM, Noll D, Cohen JD. 1998. Anterior cingulate cortex, error detection, and the online monitoring of performance. Science. 280(5364):747-749.

Citron FMM, Gray MA, Critchley HD, Weekes BS, Ferstl EC. 2014. Emotional valence and arousal affect reading in an interactive way: Neuroimaging evidence for an approach-withdrawal framework. Neuropsychologia. 56:79-89.

Clayton EC, Rajkowski J, Cohen JD, Aston-Jones G. 2004. Phasic activation of monkey locus ceruleus neurons by simple decisions in a forced-choice task. J Neurosci. 24(44):9914-9920. DOI: 10.1523/jneurosci.2446-04.2004

Clementz BA, Sweeney JA, Hamm JP, Ivleva EI, Ethridge LE, Pearlson GD, Keshavan MS, Tamminga CA. 2016. Identification of Distinct Psychosis Biotypes Using Brain-Based Biomarkers. The American journal of psychiatry. 173(4):373-384. DOI: 10.1176/appi.ajp.2015.14091200

Colton CW, Manderscheid RW. 2006. Congruencies in Increased Mortality Rates, Years of Potential Life Lost, and Causes of Death Among Public Mental Health Clients in Eight States. Preventing Chronic Disease. 3(2):A42.

Costa e Silva JA. 2013. Personalized medicine in psychiatry: new technologies and approaches. Metabolism. 62 Suppl 1:S40-44. DOI: 10.1016/j.metabol.2012.08.017

Craig AD. 2009. How do you feel--now? The anterior insula and human awareness. Nat Rev Neurosci. 10(1):59-70. DOI: 10.1038/nrn2555

Critchley HD. 2005. Neural mechanisms of autonomic, affective, and cognitive integration. J Comp Neurol. 493(1):154-166. DOI: 10.1002/cne.20749

Critchley HD, Elliott R, Mathias CJ, Dolan RJ. 2000. Neural activity relating to generation and representation of galvanic skin conductance responses: a functional magnetic resonance imaging study. J Neurosci. 20(8):3033-3040.

Cunningham ET, Jr., Sawchenko PE. 1988. Anatomical specificity of noradrenergic inputs to the paraventricular and supraoptic nuclei of the rat hypothalamus. J Comp Neurol. 274(1):60-76. DOI: 10.1002/cne.902740107

Cuthbert BN, Insel TR. 2013. Toward the future of psychiatric diagnosis: the seven pillars of RDoC. BMC Med. 11:126. DOI: 10.1186/1741-7015-11-126

Daube JR. 1986. Medical Neurosciences: An Approach to Anatomy, Pathology, and Physiology by Systems and Levels. Boston: Little, Brown and Co.

de Kloet ER, Karst H, Joels M. 2008. Corticosteroid hormones in the central stress response: quick-and-slow. Front Neuroendocrinol. 29(2):268-272. DOI: 10.1016/j.yfrne.2007.10.002

De Kloet ER, Vreugdenhil E, Oitzl MS, Joels M. 1998. Brain corticosteroid receptor balance in health and disease. Endocr Rev. 19(3):269-301. DOI: 10.1210/edrv.19.3.0331

Devilbiss DM, Waterhouse BD. 2000. Norepinephrine exhibits two distinct profiles of action on sensory cortical neuron responses to excitatory synaptic stimuli. Synapse. 37(4):273-282.

Devilbiss DM, Waterhouse BD. 2004. The effects of tonic locus ceruleus output on sensory-evoked responses of ventral posterior medial thalamic and barrel field cortical neurons in the awake rat. J Neurosci. 24(48):10773-10785. DOI: 10.1523/jneurosci.1573-04.2004

Devinsky O, Morrell MJ, Vogt BA. 1995. Contributions of anterior cingulate cortex to behaviour. Brain. 118 (Pt 1):279-306.

Diamond ME, Ahissar E. 2007. When outgoing and incoming signals meet: new insights from the zona incerta. Neuron. 56(4):578-579. DOI: 10.1016/j.neuron.2007.11.006

Downar J, Blumberger DM, Daskalakis ZJ. 2016. The Neural Crossroads of Psychiatric Illness: An Emerging Target for Brain Stimulation. Trends Cogn Sci. 20(2):107-120. DOI: 10.1016/j.tics.2015.10.007

Dunn AJ, Swiergiel AH, Palamarchouk V. 2004. Brain circuits involved in corticotropin-releasing factor-norepinephrine interactions during stress. Ann N Y Acad Sci. 1018:25-34. DOI: 10.1196/annals.1296.003

Eldar E, Cohen JD, Niv Y. 2013. The effects of neural gain on attention and learning. Nat Neurosci. 16(8):1146-1153. DOI: 10.1038/nn.3428

Faravelli C, Lo Sauro C, Lelli L, Pietrini F, Lazzeretti L, Godini L, Benni L, Fioravanti G, Talamba GA, Castellini G et al. . 2012. The role of life events and HPA axis in anxiety disorders: a review. Curr Pharm Des. 18(35):5663-5674.

Fernandes P, Regala J, Correia F, Gonçalves-Ferreira AJ. 2012. The human locus coeruleus 3-D stereotactic anatomy. Surgical and Radiologic Anatomy. 34(10):879-885. DOI: 10.1007/s00276-012-0979-y

Fountoulakis K, Fotiou F, Iacovides A, Tsiptsios J, Goulas A, Tsolaki M, Ierodiakonou C. 1999. Changes in pupil reaction to light in melancholic patients. Int J Psychophysiol. 31(2):121-128.

Fox KC, Spreng RN, Ellamil M, Andrews-Hanna JR, Christoff K. 2015. The wandering brain: meta-analysis of functional neuroimaging studies of mind-wandering and related spontaneous thought processes. Neuroimage. 111:611-621. DOI: 10.1016/j.neuroimage.2015.02.039

Frodl T, O'Keane V. 2013. How does the brain deal with cumulative stress? A review with focus on developmental stress, HPA axis function and hippocampal structure in humans. Neurobiol Dis. 52:24-37. DOI: 10.1016/j.nbd.2012.03.012

Gold JI, Shadlen MN. 2000. Representation of a perceptual decision in developing oculomotor commands. Nature. 404(6776):390-394. DOI: 10.1038/35006062

Goldberg D. 2011. The heterogeneity of "major depression". World Psychiatry. 10(3):226-228.

Goodkind M, Eickhoff SB, Oathes DJ, Jiang Y, Chang A, Jones-Hagata LB, Ortega BN, Zaiko YV, Roach EL, Korgaonkar MS et al. . 2015. Identification of a common neurobiological substrate for mental illness. JAMA Psychiatry. 72(4):305-315. DOI: 10.1001/jamapsychiatry.2014.2206

Gorka SM, Huggins AA, Fitzgerald DA, Nelson BD, Phan KL, Shankman SA. 2014. Neural response to reward anticipation in those with depression with and without panic disorder. J Affect Disord. 164:50-56. DOI: 10.1016/j.jad.2014.04.019

Gottesman, II, Gould TD. 2003. The endophenotype concept in psychiatry: etymology and strategic intentions. Am J Psychiatry. 160(4):636-645. DOI: 10.1176/appi.ajp.160.4.636

Grant SJ, Aston-Jones G, Redmond DE, Jr. 1988. Responses of primate locus coeruleus neurons to simple and complex sensory stimuli. Brain Res Bull. 21(3):401-410.

Gustavsson A, Svensson M, Jacobi F, Allgulander C, Alonso J, Beghi E, Dodel R, Ekman M, Faravelli C, Fratiglioni L et al. . 2011. Cost of disorders of the brain in Europe 2010. Eur Neuropsychopharmacol. 21(10):718-779. DOI: 10.1016/j.euroneuro.2011.08.008

Haber SN, Knutson B. 2010. The reward circuit: linking primate anatomy and human imaging. Neuropsychopharmacology. 35(1):4-26. DOI: 10.1038/npp.2009.129

Habib KE, Gold PW, Chrousos GP. 2001. Neuroendocrinology of stress. Endocrinol Metab Clin North Am. 30(3):695-728; vii-viii.

Hamilton JP, Etkin A, Furman DJ, Lemus MG, Johnson RF, Gotlib IH. 2012. Functional neuroimaging of major depressive disorder: a meta-analysis and new integration of base line activation and neural response data. Am J Psychiatry. 169(7):693-703. DOI: 10.1176/appi.ajp.2012.11071105

Hanes DP, Schall JD. 1996. Neural control of voluntary movement initiation. Science. 274(5286):427-430.

Heller PH, Perry F, Jewett DL, Levine JD. 1990. Autonomic components of the human pupillary light reflex. Invest Ophthalmol Vis Sci. 31(1):156-162.

Herman JP, McKlveen JM, Ghosal S, Kopp B, Wulsin A, Makinson R, Scheimann J, Myers B. 2016. Regulation of the hypothalamic-pituitary-adrenocortical stress response. Comprehensive Physiology. 6(2):603-621. DOI: 10.1002/cphy.c150015

Herve-Minvielle A, Sara SJ. 1995. Rapid habituation of auditory responses of locus coeruleus cells in anaesthetized and awake rats. Neuroreport. 6(10):1363-1368.

Hobson JA, McCarley RW, Wyzinski PW. 1975. Sleep cycle oscillation: reciprocal discharge by two brainstem neuronal groups. Science. 189(4196):55-58.

Hurley LM, Devilbiss DM, Waterhouse BD. 2004. A matter of focus: monoaminergic modulation of stimulus coding in mammalian sensory networks. Curr Opin Neurobiol. 14(4):488-495. DOI: 10.1016/j.conb.2004.06.007

Ide JS, Li C-sR. 2011. A cerebellar thalamic cortical circuit for error-related cognitive control. NeuroImage. 54(1):455-464. DOI: 10.1016/j.neuroimage.2010.07.042

Ito S, Stuphorn V, Brown JW, Schall JD. 2003. Performance monitoring by the anterior cingulate cortex during saccade countermanding. Science. 302(5642):120-122. DOI: 10.1126/science.1087847

Joshi S, Li Y, Kalwani RM, Gold JI. 2016. Relationships between Pupil Diameter and Neuronal Activity in the Locus Coeruleus, Colliculi, and Cingulate Cortex. Neuron. 89(1):221-234. DOI: 10.1016/j.neuron.2015.11.028

Juruena MF. 2014. Early-life stress and HPA axis trigger recurrent adulthood depression. Epilepsy Behav. 38:148-159. DOI: 10.1016/j.yebeh.2013.10.020

Kang OE, Huffer KE, Wheatley TP. 2014. Pupil dilation dynamics track attention to high-level information. PLoS One. 9(8):e102463. DOI: 10.1371/journal.pone.0102463

Kerns JG, Cohen JD, MacDonald AW, 3rd, Cho RY, Stenger VA, Carter CS. 2004. Anterior cingulate conflict monitoring and adjustments in control. Science. 303(5660):1023-1026. DOI: 10.1126/science.1089910

Kerr FA, Szabadi E. 1985. Comparison of the effects of chronic administration of ciclazindol and desipramine on pupillary responses to tyramine, methoxamine and pilocarpine in healthy volunteers. Br J Clin Pharmacol. 19(5):639-647.

Knutson B, Bhanji JP, Cooney RE, Atlas LY, Gotlib IH. 2008. Neural responses to monetary incentives in major depression. Biol Psychiatry. 63(7):686-692. DOI: 10.1016/j.biopsych.2007.07.023

Knutson B, Cooper JC. 2005. Functional magnetic resonance imaging of reward prediction. Curr Opin Neurol. 18(4):411-417.

Knutson B, Fong GW, Adams CM, Varner JL, Hommer D. 2001. Dissociation of reward anticipation and outcome with event-related fMRI. Neuroreport. 12(17):3683-3687.

Knutson B, Westdorp A, Kaiser E, Hommer D. 2000. FMRI Visualization of Brain Activity during a Monetary Incentive Delay Task. NeuroImage. 12(1):20-27.

Koenig S, Uengoer M, Lachnit H. 2018. Pupil dilation indicates the coding of past prediction errors: Evidence for attentional learning theory. Psychophysiology. 55(4). DOI: 10.1111/psyp.13020

Kozak MJ, Cuthbert BN. 2016. The NIMH Research Domain Criteria Initiative: Background, Issues, and Pragmatics. Psychophysiology. 53(3):286-297. DOI: 10.1111/psyp.12518

Krugers HJ, Karst H, Joels M. 2012. Interactions between noradrenaline and corticosteroids in the brain: from electrical activity to cognitive performance. Frontiers in Cellular Neuroscience. 6:15. DOI: 10.3389/fncel.2012.00015

Larsen RS, Waters J. 2018. Neuromodulatory Correlates of Pupil Dilation. Front Neural Circuits. 12:21. DOI: 10.3389/fncir.2018.00021

Lee T-H, Greening SG, Ueno T, Clewett D, Ponzio A, Sakaki M, Mather M. 2018. Arousal increases neural gain via the locus coeruleus–noradrenaline system in younger adults but not in older adults. Nature Human Behaviour. 2(5):356-366. DOI: 10.1038/s41562-018-0344-1

Leuchs L, Schneider M, Czisch M, Spoormaker VI. 2016. Neural correlates of pupil dilation during human fear learning. Neuroimage. 147:186-197. DOI: 10.1016/j.neuroimage.2016.11.072

Linton EA, Tilders FJ, Hodgkinson S, Berkenbosch F, Vermes I, Lowry PJ. 1985. Stress-induced secretion of adrenocorticotropin in rats is inhibited by administration of antisera to ovine corticotropin-releasing factor and vasopressin. Endocrinology. 116(3):966-970. DOI: 10.1210/endo-116-3-966

Liu KY, Marijatta F, Hammerer D, Acosta-Cabronero J, Duzel E, Howard RJ. 2017. Magnetic resonance imaging of the human locus coeruleus: A systematic review. Neurosci Biobehav Rev. DOI: 10.1016/j.neubiorev.2017.10.023

Loewenfeld I. 1993. The pupil. Detroit, Michigan: Wayne State University Press.

Longtin A, Milton JG. 1989. Insight into the transfer function, gain, and oscillation onset for the pupil light reflex using nonlinear delay-differential equations. Biol Cybern. 61(1):51-58.

Longtin A, Milton JG, Bos JE, Mackey MC. 1990. Noise and critical behavior of the pupil light reflex at oscillation onset. Phys Rev A. 41(12):6992-7005.

Lowenstein O, Loewenfeld IE. 1964. The sleep-waking cycle and pupillary activity. Ann N Y Acad Sci. 117:142-156.

Ludtke H, Wilhelm B, Adler M, Schaeffel F, Wilhelm H. 1998. Mathematical procedures in data recording and processing of pupillary fatigue waves. Vision Res. 38(19):2889-2896.

Mather M, Clewett D, Sakaki M, Harley CW. 2016. Norepinephrine ignites local hotspots of neuronal excitation: How arousal amplifies selectivity in perception and memory. Behav Brain Sci. 39:e200. DOI: 10.1017/s0140525x15000667

McCall JG, Al-Hasani R, Siuda ER, Hong DY, Norris AJ, Ford CP, Bruchas MR. 2015. CRH engagement of the locus coeruleus noradrenergic system mediates stress-induced anxiety. Neuron. 87(3):605-620. DOI: 10.1016/j.neuron.2015.07.002

McCarrick AK, Manderscheid RW, Bertolucci DE, Goldman H, Tessler RC. 1986. Chronic medical problems in the chronic mentally ill. Hosp Community Psychiatry. 37(3):289-291.

McKay LI, Cidlowski JA. 2003. Physiologic and Pharmacologic Effects of Corticosteroids. In: Kufe DW, Pollock RE, Weichselbaum RR, editors. Holland-Frei Cancer Medicine. 6 ed. Hamilton: BC Decker.

Medford N, Critchley HD. 2010. Conjoint activity of anterior insular and anterior cingulate cortex: awareness and response. Brain Struct Funct. 214(5-6):535-549. DOI: 10.1007/s00429-010-0265-x

Miltner WH, Braun CH, Coles MG. 1997. Event-related brain potentials following incorrect feedback in a time-estimation task: evidence for a "generic" neural system for error detection. J Cogn Neurosci. 9(6):788-798. DOI: 10.1162/jocn.1997.9.6.788

Mitchell AS, Browning PG, Baxter MG. 2007. Neurotoxic lesions of the medial mediodorsal nucleus of the thalamus disrupt reinforcer devaluation effects in rhesus monkeys. J Neurosci. 27(42):11289-11295. DOI: 10.1523/jneurosci.1914-07.2007

Morilak DA, Barrera G, Echevarria DJ, Garcia AS, Hernandez A, Ma S, Petre CO. 2005. Role of brain norepinephrine in the behavioral response to stress. Prog Neuropsychopharmacol Biol Psychiatry. 29(8):1214-1224. DOI: 10.1016/j.pnpbp.2005.08.007

Murphy PR, O'Connell RG, O'Sullivan M, Robertson IH, Balsters JH. 2014. Pupil diameter covaries with BOLD activity in human locus coeruleus. Hum Brain Mapp. 35(8):4140-4154. DOI: 10.1002/hbm.22466

Naber M, Frassle S, Rutishauser U, Einhauser W. 2013. Pupil size signals novelty and predicts later retrieval success for declarative memories of natural scenes. J Vis. 13(2):11. DOI: 10.1167/13.2.11

Nassar MR, Rumsey KM, Wilson RC, Parikh K, Heasly B, Gold JI. 2012. Rational regulation of learning dynamics by pupil-linked arousal systems. Nat Neurosci. 15(7):1040-1046. DOI: 10.1038/nn.3130

Nemeroff CB. 1988. The role of corticotropin-releasing factor in the pathogenesis of major depression. Pharmacopsychiatry. 21(2):76-82. DOI: 10.1055/s-2007-1014652

Nieuwenhuis S, de Geus EJ, Aston-Jones G. 2011. The anatomical and functional relationship between the P3 and autonomic components of the orienting response. Psychophysiology. 48(2):162-175. DOI: 10.1111/j.1469-8986.2010.01057.x

Nusslock R, Alloy LB. 2017. Reward processing and mood-related symptoms: An RDoC and translational neuroscience perspective. J Affect Disord. 216:3-16. DOI: 10.1016/j.jad.2017.02.001

Ong JL, Kong D, Chia TT, Tandi J, Thomas Yeo BT, Chee MW. 2015. Co-activated yet disconnected-Neural correlates of eye closures when trying to stay awake. Neuroimage. 118:553–562. DOI: 10.1016/j.neuroimage.2015.03.085

Ongur D, Price JL. 2000. The organization of networks within the orbital and medial prefrontal cortex of rats, monkeys and humans. Cereb Cortex. 10(3):206-219.

Ozomaro U, Wahlestedt C, Nemeroff CB. 2013. Personalized medicine in psychiatry: problems and promises. BMC Med. 11:132. DOI: 10.1186/1741-7015-11-132

Pacak K, Palkovits M. 2001. Stressor specificity of central neuroendocrine responses: implications for stress-related disorders. Endocr Rev. 22(4):502-548. DOI: 10.1210/edrv.22.4.0436

Page ME, Abercrombie ED. 1999. Discrete local application of corticotropin-releasing factor increases locus coeruleus discharge and extracellular norepinephrine in rat hippocampus. Synapse. 33(4):304-313.

Paus T. 2001. Primate anterior cingulate cortex: where motor control, drive and cognition interface. Nat Rev Neurosci. 2(6):417-424. DOI: 10.1038/35077500

Perez H, Ruiz S, Nunez H, White A, Gotteland M, Hernandez A. 2006. Paraventricular-coerulear interactions: role in hypertension induced by prenatal undernutrition in the rat. Eur J Neurosci. 24(4):1209-1219. DOI: 10.1111/j.1460-9568.2006.04997.x

Peters SK, Dunlop K, Downar J. 2016. Cortico-Striatal-Thalamic Loop Circuits of the Salience Network: A Central Pathway in Psychiatric Disease and Treatment. Front Syst Neurosci. 10:104. DOI: 10.3389/fnsys.2016.00104

Phillips ML, Gregory LJ, Cullen S, Coen S, Ng V, Andrew C, Giampietro V, Bullmore E, Zelaya F, Amaro E et al. . 2003. The effect of negative emotional context on neural and behavioural responses to oesophageal stimulation. Brain. 126(Pt 3):669-684.

Poudel GR, Innes CR, Bones PJ, Watts R, Jones RD. 2014. Losing the struggle to stay awake: divergent thalamic and cortical activity during microsleeps. Hum Brain Mapp. 35(1):257-269. DOI: 10.1002/hbm.22178

Prange AJ, Jr. 1964. The Pharmacology and biochemistry of depression. Dis Nerv Syst. 25:217-221.

Preuschoff K, t Hart BM, Einhauser W. 2011. Pupil Dilation Signals Surprise: Evidence for Noradrenaline's Role in Decision Making. Front Neurosci. 5:115. DOI: 10.3389/fnins.2011.00115

Rajkowski J, Kubiak P, Aston-Jones G. 1993. Correlations between locus coeruleus (LC) neural activity, pupil diameter and behavior in monkey support a role of LC in attention. Society for Neuroscience Abstracts. 19(1-3):974-974.

Rajkowski J, Kubiak P, Ivanova S, Aston-Jones G. 1998. State-related activity, reactivity of locus ceruleus neurons in behaving monkeys. Adv Pharmacol. 42:740-744.

Rasmussen K, Morilak DA, Jacobs BL. 1986. Single unit activity of locus coeruleus neurons in the freely moving cat. I. During naturalistic behaviors and in response to simple and complex stimuli. Brain Res. 371(2):324-334.

Reinhard G, Lachnit H. 2002. Differential conditioning of anticipatory pupillary dilation responses in humans. Biol Psychol. 60(1):51-68.

Reinhard G, Lachnit H, Konig S. 2006. Tracking stimulus processing in Pavlovian pupillary conditioning. Psychophysiology. 43(1):73-83. DOI: 10.1111/j.1469-8986.2006.00374.x

Roehrig C. 2016. Mental Disorders Top The List Of The Most Costly Conditions In The United States: $201 Billion. Health Aff (Millwood). 35(6):1130-1135. DOI: 10.1377/hlthaff.2015.1659

Rudebeck PH, Putnam PT, Daniels TE, Yang T, Mitz AR, Rhodes SE, Murray EA. 2014. A role for primate subgenual cingulate cortex in sustaining autonomic arousal. Proc Natl Acad Sci U S A. 111(14):5391-5396. DOI: 10.1073/pnas.1317695111

Sämann PG, Tully C, Spoormaker VI, Wetter TC, Holsboer F, Wehrle R, Czisch M. 2010. Increased sleep pressure reduces resting state functional connectivity. Magma. 23(5-6):375-389. DOI: 10.1007/s10334-010-0213-z

Sämann PG, Wehrle R, Hoehn D, Spoormaker VI, Peters H, Tully C, Holsboer F, Czisch M. 2011. Development of the brain's default mode network from wakefulness to slow wave sleep. Cereb Cortex. 21(9):2082-2093. DOI: 10.1093/cercor/bhq295

Sambataro F, Doerig N, Hanggi J, Wolf RC, Brakowski J, Holtforth MG, Seifritz E, Spinelli S. 2018. Anterior cingulate volume predicts response to psychotherapy and functional connectivity with the inferior parietal cortex in major depressive disorder. Eur Neuropsychopharmacol. 28(1):138-148. DOI: 10.1016/j.euroneuro.2017.11.008

Samuels ER, Szabadi E. 2008. Functional neuroanatomy of the noradrenergic locus coeruleus: its roles in the regulation of arousal and autonomic function part II: physiological and pharmacological manipulations and pathological alterations of locus coeruleus activity in humans. Curr Neuropharmacol. 6(3):254-285. DOI: 10.2174/157015908785777193

Saper CB, Scammell TE, Lu J. 2005. Hypothalamic regulation of sleep and circadian rhythms. Nature. 437(7063):1257-1263. DOI: 10.1038/nature04284

Saphier D. 1993. Electrophysiology and neuropharmacology of noradrenergic projections to rat PVN magnocellular neurons. Am J Physiol. 264(5 Pt 2):R891-902. DOI: 10.1152/ajpregu.1993.264.5.R891

Schall JD, Thompson KG. 1999. Neural selection and control of visually guided eye movements. Annu Rev Neurosci. 22:241-259. DOI: 10.1146/annurev.neuro.22.1.241

Schildkraut JJ. 1965. The catecholamine hypothesis of affective disorders: a review of supporting evidence. Am J Psychiatry. 122(5):509-522. DOI: 10.1176/ajp.122.5.509

Seifert S, von Cramon DY, Imperati D, Tittgemeyer M, Ullsperger M. 2011. Thalamocingulate interactions in performance monitoring. J Neurosci. 31(9):3375-3383. DOI: 10.1523/jneurosci.6242-10.2011

Servan-Schreiber D, Printz H, Cohen JD. 1990. A network model of catecholamine effects: gain, signal-to-noise ratio, and behavior. Science. 249(4971):892-895.

Shur E, Checkley S. 1982. Pupil studies in depressed patients: an investigation of the mechanism of action of desipramine. Br J Psychiatry. 140:181-184.

Siepmann T, Ziemssen T, Mueck-Weymann M, Kirch W, Siepmann M. 2007. The effects of venlafaxine on autonomic functions in healthy volunteers. J Clin Psychopharmacol. 27(6):687-691. DOI: 10.1097/jcp.0b013e31815a255b

Smith SM, Vale WW. 2006. The role of the hypothalamic-pituitary-adrenal axis in neuroendocrine responses to stress. Dialogues in Clinical Neuroscience. 8(4):383-395.

Soni A. 2009. The five most costly conditions, 1996 and 2006: Estimates for the US civilian noninstitutionalized population (Statistical Brief# 248). Rockville, MD: Agency for Healthcare Research and Quality.

Spoormaker VI, Schröter MS, Gleiser PM, Andrade KC, Dresler M, Wehrle R, Sämann PG, Czisch M. 2010. Development of a large-scale functional brain network during human non-rapid eye movement sleep. J Neurosci. 30(34):11379-11387. DOI: 10.1523/jneurosci.2015-10.2010

Sterner EY, Kalynchuk LE. 2010. Behavioral and neurobiological consequences of prolonged glucocorticoid exposure in rats: relevance to depression. Prog Neuropsychopharmacol Biol Psychiatry. 34(5):777-790. DOI: 10.1016/j.pnpbp.2010.03.005

Stetler C, Miller GE. 2011. Depression and hypothalamic-pituitary-adrenal activation: a quantitative summary of four decades of research. Psychosom Med. 73(2):114-126. DOI: 10.1097/PSY.0b013e31820ad12b

Szabadi E. 2012. Modulation of physiological reflexes by pain: role of the locus coeruleus. Front Integr Neurosci. 6:94. DOI: 10.3389/fnint.2012.00094

Szabadi E. 2013. Functional neuroanatomy of the central noradrenergic system. J Psychopharmacol. 27(8):659-693. DOI: 10.1177/0269881113490326

Tagliazucchi E, Laufs H. 2014. Decoding wakefulness levels from typical fMRI resting-state data reveals reliable drifts between wakefulness and sleep. Neuron. 82(3):695-708. DOI: 10.1016/j.neuron.2014.03.020

Tank AW, Lee Wong D. 2015. Peripheral and central effects of circulating catecholamines. Compr Physiol. 5(1):1-15. DOI: 10.1002/cphy.c140007

Theofilopoulos N, McDade G, Szabadi E, Bradshaw CM. 1995. Effects of reboxetine and desipramine on the kinetics of the pupillary light reflex. British Journal of Clinical Pharmacology. 39(3):251-255.

Trautmann S, Rehm J, Wittchen HU. 2016. The economic costs of mental disorders: Do our societies react appropriately to the burden of mental disorders? EMBO Reports. 17(9):1245-1249. DOI: 10.15252/embr.201642951

Uddin LQ. 2015. Salience processing and insular cortical function and dysfunction. Nat Rev Neurosci. 16(1):55-61. DOI: 10.1038/nrn3857

Ulrich-Lai YM, Herman JP. 2009. Neural regulation of endocrine and autonomic stress responses. Nat Rev Neurosci. 10(6):397-409. DOI: 10.1038/nrn2647

Visser RM, Kunze AE, Westhoff B, Scholte HS, Kindt M. 2015. Representational similarity analysis offers a preview of the noradrenergic modulation of long-term fear memory at the time of encoding. Psychoneuroendocrinology. 55:8-20. DOI: 10.1016/j.psyneuen.2015.01.021

Visser RM, Scholte HS, Beemsterboer T, Kindt M. 2013. Neural pattern similarity predicts long-term fear memory. Nat Neurosci. 16(4):388-390. DOI: 10.1038/nn.3345

Wagner G, Koch K, Reichenbach JR, Sauer H, Schlosser RG. 2006. The special involvement of the rostrolateral prefrontal cortex in planning abilities: an event-related fMRI study with the Tower of London paradigm. Neuropsychologia. 44(12):2337-2347. DOI: 10.1016/j.neuropsychologia.2006.05.014

Walker ER, McGee RE, Druss BG. 2015. Mortality in mental disorders and global disease burden implications: a systematic review and meta-analysis. JAMA Psychiatry. 72(4):334-341. DOI: 10.1001/jamapsychiatry.2014.2502

Wang CA, Boehnke SE, White BJ, Munoz DP. 2012. Microstimulation of the monkey superior colliculus induces pupil dilation without evoking saccades. J Neurosci. 32(11):3629-3636. DOI: 10.1523/jneurosci.5512-11.2012

Warga M, Ludtke H, Wilhelm H, Wilhelm B. 2009. How do spontaneous pupillary oscillations in light relate to light intensity? Vision Res. 49(3):295-300. DOI: 10.1016/j.visres.2008.09.019

Waterhouse BD, Moises HC, Woodward DJ. 1998. Phasic activation of the locus coeruleus enhances responses of primary sensory cortical neurons to peripheral receptive field stimulation. Brain Res. 790(1-2):33-44.

Whitnall MH, Smyth D, Gainer H. 1987. Vasopressin coexists in half of the corticotropin-releasing factor axons present in the external zone of the median eminence in normal rats. Neuroendocrinology. 45(5):420-424. DOI: 10.1159/000124768

Whitton AE, Treadway MT, Pizzagalli DA. 2015. Reward processing dysfunction in major depression, bipolar disorder and schizophrenia. Curr Opin Psychiatry. 28(1):7-12. DOI: 10.1097/yco.0000000000000122

Wierda SM, van Rijn H, Taatgen NA, Martens S. 2012. Pupil dilation deconvolution reveals the dynamics of attention at high temporal resolution. Proc Natl Acad Sci U S A. 109(22):8456-8460. DOI: 10.1073/pnas.1201858109

Wilhelm B, Giedke H, Ludtke H, Bittner E, Hofmann A, Wilhelm H. 2001. Daytime variations in central nervous system activation measured by a pupillographic sleepiness test. J Sleep Res. 10(1):1-7.

Wilhelm B, Wilhelm H, Ludtke H, Streicher P, Adler M. 1998. Pupillographic assessment of sleepiness in sleep-deprived healthy subjects. Sleep. 21(3):258-265.

Wittchen HU, Jacobi F. 2005. Size and burden of mental disorders in Europe--a critical review and appraisal of 27 studies. Eur Neuropsychopharmacol. 15(4):357-376. DOI: 10.1016/j.euroneuro.2005.04.012

Wittchen HU, Jacobi F, Rehm J, Gustavsson A, Svensson M, Jonsson B, Olesen J, Allgulander C, Alonso J, Faravelli C et al. . 2011. The size and burden of mental disorders and other disorders of the brain in Europe 2010. Eur Neuropsychopharmacol. 21(9):655-679. DOI: 10.1016/j.euroneuro.2011.07.018

Wittchen HU, Jonsson B, Olesen J. 2005. Towards a better understanding of the size and burden and cost of brain disorders in Europe. Eur Neuropsychopharmacol. 15(4):355-356. DOI: 10.1016/j.euroneuro.2005.04.001

Woody ML, Gibb BE. 2015. Integrating NIMH Research Domain Criteria (RDoC) into Depression Research. Curr Opin Psychol. 4:6-12. DOI: 10.1016/j.copsyc.2015.01.004

Yellin D, Berkovich-Ohana A, Malach R. 2015. Coupling between pupil fluctuations and resting-state fMRI uncovers a slow build-up of antagonistic responses in the human cortex. Neuroimage. 106:414-427. DOI: 10.1016/j.neuroimage.2014.11.034

Acknowledgements

This dissertation would not have been possible without the guidance and the help of many people who in one way or another contributed to this work.

First of all, I would like to express my sincere gratitude to Dr. Victor Spoormaker as my supervisor and leader of the Psychophysiology Project Group, for giving me the great opportunity to conduct these studies, for his constantly available and skillful scientific support, and for his outstanding sense of humor and relaxed attitude which always promoted an open and friendly work atmosphere. Without him, I also probably would never have met my girlfriend Borbála, who came to our lab as a PhD student from Budapest for a cooperation in sleep research. I truly could not have imagined having a better advisor and mentor for my PhD study.

My sincere thanks also goes to the leader of the neuroimaging core unit Dr. Michael Czisch, who provided access to the MR research facilities and whose vast methodological experience and numerous advices strongly contributed to this work.

I also would like to deeply thank Dr. Philipp Sämann as neuroradiologist and research associate of the neuroimaging core unit for his constant interest in my studies and for providing valuable inspirations and helpful corrections.

Moreover, I am pleased to acknowledge my thesis advisory committee including Dr. Virginia Flanagin, PD Dr. Kathrin Koch and Prof. Dr. Dr. Elisabeth Binder, for the fruitful discussions and scientific advice through the last three and a half years.

I also express my gratitude to the Graduate School of Systemic Neurosciences (LMU) which allowed me to start my PhD at the Max Planck Institute of Psychiatry by granting my a yearlong stipend.

Special mention goes to Taechawidd “Fu” Nantawisarakul for proof-reading this thesis and to all technical assistants of the MR unit, particularly to Ines Eidner, Anna Hetzel and Rene Schranzer, for their tremendous support in collecting the data.

These acknowledgements would not be complete without mentioning my PhD colleague Laura Leuchs, who became a close friend over the years and whose astuteness and emotional support

helped carrying me through this work. Similar, profound gratitude goes to my brother and all of my friends for spending their Friday and Saturday evenings with me and providing the necessary balance to work.

Above all I want to deeply acknowledge my girlfriend and true soulmate Borbála, who greatly contributed to my well-being in the last phase of this work and who decided to stay with me in Munich.

Last but not least I greatly thank my parents who financially supported me throughout the years as a student and who left me a room in their house for all my musical instruments, without which I probably would have lost contact to my artistic vein and source of creativity.

„Alles Wissen und alles Vermehren unseres Wissens endet nicht mit einem Schlußpunkt, sondern mit einem Fragezeichen.“

– Hermann Hesse

Eidesstattliche Versicherung/Affidavit

Hiermit versichere ich an Eides statt, dass ich die vorliegende Dissertation „*Simultaneous pupillometry and functional magnetic resonance imaging (fMRI) for the detection of stress-related endophenotypes“* selbstständig angefertigt habe, mich außer der angegebenen keiner weiteren Hilfsmittel bedient und alle Erkenntnisse, die aus dem Schrifttum ganz oder annähernd übernommen sind, als solche kenntlich gemacht und nach ihrer Herkunft unter Bezeichnung der Fundstelle einzeln nachgewiesen habe.

I hereby confirm that the dissertation *“Simultaneous pupillometry and functional magnetic resonance imaging (fMRI) for the detection of stress-related endophenotypes“* is the result of my own work and that I have only used sources or materials listed and specified in the dissertation.

Munich, 26.07.2018

_____

Maximilian Schneider

Declaration of Author Contribution

Spontaneous pupil dilations during the resting state are associated with activation of the salience network.

Schneider M, Hathway P, Leuchs L, Samann PG, Czisch M, Spoormaker VI. 2016. Neuroimage.

The author of this thesis is the first author of the publication; M.S. and V.S. designed research and wrote the manuscript; M.S., P.H. and V.S. analyzed the data; M.S. and P.H. collected the data; L.L., P.S. and M.C. critically revised the manuscript.

Disentangling reward anticipation with simultaneous pupillometry / fMRI.

Schneider M, Leuchs L, Czisch M, Samann PG, Spoormaker VI. 2016. Neuroimage.

The author of this thesis is the first author of the publication; M.S. and V.S. designed research and wrote the manuscript; the data was collected within the framework of the BeCOME study; M.S. and V.S. analyzed the data; L.L., M.C. and P.S. critically revised the manuscript.

Munich, 26.07.2018

_____

Maximilian Schneider

Hereby confirms the first supervisor the listed contributions of Maximilian Schneider to the publications included in this thesis.

Munich, 26.07.2018

_____

Dr. Victor Spoormaker